NTNU – Trondheim
Norwegian University of
Science and Technology

Tailoring of alginate gel properties with mannuronan C-5 epimerases

Correlations between structural and physical properties

Johan Robert Berg

Chemical Engineering and Biotechnology
Submission date: July 2013
Supervisor: Berit Løkensgard Strand, IBT
Co-supervisor: Gudmund Skjåk-Bræk, IBT

Norwegian University of Science and Technology
Department of Biotechnology

Acknowledgements

This report is an individual master thesis conducted at the Department of Biotechnology, Faculty of Natural Science and Technology at the Norwegian University of Science and Technology.

I am very grateful for the help and support I have received from several persons during my work. Most of all, I would like to thank my supervisor professor Berit L. Strand for welcoming me to NTNU and her great guidance during the whole work. Her positive and kind attitude has given me a lot of energy. I am thankful for the support I have received from professor Gudmund Skjåk-Bræk, his great expertise in the field of polysaccharides has been valuable and his door has always been open. I would also like to express my thankfulness to Wenche I. Strand for being very helpful during my practical lab work, in addition to analyzing all my NMR- samples. She has given me great support and I have learnt many valuable things from her. Furthermore, I am very grateful for the encouragement I have received from Dr. Olav Andreas Aarstad and for performing the HPAEC-PAD analyze. I would as well like to thank Ann-Sissel Teialeret Ulset for performing the SEC-MALLS analyze and Dr. Finn Aachmann for providing the enzyme AlgE4 and for his help to isolate it.

Finally, the support and love from Julia has been vital for me during the work as well as the encouragement from friends and family.

Trondheim, July 15th

Johan Berg

Abstract

Alginate gels are one of the most used materials for immobilization of living cells due to the gels are structurally similar to the extracellular matrices in tissues. Alginate is a naturally occurring anionic polymer typically obtained from brown seaweed. It is a polysaccharide that consists of (1 →4)-linked β-D-mannuronic acid (M) and α-L-guluronic acid (G) residues. The C-5 epimerases is a family of enzymes that converts β-D-mannuronic acid (M) to α-L-guluronic acid (G). Since the C-5 epimerases have unique epimerization patterns it is possible to tailor the structure of alginate in order to alter its physical properties.

In this thesis, polymers only consisting of M-blocks were used as starting material and by varying the epimerization time with AlgE6 G contents between 48-85% were achieved, as determined by ^{1}H-NMR. A control alginate rich of alternating blocks, and relative short G-blocks, was made by first performing an AlgE4 epimerization in polyM, followed by an AlgE6 epimerization. Evidently, the used C-5 epimerases readily modified the structure of alginate.

The epimerized alginates were degraded with M-lyase from *Haliotis tuberculata* and G-lyase from *Klebsiella aerogenes* to study the block structures more carefully. The degraded alginates were analyzed by high pressure anion-exchange chromatography with pulsed amperometric detection (HPAEC-PAD). The data revealed that the number of long G-blocks (DP>40), among the AlgE6 epimerized mannuronan samples, increased with an increasing G-content. The natural alginate *Laminaria hyperborean* stipe was used as a reference in the work and it was shown to consist of large quantities of very long G-blocks that were not present in the epimerized alginates. The epimerized alginates contained relatively short M blocks, in relation to their G block lengths. An increasing G-content resulted in M distributions mostly consisting of short M blocks.

To be able to compare physical properties of the alginates Ca^{2+} gel cylinders were made by internal gelling. All cylinders were saturated in Ca^{2+} except for one of the AlgE6 epimerized alginates, which instead was saturated in both Ba^{2+} and Ca^{2+}. This was done to examine the effect of Ba^{2+} ions in an alginate rich of both G and M-blocks. Among the AlgE6 epimerized mannuronan alginates, the G-content and G-block lengths, significantly affected their physical properties. As observed, the Young´s modulus of the alginate with the highest G-content was about the double

strength of the alginate with the smallest G-content. The alginate that contained a high quantity of alternating blocks underwent the highest syneresis of all alginates. Moreover, it had a comparatively low Young´s modulus and was very compressible as seen by the high elasticity and rupture strength. The gels that were saturated in Ba^{2+} and Ca^{2+} had different physical properties than the Ca^{2+} saturated alginates, remarkably, the gels were shaped as small bullets. Surprisingly, the Young´s modulus and rupture strength of the alginate was low. Finally, the stability of the gel cylinders was tested upon repeating saline treatments and an increasing gel stability was observed in alginate gels with the following structural features: G- and M-blocks (stability increasing with an increasing G-content) < long G-blocks < MG-blocks < saturation with the high affinity ion Ba^{2+}.

This thesis demonstrates that the physical properties of alginate can be highly designed to meet specific application requirements. Both the data from the work, and a developed guide from a literature study, ensures it.

List of abbreviations

Ascophyllum nodosum	*A. nod.*
Azotobacter vinelandii	*A. vinelandii*
Ca-G-gels	The Ca^{2+} saturated gel batches formed from AlgE6 epimerized mannuronan (F_G=0,48 (not stirred), F_G =0,48, F_G =0,60, F_G =0,68, F_G =0,85)
DP	Degree of polymerisation
E	Young's modulus
EDTA	Ethylenediaminetetraacetic acid
G	α-L-guluronic acid
G-blocks	Homopolymeric regions of guluronic acid
GDL	D -glucono-δ-lactone
^{1}H-NMR	Hydrogen Nuclear Magnetic Resonance
HPAEC-PAD	High performance anion exchange chromatography with pulsed amperometric detection
M	β-D-mannuronic acid
Macrocystis pyrifera	*M. pyr.*
Mannuronan	Pure polyM alginate (F_M=1), [n]=1548 ml/g
M-blocks	Homopolymeric regions of mannuronic β-D-mannuronic acid
MG-blocks	Alternating sequences of mannuronic- and guluronic acid
MOPS	3(N-morpholino)propanesulfonic acid

MQ	MilliQ-water (ultra pure water)
SF60	*Laminaria hyberborea* stipe, Bl: 54/7422, [η]=980 ml/g, 199,5 kDa, F_G=0.64
TTHA	Triethylene tetraamine hexaacetat

Table of contents

1 Introduction

1.1 Alginate

1.1.1 Source and applications

Alginate is a polysaccharide that is used in numerous of different applications and industrial fields due to its gelling properties and ability to retain water (Moe, Draget, Skjåk-Bræk, & Smidsrød, 1995). Alginate is rather abundant in nature (Moe et al., 1995) and there seem to be no global shortage of it (Ingar Draget, Østgaard, & Smidsrød, 1990). Alginate is mainly occurring as a structural component in marine brown algae (*Phaeophyta*) where it is comprising up to 40% of the dry weight (Moe et al., 1995). Currently, commercial alginates mostly are subtracted from algal sources (Moe et al., 1995). However, bacterial alginates are as well produced by some members of the *Pseudomonas* genera family (Aarstad, 2013). The alginate is secreted from the bacteria and it can form a biofilm that protects against a host immune system (Aarstad, 2013).

Alginate is used in many food products and is generally recognized as safe (GRAS) by the Food and Drug administration in the United states (Dornish, Kaplan, & Skaugrud, 2001). Also, alginate has been used as a matrix in drug delivery systems and is considered to be non-toxic and biodegradable (Aarstad, 2013). Alginate hydrogels are one of the most used materials for immobilization of living cells (Smidsrød, 1990), particularly within the scientific fields of wound healing and tissue engineering due to the gels maintain structural similarity to the extracellular matrices in tissues and readily are customized (Lee & Mooney, 2012). Importantly, alginate gels are stable in physiological conditions, and so far, no alginate-degrading enzymes have been reported in humans (Yrr A Mørch, 2008). There are several examples of when immunoisolation of cells have been successful and the small pores of the alginate gel have prevented the passage of host immune system substances, such as large antibodies, and at the same time allowed free passage of smaller molecules like nutrients, electrolytes and oxygen (Yrr A Mørch, 2008). In the described example it is essential that the

alginate gel is stable over time so the cells can grow and avoid being detected by the host immune system. In other applications, e.g. bone tissue engineering, it is desired to have a dissolving alginate gel so the cells come in direct contact with the host tissue (Aarstad, 2013). Evidently, depending on the application the alginate must be carefully chosen and modified.

1.1.2 Alginate composition

Alginate is a group of unbranched binary anionic co-polymers, consisting of (1 →4)-linked β-D-mannuronic acid (M) and α-L-guluronic acid (G) residues (Figure 1a) (Moe et al., 1995). When the monomer sequence of natural alginates are studied (Smidsrød, 1990) it is clear that the order of monomers differs greatly and depends on the alginates origin. Since there are no ordered pattern for the monomers, the distribution of them along the polymer chain cannot be described by the Bernoullian distribution (Skják-Bræk, Smidsrød, & Larsen, 1986). However, the monomers are organized in blocks of various lengths along the chain (Figure 1b) (Christensena, 2011), with G-blocks consisting of only guluronic acid monomers, M-blocks comprising of only mannuronic acid monomers and MG-blocks consisting of alternating residues. As seen in (Figure 1c), due to the conformational difference of G and M residues the three different types of blocks have a diverse orientation along the alginate peptide. M-blocks are coupled by a diequatorial linkage, which results in a flat structure (Figure 1c top), while G-blocks are connected diaxially (Figure 1c bottom) and shorter than M-blocks. Therefore, G-blocks are less flexible than M-blocks and as illustrated in (Figure 2) the G-blocks are as well stabilized by intramolecular hydrogen bondings. MG-blocks contain both equatorial-axial and axial-equatorial bonds (Figure 1c middle) and due to the opposing degrees of freedom these blocks are more flexible than MM-blocks (Yrr A Mørch, 2008). In conclusion, the inflexibility of the residues increase in the order MG < MM < GG (Smidsrød, Glover, & Whittington, 1973).

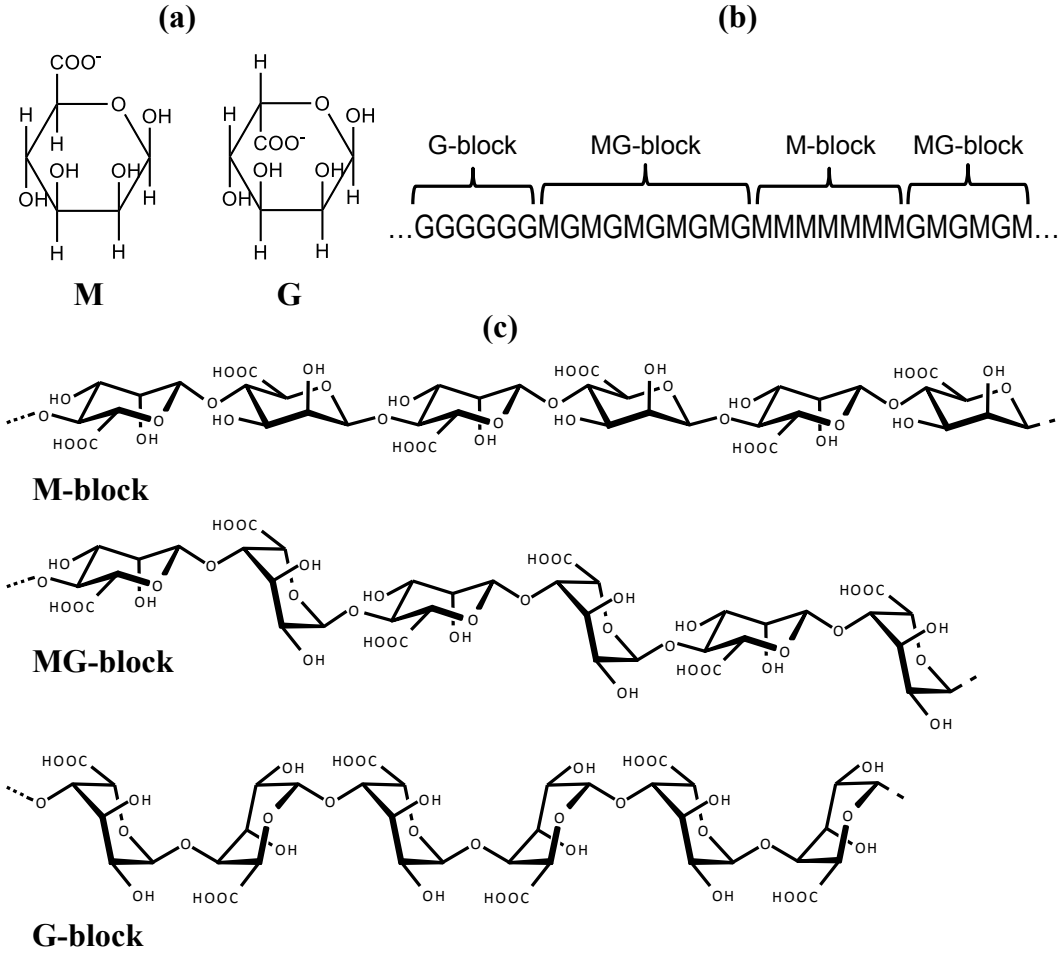

Figure 1. The chemical structure of alginate. a) Illustration of the Haworth formula of the M monomer β-D-mannuronic acid and the G-monomer α-L-guluronic acid. b) Possible block combinations in alginate. c) Ring conformations in M-block (4C1), G-blocks (1C4) and MG-blocks. Ring protons are not shown. Directly reproduced from (Yrr A Mørch, 2008).

1.1.3 Gelling properties

The pK value in alginates is about 3,6, therefore, alginates have a uniformly distributed net negative charge at neutral pH (Simsek-Ege, Bond, & Stringer, 2003). Evidently, alginate is a polyanion and it has been shown that alginate have a preference for divalent cations. In detail, alginate´s affinity toward the following divalent ions has been shown to decrease in the order: Pb > Cu

> Cd > Ba > Sr > Ca > Co, Ni, Zn> Mn (Haug & Smidsrod, 1970). Moreover, it has been reported (Ý. A. Mørch, Donati, Berit, & Skjåk-Bræk, 2006) that Ca^{2+} binds to G- and MG-blocks, Ba^{2+} to G- and M-blocks, and Sr^{2+} to G-blocks. This means that the preference for cations, and thereby gel properties, depend on the block composition of the alginate. Since two G residues are linked diaxially there is a cavity between them (Figure 2) and it has been shown that Ca^{2+} prefers to bind in these junctions.

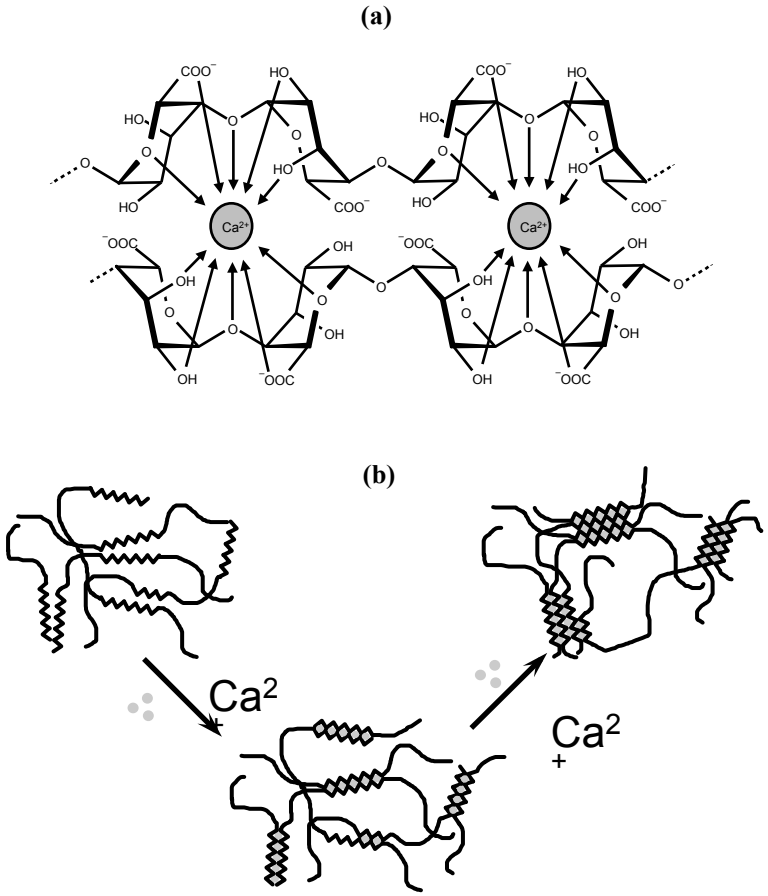

Figure 2. Schematic drawing of the egg-box model. a) Ionic crosslinking of two blocks of G-residues by the egg-box model. b) Lateral association of G-blocks. Directly reproduced from (Yrr A Mørch, 2008).

As illustrated in (Figure 2) each Ca^{2+} interacts with two neighbouring G residues, as well as, with two G residues in an opposing chain, this has been described as "the egg-box model" (Sikorski, Mo, Skjåk-Bræk, & Stokke, 2007). The formed crosslinks are, together with elastic segments, required for a stable gel network. Finally, stable Ca^{2+} gels have been formed from polyalternating alginate, evidently, Ca^{2+} ions can, in addition to GG/GG junctions, bind GG/MG or MG/MG junctions as well (Donati, Mørch, Strand, Skjåk-Bræk, & Paoletti, 2009). As expected, circular dichroism experiments showed in the same article that Ca^{2+} ions had the highest affinity for GG/GG-junctions.

1.1.4 Formation of gels

The internal gelation method (Moe et al., 1995) is used in this work (Figure 3) and it is started by adding calcium in an inactive form, usually as $CaCO_3$. When adding D-(+)-Gluconic acid δ-lactone (GDL) to the solution, it is slowly hydrolyzed to guluronic acid. The acid dissociates and releases protons, which results in a decrease of the pH. The protons react with $CaCO_3$ and release Ca^{2+} homogeneously into the solution. This method usually results in homogeneous distribution of alginate within the gel.

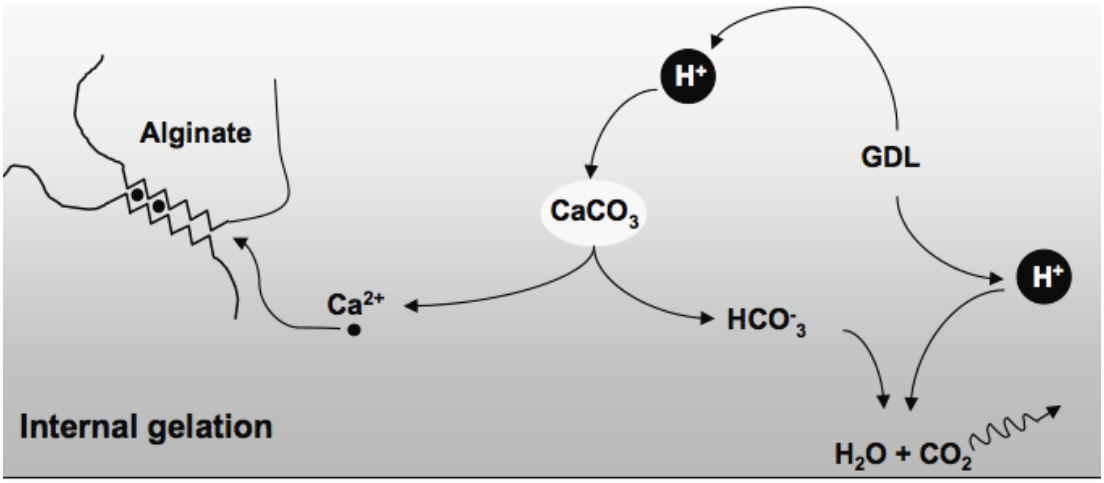

Figure 3. Illustration of the internal gelation method. When GDl is added to the alginate solution protons are released that react with $CaCO_3$. In this way, the release of Ca^{2+} is controlled. Directly reproduced from (Yrr A Mørch, 2008).

1.1.5 Water loss

When an alginate gel is fully compressed water is pressed out and the water amount, as well as the gel structure, varies according to the state of the gel. In this project the water loss after the rupture strength compression studies were documented. By taking the initial gel weight in account the water loss is normalized and the estimation was calculated from the following equation:

$$(1-(Wac/W_0)) * 100 \qquad (1.1)$$

where Wo and Wac are the gel weight before, and after, the rupture strength compression studies, respectively.

1.2 Mannuronan C-5 epimerases

Epimerization is a process where an epimer is re-configured into its chiral counterpart. During the epimerization in alginates, carbon 5 of D-mannuronic acid (M) is re-arranged into the epimer L-guluronic acid (G). Specifically, the most stable conformation for the M monomer is the $^4C_1$, however, during epimerization the hexapyranose ring is re-arranged into the inverted $^1C4$ conformation (Figure 1a). The epimerization of carbohydrates is catalyzed by enzymes known as epimerases and in this work C-5 epimerases are used to alter alginate chains and thereby the physical properties. In the genome of the bacteria *Azotobacter vinelandii (A. vinelandii)* there are at least seven distinctive mannuronan C-5 epimerases and these are denoted AlgE1-AlgE7 (Ertesvåg, Høidal, Schjerven, Svanem, & Valla, 1999). The C-5 epimerases used in this work were expressed in *Escherichia coli* (*E.coli*) and studies have reported of the successful use of C-5 epimerases expressed in *E.coli* (Campa et al., 2004; Ertesvåg, Doseth, Larsen, Skjåk-Bræk, & Valla, 1994; Ertesvåg et al., 1999; Holtan, Bruheim, & Skjak-Braek, 2006).

1.2.1 Epimerization pattern of C-5 epimerases

The epimerization patterns of the C-5 epimerases AlgE1-AlgE7 vary. Six of them introduce a combination of continuous stretches of G blocks and alternating blocks while AlgE4 strictly introduce alternating blocks (Ertesvåg et al., 1999). Ca^{2+} ions are needed for enzyme activity and the optimal concentration varies between AlgE1-AlgE7. AlgE6 introduces long G-blocks and as shown (Figure 2) Ca^{2+} ions bind in junctions that are formed between G-residues, consequently, during the epimerization alginate aggregation can occur. Aggregation is not desired during *in vitro* epimerization, therefore, the non-gelling Na^{+} ion is present in relative high concentration in the reaction buffer. The Na^{+} ions bind to the G-blocks and reduce the non-wanted aggregation. When epimerization is performed with AlgE4 a smaller concentration of Na^{+} ions are used since the enzyme introduces alternating sequences and no long G-blocks. In (Figure 4) the epimerization patterns of AlgE1-AlgE7 are presented and by using one of the enzymes, or performing several epimerizations with a selection of enzymes, the alginate can be modified as preferred. An example of using two C-5 epimerases to modify alginate is presented in (Figure 5).

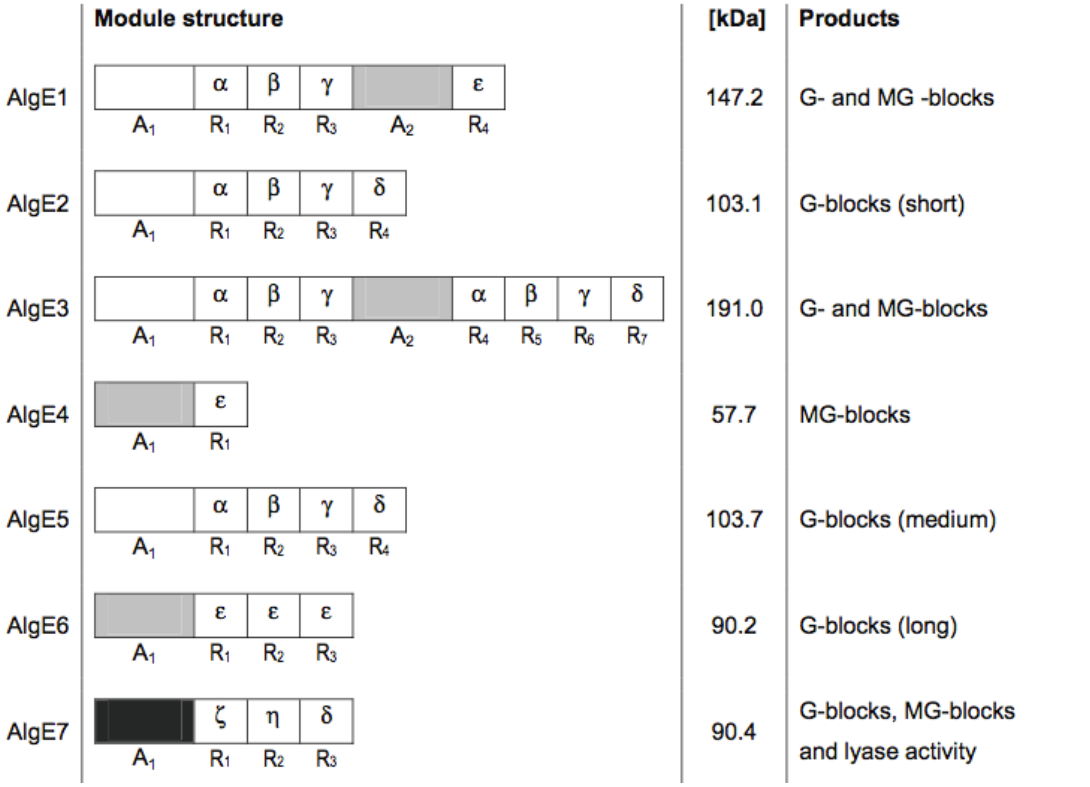

Figure 4. The modular structure, molecular weight and enzyme activities of the extracellular mannuronan C-5 epimerases AlgE1-AlgE7 *from A. vinelandii*. Each mannuronan C-5 epimerase is composed of different numbers of A modules (385 amino acids) and R modules (153 amino acids), designated A1-A2 and R1-R7. Closely related A-modules are indicated with identical shading. Closely related R-modules are indicated with identical Greek letters (α, β, γ , δ ,ε ,ζ ,η). Directly reproduced from (Yrr A Mørch, 2008).

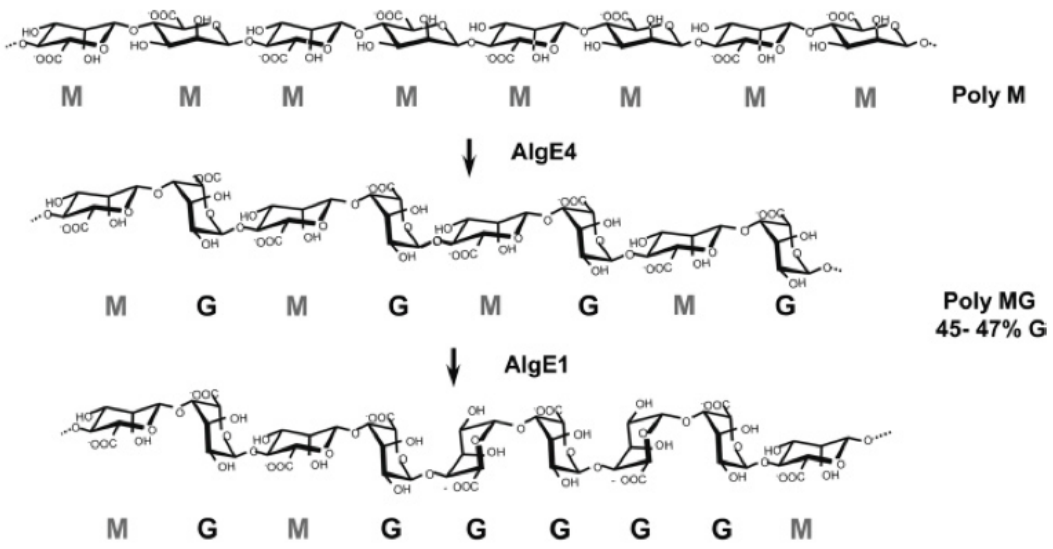

Figure 5. Scheme of the epimerization of mannuronan with two C-5 epimerases to form an alginate containing G blocks and MG blocks solely (no M blocks). The first step using AlgE4 introduces singe G residues, resulting in an alginate with alternating structure (polyMG) containing 45-47% G. The second step, involving AlgE1, introduces G blocks into the alginate chain. Directly reproduced from (Ý. Mørch, Donati, Strand, & Skjåk-Bræk, 2007)**.**

1.2.2 The structure of mannuronan C-5 epimerases

As seen in (Figure 4) AlgE1-AlgE7 are constructed by two types of modules named A and R which consist of 385 and 155 amino acids, respectively. The amino acids of the two modules are highly conserved among AlgE1-7 and closely related sequences are highlighted in fig X. The A module contains the alginate binding site and performs the catalytic activity (Ertesvåg & Valla, 1999) and the R module seems to control the affinity for the substrates (Sletmoen, Skjåk-Bræk, & Stokke, 2005). Finally, both the A and R module bind Ca^{2+} during the epimerization (Ertesvåg & Valla, 1999).

1.3 Structural characterization

1.3.1 ^{1}H-NMR

Nuclear magnetic resonance (NMR) is a commonly used method in biochemistry and organic chemistry to determine the chemical composition and sequence structure of molecules, such as alginates (Grasdalen, Larsen, & Smidsrød, 1979). The method is based on quantum mechanical magnetic properties of atomic nuclei. When a sample is placed in a strong magnetic field the nuclei of the different molecules behave characteristic according to the chemical surrounding. ^{1}H-NMR is used in this work to analyze how protons in the alginate act when irradiated with an electromagnetic pulse. Depending on the protons location, and the nearby monomers, energy at various frequencies are absorbed. These so called differences in chemical shifts are registered and integrated to obtain the average fraction of G and M (F_G and F_M), and of the four diads (F_{MM}, F_{GG} F_{MG}, F_{GM} and) as well as the triads (F_{MMM}, F_{MMG}, F_{GMM}, F_{GGG}, F_{GGM}, F_{MGG}, F_{MGM}, and F_{GMG}) in the polymer (Grasdalen, 1983a).

To determine the molar fractions of the monomers, dimers and trimers the characteristic signals are integrated by using the following relationships (Skják-Bræk et al., 1986):

$$F_G = I_G / I_{total} \quad (1.2)$$

$$F_M = I_M / I_{total} \quad (1.3)$$

$$F_{GG} + F_{GM} = F_G \quad (1.4)$$

$$F_{MM} + F_{MG} = F_M \quad (1.5)$$

$$F_G = F_{GGG} + F_{MGG} + F_{GGM} + F_{MGM} \quad (1.6)$$

$$F_{MG} = F_{GM} = F_{GGM} + F_{MGM} \quad (1.7)$$

$$F_{MGG} = F_{GG} \quad (1.8)$$

When the fractions have been calculated the following equation can be used to determine the average G-block length:

$$N_{G>1} = (F_G - F_{MGM}) / F_{MGG} \quad (1.9)$$

^{1}H-NMR provides average values of the residue lengths and the fractions of monomers, dimers and trimers. By degrading alginate with lyase enzymes and separating and quantifying the peptides by high-performance anion-exchange chromatography with pulsed amperometric detection (HPAEC-PAD) more information of the block structure is acquired.

1.3.2 Alginate lyase degradation

Alginate lyases are enzymes that degrade alginates in a specific way by cleaving glycosidic bonds by a β-elimination mechanism (Wong, Preston, & Schiller, 2000). Alginate lyases with different cleaving patterns have been isolated from several sources such as marine algae and microorganisms(Wong et al., 2000). Depending on these patterns and substrate preferences, alginate lyases are classified as G- or M lyase. G-lyase mostly degrades M-blocks and rarely G blocks in the alginate. However, M-lyase predominantly breaks G blocks but seldom M blocks (Tøndervik et al., 2010). Both groups of lyases can degrade MG blocks, an illustration of the specificity of alginate lyases is presented below in (Figure 6).

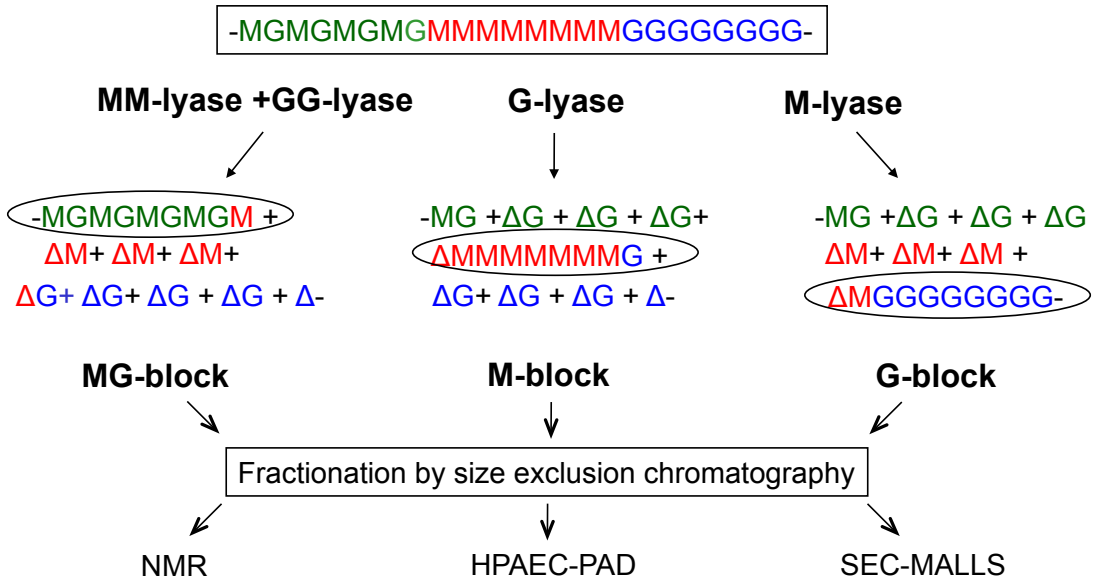

Figure 6. Scheme of the alginate lyase activity. M-lyase leaves the G-blocks intact, while G-lyase is unable to degrade M-blocks. NMR, HPAEC-PAD and SEC-MALLS can determine the block structure of the obtained polymers. Directly reproduced from (Aarstad, Tøndervik, Sletta, & Skjåk-Bræk, 2011).

Due to the high specificity of alginate lyases articles have been able to present comprehensive descriptions of the epimerization patterns of the mannuronan C-5 epimerases AlgE1 and AlgE6 (Holtan et al., 2006) as well as AlgE4 (Campa et al., 2004).

1.3.3 HPAEC-PAD

High performance anion exchange chromatography with pulsed amperiometric detection (HPAEC-PAD) is a chromatography method used for analysis of mono and oligosaccharides (Aarstad, 2013). Carbohydrates are weakly acidic and by using a strong anion-exchange stationary phase they can be separated according to their composition and length (Dionex, 2004). After the separation the peptides are detected by a PAD detector that detects carbohydrates down to approximately 10 picomoles without requiring derivatization (Dionex, 2004). By measuring the electrical current generated by the oxidation of oligosaccharides, which is proportional to the concentration, at the surface of a gold electrode the oligosaccharides are detected (Aarstad, 2013). HPAEC-PAD is very selective for oligosaccharides, since pulsed amperometry only detects compounds that contain functional groups that are oxidizable at the used detection voltage (Dionex, 2004). After the oxidation reaction the surface must be cleaned before the next measurement can start and this is done by regulating the electrode potential(Dionex, 2004). The sequence of potential changes are denoted as a waveform and pulsed amperometry is based on the repeated use of a waveform (Dionex, 2004). To perform a quantitative analysis of alginate digests, standards must be used to determine the detector-response factors for G- and M-peptides as a function of peptide length (Aarstad, 2013). Finally, the discussed method generates chromatograms of the separated oligosaccharides. By outlining baselines in the chromatograms the peaks can be integrated. For each peak, the area is given as retention-time (min) x signal (nC).

1.3.4 SEC-MALLS

Size exclusion chromatography - multi-angle laser light scattering (SEC-MALLS) is commonly used to determine the molecular weight and size (root mean square radius) of larger macromolecules such as polysaccharides. A sample is first processed in a size-exclusion column where the larger molecules are eluted out first. In this way, the weight range of the individual samples is obtained, as well as the relative disparity between the samples. The molecular weight and size can be determined independently of the elution position since the light scattering and concentration are measured for each eluting fraction(Technology, 2013).

Alginates are polydisperse with respect to molecular weight, therefore, the molecular weight is a mean value of the complete distribution of molecular masses (Aarstad, 2013). The molecular weight is defined as

$$M_W = \frac{\sum_i c_i M_i}{\sum_i c_i} \qquad (1.10)$$

where c_i is the weight concentration [g/l], and M_i is the molecular weight .

1.4 Correlations between structural and physical properties of alginate

An alginate gel contains large amount of water and is a continuous polymer network where the peptides are bound by non-covalent crosslinks. The physical properties of alginate gels are highly dependent on the structure and in this part the relationships between the structural and physical properties of alginates and alginate gels are presented and discussed.

1.4.1 Syneresis

Alginate gels are formed in wells and during the formation process the sizes of the gels are reduced due to release of water. This volume decrease, or shrinkage, is defined as syneresis and results in an increased alginate concentration (Ý. Mørch et al., 2007).

In this work syneresis was determined as the weight reduction of the gel cylinders with respect to the initial weight, assuming no significant change in density during the gel formation process. Syneresis was calculated from the equation below:

$$(1- (W/W_0)) * 100 \qquad (1.11)$$

where W_0 is the initial weight at the start of the gel formation process and W is the weight before the compression measurement during the gel rheology study.

The formation of junctions (Figure 2) during the gel formation is an equilibrium process and syneresis is a measure of how rapid and how much they are restructured (Kurt I. Draget et al., 2000).

1.4.1.1 Factors leading to increased syneresis

Short G-blocks are less able, compared to longer G-blocks, to form strong permanent junctions that obstruct the reformation of the network structure, therefore, alginate gels with short G-blocks shrink more during gel formation (Kurt Ingar Draget et al., 2001).

Alginates with a high composition of M-sequences undergo syneresis more increasingly than G-rich alginates upon gelation with calcium ions (Moe et al., 1995).

Studies where alginates from different origins have been epimerized with AlgE4, in order to establish and elongate MG-blocks, have concluded that the introduced MG-sequences lead to higher syneresis (Kurt Ingar Draget et al., 2001; Kurt I. Draget et al., 2000; Ý A Mørch, Holtan, Donati, Strand, & Skjåk-Bræk, 2008; Strand, Mørch, Syvertsen, Espevik, & Skjåk‐Bræk, 2003). The mechanism behind has been suggested to be due to the more flexible elastic segments (the introduced MG-blocks) that allow a denser packing of the alginate chains (Kurt Ingar Draget et al., 2001).Moreover, the formation of MG/MG junctions by a "zipping" mechanism can lead to gel collapsing in MG-block rich sections that ultimately results in higher syneresis (Donati et al., 2005; Donati et al., 2009).

During the gel formation process there are several factors that affect the final syneresis level. It has been shown that up to an extent a longer gelling time (Martinsen, Skjåk‐Bræk, & Smidsrød, 1989), as well as an increasing molecular weight (Kurt Ingar Draget et al., 2001), results in higher syneresis. Additionally, the amount of Ca^{2+} ions in the environment around the gel during gel formation affects the syneresis. In the studies (Donati et al., 2009; Ý A Mørch et al., 2008) gels were prepared from alginates of different source and the calcium saturated gels had significantly higher degree of syneresis than the non-saturated cylinders. Furthermore, studies (Kong, Lee, & Mooney, 2003; Martinsen et al., 1989; Saitoh, Araki, Kon, Katsura, & Taira, 2000) have shown that the syneresis increase for alginate gels that are put in increasing concentrations of Ca^{2+}. These results are partly due to that the Ca^{2+} saturation of the G-blocks leads to a denser packing of the polymer chains. Non-saturated cylinders have less crosslinks and a weaker gel network which leads to lower syneresis.

1.4.1.2 Factors leading to reduced syneresis

Long G-blocks in alginate gels seem to lower the extent of syneresis. In a recent study (Aarstad, 2013) long G-blocks (G> 98%, DP>100) from dialysed *L. hyp.,* stipe were added to mannuronan, which had been epimerized with AlgE6 (F_G=0,51), to give an alginate with the total G-content F_G=0,67. The addition of long G-blocks resulted in gels that experienced significantly lower syneresis compared to two control gels of mannuronan that had been epimerized with AlgE6. The first control was the original alginate (F_G=0,51) and the second was an alginate with a similar total G-content (F_G=0,68) as the alginate where long G-blocks had been added. Finally, the addition of the long G-blocks lowered the syneresis to a similar level as the natural alginate *L. hyp.,* stipe.

In the study (Saitoh et al., 2000) swollen alginate samples were immersed in various types of solutions of different concentrations and gels immersed in solutions containing K^+, KCl or K_2SO_4 swelled as a result.

1.4.2 Swelling and stability measurements

Ca^{2+} is one of the most used ions in the formation of alginate gels, however, these gels are vulnerable toward chelating compounds, like phosphate and citrate, and non-inducing gel agents such as magnesium and sodium ions (Ý. A. Mørch et al., 2006). The latter ion is used in this work to examine the stability of the alginate gels by putting them in saline solution (50mM NaCl) and documenting the swelling behaviour. There are mainly two explanations behind the swelling. Firstly, Ca^{2+} can be replaced with other cations and if these are non-gel inducing ions, such as Na^+ or Mg^{2+}, the result is a weaker gel network (Smidsrød, 1990). Secondly, due to the higher concentration of Na^+ water will flow into the gel which causes osmotic swelling (Thu et al., 1996). Depending on the application stable or swelling properties of the gels are desired or not. If alginate is to be used for immunoisolation, or immobilization, stable gels are wanted since swelling leads to enlarged porosity and no control over the pore size (Yrr A Mørch, 2008). Ultimately, these events can lead to a rupture of the gel that triggers the receiver's immune system to a rejection reaction against the uncovered transplanted cells.

Calcium alginate gels swell under physiological conditions depending on the composition and sequential structure of the polymer (Martinsen et al., 1989) and some of these factors are presented below.

1.4.2.1 Factors to achieve less stable alginates

In the literature there are examples of that Ca^{2+} saturated alginate gels, with a low G-content, swell more than alginates with a high G-content, when treated with saline solution (Martinsen et al., 1989; Strand, Mørch, Syvertsen, et al., 2003; Thu et al., 1996). Partly, this is due to the exchange of ions, in an alginate with few G-blocks, affects a higher part of the total G-blocks, which leads to increased swelling.

1.4.2.2 Factors to achieve more stable alginates

Studies have shown that the introduction and elongation of alternating blocks by AlgE4 epimerization in natural alginates results in more stable alginate gels (Donati et al., 2009) and alginate capsules (Strand, Mørch, Syvertsen, et al., 2003). This could be due to that the alternating blocks makes the gel network more dense and the effect is that more crosslinks are formed (Yrr A Mørch, 2008). Moreover, Ca^{2+} can bind to the MG-blocks (Donati et al., 2005) and this further stabilizes the gel.

Alginates have different affinity toward divalent ions and by replacing the commonly used Ca^{2+} as gel formation ion with stronger binding ions such as Sr^{2+} or Ba^{2+}, the stability of the gels increase (Ý. A. Mørch et al., 2006; Thu et al., 1996).

Polyanion-polycation complex membranes can be used to stabilize alginate gels against swelling. The polycations work by discharging the alginate network and lowering the number of osmotic active counter ions (Thu et al., 1996). One of the most tried polycations is poly-l-lysine (PLL) and when it binds to alginate it forms a polyanion-polycation complex membrane. The membrane reduces the pore area of the gels, in this way, it works as an immune protective barrier (King et al., 2003). Lately, the polyanion poly-l-ornithine (PLO) has shown excellent resistance to swelling and damage

under osmotic stress (Tam et al., 2011) and thiolated polymers, which form disulphide bonds, (George & Abraham, 2006) have been used to improve the stability of alginate gels (Bernkop-Schnürch, Kast, & Richter, 2001). Nevertheless, one should be aware of that polypetides such as PLL is toxic to many cell lines (Strand et al., 2001). Furthermore, PLL can activate an immune response, including macrophages (Vandenbossche et al., 1993) and the complement pathway (Darquy, Pueyo, Capron, & Reach, 1994), which may result in fibrotic overgrowth (Darquy et al., 1994; Strand et al., 2001; Vandenbossche et al., 1993) . Conclusively, to improve the biocompatibility the use of PLL in transplantation procedures should be limited (Strand et al., 2001).

1.4.3 Young´s modulus

The strength of alginate gels are commonly measured by their Young´s modulus and it is a constant (E) that is obtained by compressing a gel in one direction (Yrr A Mørch, 2008). This is done in a texture analyser, where a force (F) is applied to the gel and the resultant compression (ΔL) is registered.

As the force is steadily amplified, a plot of stress/strain =F/A versus compression (ΔL/L) is obtained, an illustration of this is presented below (Figure 7).

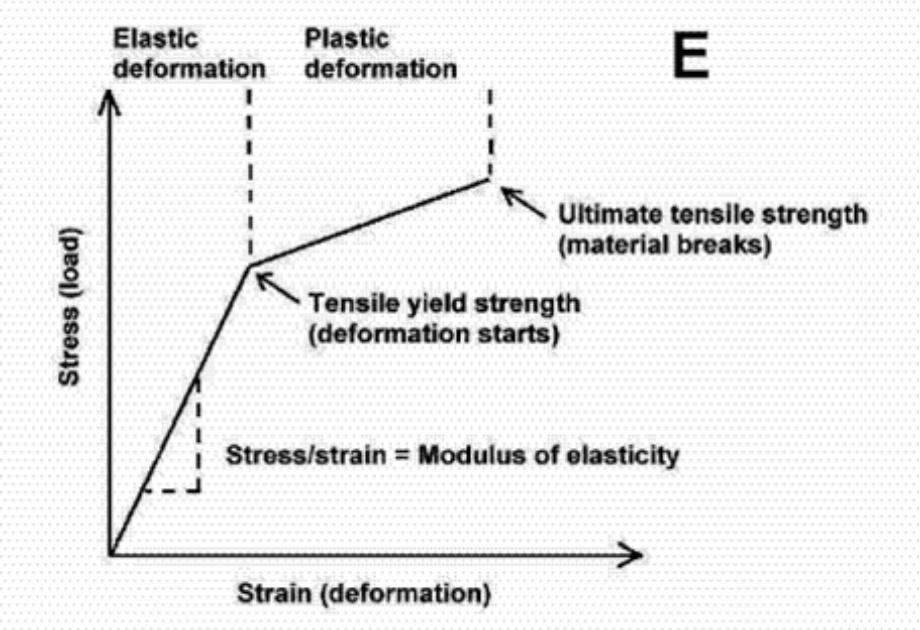

Figure 7. Illustration of how Young´s modulus is determined (Sandoval, 2010).

Young's modulus is decided from the compression of gel cylinders and is calculated from the initial slope in the elastic region of the force/deformation curve (Smidsrød, Haug, & Lian, 1972) by using the following equation:

$$F/A = E \times (\Delta l / l) \qquad (1.12)$$

where F is the forced used to compress the cylinder with a contact surface A and (Δl/ l) is the fraction of the compression length and total length. The physical quantity of E is pressure, commonly measured in the unit Pa.

As Young´s modulus is a measure of gel strength it highly depends on the quantity and strength of the crosslinks, and additionally, the flexibility of the crosslinks (Moe et al., 1995). Moreover, syneresis, which results in higher alginate concentrations due to the loss of water, must be considered when the gel strength is compared between alginate gels since $E = k \cdot C^2_{alginate}$ (Martinsen et al., 1989). Conclusively, several elements affect the gel strength and it is demonstrated below how various key factors - such as

molecular weight, block composition and type of ion used for gelation - makes gels stronger and weaker, respectively.

1.4.3.1 Increased Young´s modulus

In calcium gels G-blocks are ion binding, so, alginates with high G-content have increased ion binding and in this way more crosslinks are formed and the result are stronger gels (Ý. A. Mørch et al., 2006). In addition, longer G-blocks lead to stronger junctions and mechanical properties (Ingar Draget et al., 1990; Moe et al., 1995; Skják-Bræk et al., 1986). This trend has been explained to be due to the connection of long G-blocks and the reduction of elastic segments (Yrr A Mørch, 2008).

In a recent study (Aarstad, 2013) gels were formed from AlgE6 epimerized polyM, as well as, from the natural alginate *L. hyp.,* stipe. The natural alginate had a similar G-content as one of the epimerized gels, however, the NMR data revealed that its average G-block length was somewhat shorter compared to the epimerized alginate. Even though the average G-block length of the epimerized gels were longer and their molecular weights were higher, the Young´s modulus of the gels from *L. hyp.,* stipe were 2,5 and 5 times higher compared to the epimerized gels. However, HPAEC-PAD experiments revealed that the *L.hyp*., consisted of some very long G-blocks that were not present in the epimerized alginates. Taken together, the experiments suggested that very prolonged G-blocks, which are found in several natural alginates (Aarstad et al., 2011), form gels with high Young´s modulus.

The gel strength increases slightly when alternating sequences are introduced in natural alginates (Donati et al., 2005; Ý A Mørch et al., 2008). One explanation to this is that alternating sequences can form optimal crosslinks between less extended chains (Kurt I. Draget et al., 2000). Yet, in the study (Ý A Mørch et al., 2008) where G-blocks were inserted by AlgE1 or AlgE6 in an alginate mostly consisting of alternating blocks (F_{MG}=F_{GM}=F_{MGM}=0,46) it was showed that the Young´s modulus was relatively small for gels prepared from the alternating alginate compared to the gels prepared from alginate where G-blocks had been introduced. So, it

is important to keep in mind that a high content of alternating blocks in an alginate do not necessarily guarantee a strong gel.

Young´s modulus depends on the kind of divalent ion used for gelation since the gel strength increases with the attraction between the alginate chain and the crosslinking ion (Haug & Smidsrod, 1970). Furthermore, it has been shown that the minimum length of G blocks required for junction formation reduces with increasing affinity of ions toward the alginate polymer and this can result in a higher density of stable crosslinks in the gel network (Bjørn T. Stokke, Smidsrød, Zanetti, Strand, & Skjåk-Bræk, 1993). In conclusion, an increase in mechanical strength due to ion affinity could either be a result from more stable junctions, a higher number of crosslinks or a combination of the two (Smidsrød, 1974). Nevertheless, it should be noted that no proof for the mechanism or mechanisms have been presented yet (Moe et al., 1995).

Young´s modulus increases up to a certain molecular weight and then becomes constant. Studies have reported that the Young´s modulus of Ca^{2+} saturated alginate gels increases for molecular weights up to around 100 kDa (K. Draget, Simensen, Onsøyen, & Smidsrød, 1993) or 240 kDa in Ca^{2+} saturated beads (Martinsen et al., 1989). However, Young´s modulus for Ca^{2+} limited gels increased with increasing molecular weight up to 320-340 kD (K. Draget et al., 1993), meaning that Ca-limited gels are more molecular weight sensitive than Ca^{2+} saturated gels. Ultimately, the gel strength of Ca^{2+} alginate gels with equal polymer concentration and with molecular weight above a certain threshold depends only on the average G-block length of the polymer (Smidsrød & Haug, 1972).

1.4.3.2 Decreased Young´s modulus

Alginate wit a high content of M-blocks form weaker gels (Kurt I. Draget et al., 2000; Skjåk-Bræk et al., 1986). Additionally, alginates with a low molecular weight (K. Draget et al., 1993; Martinsen et al., 1989) and short average G-blocks (Ingar Draget et al., 1990; Moe et al., 1995; Skjåk-Bræk et al., 1986) form gels with low Young´s modulus. Finally, less strong alginate gels are formed by using divalent gelling ions that have weak binding

affinity for alginate, for instance Mg^{2+}, which have a lower or equal affinity to G-, M and MG-blocks, compared to Ca^{2+} (Smidsrød, 1974).

1.4.4 Elasticity and rupture strength

The force needed to rupture a gel reflects the gel behaviour at large deformation and this property is an important factor in applications where alginate gels are used to immobilize cells, for example in bone tissue engineering (Aarstad, 2013). Also, the differentiation of stem cells is highly dependent on the elasticity of a material (Huebsch et al., 2010). Obviously, the elasticity and rupture strength of alginate gels are important in tissue engineering applications and as will be presented, the same structural features of the alginate, in general, affect the two physical properties.

When a force is applied to a gel the crosslink that is under the highest stress, usually the shortest one, breaks first and the released energy rushes the rupture of neighbouring junctions in a chain-reaction manner(Zhang, Daubert, & Allen Foegeding, 2007). Furthermore, stiff and short polymers between crosslinks will transmit more energy to the junctions that as well accelerates the rupture (Ý A Mørch et al., 2008). The described process indicates that the rupture strength is related to the number and length of junctions in the network, and one could suspect that a gel with a high Young´s modulus also posses a high rupture strength. Nevertheless, this is not always the case and one explanation to this is that the two properties in different ways depend on the main molecular weight of the alginate polymer from which the gel is created (Mitchell, 1980). In the following section structural features of alginates are presented that affect the elasticity and rupture strength.

1.4.4.1 Increased elasticity and rupture strength

Commonly, alginate gels that are rich in M-blocks appear to be softer and more elastic than alginates with a high fraction of G-blocks (Mancini, Moresi, & Rancini, 1999; Mitchell & Blanshard, 1976), additionally, these gels have a high rupture strength (Moe et al., 1995).

Rupture strength, just as Young´s modulus, increases with increasing molecular weight, but does not become constant above a certain threshold value in contrast to Young´s modulus (Moe et al., 1995).

In general, the elasticity and rupture strength is much higher for Ca^{2+} saturated gels compared to Ca^{2+} limited gels (Donati et al., 2009; Klepp-Andersen, 2010; Ý A Mørch et al., 2008) and this is due to the enhanced formation of crosslinks that results in more stable junctions. For example, the report (Klepp-Andersen, 2010) showed that Ca^{2+} saturated SF60 and AlgE6 epimerized mannuronan consistently could be more compressed than the corresponding Ca^{2+} limited gels made from the same alginate. Studies where mannuronan was epimerized with AlgE1 (Aarstad, 2013) or AlgE6 (Klepp-Andersen, 2010) have revealed how the elasticity and rupture strength of Ca^{2+} saturated gels are decreasing with increasing G-content. According to the NMR spectra in the two studies the average length of the G-blocks are almost equal for the gels that had been epimerized to different total G-content, therefore, it is hard to speculate how the average G-length affected the elasticity and rupture strength. Nonetheless, two articles (Donati et al., 2009; Ý A Mørch et al., 2008) have shown that longer average G-lengths, and also higher G-content, seem to lower the elasticity and rupture strength in Ca^{2+} saturated gels. In the article (Donati et al., 2009), where the effect of AlgE4 epimerization was studied in the natural alginates *L.hyp., M. pyr*., and *A.nod.* and also in the article (Ý A Mørch et al., 2008), where polyMG was epimerized with AlgE1 or AlgE6, longer mean G-blocks and higher G-content, generally, lead to lower rupture strengths. Taken together, it seems as higher G-content and longer G-blocks in Ca^{2+} saturated alginates lead to decreased elasticity and rupture strength in some natural alginates as well as epimerized mannuronan.

The presence of flexible MG-blocks affects the elasticity and rupture strength. In the above presented article (Donati et al., 2009) where AlgE4 epimerization was performed in three natural alginates it was shown that the elasticity and rupture strength increased from the epimerization. In another study it (Ý A Mørch et al., 2008) it has been demonstrated that alginate gels with a high content of MG-blocks ($F_{MG,GM}$=0,46) can be compressed by an exceptionally high force before rupture. Nevertheless, an introduction of just a few percent G-blocks leads to a much lower rupture strength, an explanation to this is presented in the next part (Section 1.4.4.2)

1.4.4.2 Decreased elasticity and rupture strength

Alginate gels made of polyMG tend to be elastic and have very high rupture strengths (Ý A Mørch et al., 2008). Yet, it was reported in the same article that an increase of the G-block content, by AlgE1 epimerization, of just two percent resulted in lower rupture strength. Specifically, compared to gels prepared from polyMG the rupture strength was decreased by around 60% and 80% for Ca^{2+} saturated and Ca^{2+} limited gels, correspondingly. A theory behind these observations is that long homogenous MG/MG junctions work as reels in gel networks and are able to spread put on stress by sliding over each other (Donati et al., 2009). The process is dependent of the homogenous MG/MG junctions, therefore, only a few introduced G blocks are enough to terminate the process resulting in lower elasticity and rupture strength.

As mentioned, alginate gels that are formed in Ca^{2+} limited environments are much weaker than Ca^{2+} saturated gels. When it comes to rupture strength, the relationship between chemical and physical properties of Ca^{2+} saturated and limited gels are opposite. For example, in the report (Klepp-Andersen, 2010), where G-blocks were introduced in polyM by AlgE6, an increase in G-content of the Ca^{2+} limited gels resulted in higher rupture strength. As for the previous stated articles (Donati et al., 2009; Ý A Mørch et al., 2008), again, the data showed that longer G-blocks and higher G-content increase the rupture strength. Especially, (Donati et al., 2009) emphasize that longer G-blocks in Ca^{2+} limited gels require higher energy to be disrupted. Additionally, it should be noted that the longest introduced G-blocks in mannuronan by epimerization is around 60 consecutive G-residues (Aarstad, 2013). Still, longer sequences are present in natural alginates, for example in the article (Aarstad et al., 2011) the longest G-blocks of three natural alginates varied between 120-163 residues as detected by SEC-MALLS. Thus, it is important to keep in mind in the discussion above, regarding how the length of the G-blocks affects the rupture strength, in fact is a discussion on “semi-long” G-blocks.

In several studies the elasticity of Ca^{2+} saturated natural alginates were lower and more brittle compared to epimerized mannuronan. In the article (Ý A Mørch et al., 2008) Ca^{2+} saturated gels made from polyM epimerized with AlgE1 or AlgE6 were more elastic than Ca^{2+} saturated gels prepared from

L. hyp.. stipe. Furthermore, in the article (Ý. Mørch et al., 2007) Ca^{2+} saturated gel beads were prepared from AlgE1 epimerized polyMG (AlgE4 epimerized polyM, $F_{MG}=F_{GM}=0,45$) and as well from *L. hyp.* stipe and *M. pyr*. Epimerized gel beads of different epimerization degree were prepared and all of them were more elastic than the two natural alginates. Finally, in the report (Klepp-Andersen, 2010) alginate gels were formed from AlgE6 epimerized polyM as well as SF60. The gels were made in both Ca^{2+} saturated and limited environments and in general the natural alginate had significantly lower elastic behaviour in relation to the epimerized gels.

In a study (Aarstad, 2013) were long G-blocks (DP> 100) extracted from dialysed *L.hyp.,* lysate and added to mannuronan that had been epimerized with AlgE6. Alginate gels were prepared and when gels with the added long blocks were compared to gels with an alike G-content, it was evident that that the long G-blocks lowered the rupture strength. Furthermore, rupture strength increases by the molecular weight (Moe et al., 1995) and even though the molecular weight of the epimerized mannuronan was higher than the natural control, *L. hyp.,* the epimerized gel had a lower rupture strength relative to *L. hyp.,*. Again, it was clear that long G-blocks in Ca^{2+} saturated gels lowered the rupture strength.

1.4.5 Overview of correlations between structural and physical properties of alginate gels

The presented and discussed correlations between the structural and physical properties of alginates have been summarized and are presented below in (Table 1). As seen, there are many factors that affect the properties of alginate gels and the most important block features are marked in dark while the less important are marked in grey. Finally, the table presents trends and due to the complexity of forming alginate gels it should only be used as a guide, there are no absolute guarantees that the desired property will be achieved by following it.

Table 1. Correlations between structural features of alginates and physical properties of alginate gels. The dark areas mark important block structure features that are necessary to obtain the desired physical property. The grey areas mark block structure features that are less important to obtain alginate gels with the sought gel property. White/not marked areas represent block features that the alginate should not have in order to acquire the desired gel property.

	Structure property					
Physical property	**High content of G-blocks**	**High content of short G-blocks**	**High content of long G-blocks**	**High content of M-block**	**High content of MG-blocks**	**Other**
High syneresis						Longer gelling time Increases with an increasing molecular weight Ca^{2+} saturated alginates have higher degree of syneresis than alginates formed in Ca^{2+} limited environment
High Young´s modulus						Increases up to a certain molecular weight Use gelation ion with higher affinity for the blocks Ca^{2+} saturated alginates stronger than alginates formed in Ca^{2+} limited environment
High rupture strength and elasticity						The rupture strength increases with an increasing molecular weight The rupture strength and elasticity is higher Ca^{2+} saturated alginates have higer elasticity and rupture strength than alginates formed in Ca^{2+} limited enviroments In Ca^{2+} saturated alginates less and shorter G-blocks lead to increased rupture strength and elasticity
Stable dimensional properties						Use gelation ion with higher affinity for the blocks Polyanion-polycation complex membranes can be used to stabilize alginate gels against swelling

1.5 Study aims

The aim of this project was to study physical properties of AlgE6 epimerized alginates. Mannuronan was used as start material and was epimerized with AlgE6 to five different epimerization degrees. In addition, a fraction of one AlgE6 sample was further epimerized with AlgE4, to compare the physical properties of alginates having G- and M-blocks solely with an alginate consisting of MG- and G-blocks. A control alginate consisting of a high content of MG-blocks and short G-blocks was made. This was done by first performing a full AlgE4 epimerization in mannuronan to create an alginate mostly consisting of MG-blocks. Finally, an epimerization with AlgE6 was performed to introduce G-blocks. Moreover, alginate from *L.hyp.,* stipe (SF60) was used as reference.

To be able to compare the physical properties of the alginates Ca^{2+} alginate gel cylinders were prepared by internal gelling. All alginates were then saturated in 50 mM $CaCl_2$ except for one of the AlgE6 epimerized mannuronan alginates that was saturated in 20 mM $BaCl_2$ and 30 mM $CaCl_2$. This was done to examine the effect of Ba^{2+} ions in a gel network rich of M and G-blocks. Syneresis was determined as weight reduction with respect to the initial weight, before compression measurements were performed by using a texture analyzer. From the deformation compression measurements, Young's modulus, elasticity, rupture strength and normalized water release were determined. Finally, the stability of the saturated gel cylinders was tested upon saline treatments (0.15 M NaCl). To examine the extreme effects of gel stability the saline solution was gently stirred during the treatments. Importantly, two gel batches were treated in saline solution that was not stirred, hence, the effect of the saline treatment was milder. To study this effect more carefully two alginate batches of SF60 were prepared where one was treated in stirred saline solution, while the other was treated in saline solution that was not stirred.

2 Experimental

The mannuronan used in the following experiments came from an epimerase-negative mutant (Alg^-) of *Pseudomonas fluorescens* (Nova Matrix, batch [512-216-01TP], August 2007). The intrinsic viscosity of the mannuronan was [η] =1548 ml/g and F_M=1. The alginate had to be purified before further use. SF60, an alginate sample from the stipe of *L.hyp.* (F_G=0.64) was used as a comparison of the enzymatically modified alginates to natural occurring alginates.

2.1 Purification of alginate

5 g mannuronan was dissolved in 500 ml MQ-water (devoiced and filtrated) to achieve an alginate concentration of 1 % (w/v). 1.5 g sodium chloride was mixed in 250 ml MQ water before adding it to the alginate solution, to avoid formation of aggregates. For precipitation of alginate, a similar volume (750 ml) of ethanol was added while stirring with a glass rod. The alginate solution was filtrated (Schleicher & Schuell, Microscience) using a water jet pump. Washing was performed three times with 70% ethanol and two times with 96% ethanol to remove water and salts before the alginate was dried over night. The weight of the dry alginate was measured, following addition of MQ water to dissolve the alginate once again, to 0.25%. The alginate was filtrated through a 25 µm Grade 113(Whatman, Glass Microfibre filters) followed by
2,7 GF/D filter (Whatman, Glass Microfibre filters) followed by 1.6 µm GF/A filter (Whatman, Glass Microfibre filters) using a water jet pump. The solution was freeze-dried on a vacuum freeze-dryer (Edwards RV12) for 24-48 hours.

2.2 C-5 epimerization of alginate

2.2.1 AlgE6 epimerization

Purified mannuronan was used as a start material to produce five alginate samples with various G-contents. An AlgE6 enzyme (dissolved) from recombinant *E.coli* (SINTEF) was used in the epimerization reaction. The mannuronan was epimerized with the enzyme:alginate ratio 1:100 and the epimerization times are presented in (Table 2).

Purified alginates were dissolved in MQ water on a magnetic stirrer at room temperature. A concentrated stock solution of MOPS buffer (pH 6.9) was added, giving the solutions a final concentration of 0.25% (w/v) alginate, 50 mM MOPS, 2.5 mM $CaCl_2$ and 10 mM NaCl. The mixtures were pre-heated at 37°C for at least two hours. The AlgE6 enzyme immediately added to the pre-heated solutions, before incubating the solutions at 37°C for on a magnetic stirrer. The epimerization reactions were terminated by removal of calcium with addition of EDTA stock of 0.1M, to 4 mM in the final solution. As stated in (Section 2.2.2) the alginate solutions then were put in a warm water bath for 13-15 min so that the temperature was at least 85°C for 10 min. The temperature never was higher than 88°C. Immediately after the water bath the alginate solutions were put in cold water to cool the solution. To purify the alginates, the solutions were dialyzed against 0.05M NaCl (three shifts of 7L), followed by dialysis against MQ water (7L) until the conductivities were below 2 µS. The alginate solution was filtrated through a 25 µm Grade 113(Whatman, Glass Microfibre filters). pH were adjusted to 7,0 with 1 M NaOH, before freeze-drying the samples.

Concentrated stock solution of buffer:

- 200 mM MOPS
- 10 mM $CaCl_2$ 300
- 300 mM NaCl

The pH of the buffer was adjusted with 5 M NaOH to 6.9.

2.2.2 Examination of the possible re-activation of AlgE6 & AlgE4 epimerization of AlgE6 epimerized polyM

One of the goals of this project was to examine how the physical properties of an alginate gel mostly composed of G and M-blocks was affected by an introduction of alternating blocks by AlgE4 epimerization. In the work (Klepp-Andersen, 2010) this had been tried by first introducing G-blocks in polyM followed by an AlgE4 epimerization. However, after the AlgE4 epimerization the total G-content had increased comprehensively while the alternating blocks only had increased by a few percent. To examine this result and see if AlgE4 could epimerize polyM, which had been epimerized with AlgE6, an experiment in the beginning of the project was performed. In the experiment polyM was first epimerized with AlgE6 and the alginate was

then divided into three samples. The first sample was just the alginate from the first reaction, the second sample was incubated in reaction buffer to see whether AlgE6 could be reactivated and the last sample was incubated with AlgE4. In detail, first 50 mg polyM was epimerized in an enzyme to alginate ratio of 1:150 for 42 hours under magnetic stirring in 37 ° C. The reaction was ended by adding 0,1M EDTA (pH=7,00) to a final concentration of 4 mM. After dialysis against 50 mM NaCl followed by dialysis against MQ water the alginate was freeze-dried and divided into three samples. The first sample was not processed further and was denoted 0. One of the alginate samples, denoted 1, then was AlgE4 epimerized in an enzyme to alginate ratio of 1:150 for 47 hours under magnetic stirring in 37 °C while the other sample, denoted 2, was incubated in just reaction buffer without addition of AlgE4. For the epimerization reactions the same buffer (pH=6,90) was used and the final concentrations were 50mM MOPS, 2,5 mM $CaCl_2$ and 50 mM NaCl. As seen in (Section 3.2.1) AlgE6 was re-activated and it was decided to try to use a warm water bath (95°C) to denature AlgE6 after the epimerization reaction. The first polyM batch that was epimerized with AlgE6 F_G=0,48 (not stirred), was put in the water bath for 80 min and the temperature was at least 85 for 25 min. It was observed that the molecular weight had decreased comprehensively due to the water bath treatment (Table 2). From these results it was decided that the temperature in the alginate solution should be at least 85°C for 10 min. In general it took about 3 min for the temperature to rise to 85°C (smaller volumes were heated than in the previous described experiment), and so, the alginates were treated between 13-15 min in the water bath. As seen in (Table 2), the molecular weight of the epimerized alginates were alike. To emphasize, all epimerised alginates were treated in the water bath after the first epimerization, even the alginates that were not planned to be incubated with AlgE4, this was done to ensure that all alginates had been handled in the same way.

2.2.3 AlgE4 epimerization

The epimerization with AlgE4, produced recombinant by *Hansinula polymorpha* (Sintef), was performed in the same way as the AlgE6 epimerization, but with a lower concentration of NaCl. The final buffer concentration in the solution was 50 mM MOPS, 2.5 mM $CaCl_2$ and 10 mM NaCl. The AlgE6 epimerized sample with a G-content of 60% was used as substrate for the AlgE4 epimerization. The enzyme:alginate ratio of the AlgE4 epimerization was 1:100. The epimerization time was 48 hours.

When mannuronan was AlgE4 epimerized to form the control alginate polyMG the same reaction conditions were used as when F_G=0,60 was AlgE4 epimerized. The following concentrated buffer was used:

Concentrated stock solution of buffer (pH 6.9):

- 200 mM MOPS
- 10 mM $CaCl_2$
- 40 mM NaCl

2.3 Nuclear magnetic resonance (^{1}H NMR)

The chemical compositions of the epimerized samples were analyzed by ^{1}H-NMR. Before the analyses could be performed the samples were hydrolyzed to reduce the viscosity. By using mild acid hydrolysis the alginates were degraded and consequently the viscosity was reduced.

2.3.1 Preparation of samples; acid hydrolysis

Acid hydrolysis was performed by dissolving 20 mg epimerized alginate in 60 ml MQ. pH was adjusted to 5.6 by adding 0.05 M hydrochloric acid (HCl) and the solution was placed in a water bath holding 95°C for one hour. The solution was rapidly cooled down in cold water and pH was adjusted, this time to 3.8 by adding 0.1 M HCl. The solution was placed in the water bath once again, for 50 minutes at 95°C before it was rapidly cooled down. pH was adjusted to 6.8 by adding 0.5 M NaOH and the alginate was freeze-dried.

2.3.2 ^{1}H-NMR sample

10 mg of degraded alginates was solved in deuterium oxide (D_2O) to prevent disturbing signals from ^{1}H in H_2O. 20 µl (0.3M) triethylene tetraamine hexaacetat (TTHA) and 5 µl (1%) 3-trimethylsilyl propionic acid (TSP) were mixed in to the sample in the eppendorf- tube. TTHA is a chelator that binds divalent cations and was used to prevent the cations of interacting with

the G-blocks. The solutions were mixed well and transferred to a NMR tube. The ^{1}H-NMR spectra were recorded on a Bruker Avance DPX 400 spectrometer at 90°C and a 30° magnetizing angle.

2.4 Analysis of block structure

The five AlgE6 epimerized alginates were separated and characterized by HPAEC-PAD. The technique allows separation of oligo-/polysaccharides according to their chain- length. Chromatograms were produced according to the detector signals as a function of retention time. Relative areas were obtained by integrating the peaks in the chromatograms thus allowing determination of the block structure.

2.4.1 Degradation of alginate with M-lyase and G-lyase

1 mg of each epimerized sample was dissolved in 500 µl MQ water on a shaker at room temperature. 500 µl ammonium-acetate buffer was added, giving the solutions a final concentration of 1 mg/ml alginate, 200 mM ammonium-acetate and 50 mM NaCl. The sample was divided in two parts of equal volume. 160 µl M-lyase from *H. tuberculata* was mixed in to one half and 20 µl G-lyase from *K. Aerogenes* to the other half, following incubation at 30° C temperature for 20 hours. To stop the lyase reaction, the samples were placed in boiling water (100°C) for ten minutes.

Concentrated ammonium-acetate buffer:

- 400 mM Ammonium-acetate
- 100 mM NaCl

2.4.2 HPAEC-PAD analysis

HPAEC-PAD was used to separate and characterize the degraded alginates. The alginate samples were prepared as described in (Section 2.4.1).

Carbonate-free 0.1 M NaOH, diluted from a 50% (w/v) stock solution was used as mobile phase, whilst 1M sodium-acetate in 0.1 M NaOH was used as

eluent. The solutions were degassed with helium and filtrated with a 0.22 µm filter. The analyses were performed with Waveform A.

The alginate samples were injected in a 100 µl loop, with an injection volume of 25 µl to the Ion Pac AS4A column. The elution was performed with a gradient of 0-70% 1M NaAC for 80 minutes. The elution speed was set to 1 ml/min, with a pressure of 550-700 psi. The chromatograms were produced and integrated with the program Chromeleon 6.7.

2.5 SEC-MALLS

As the physical properties of alginates are affected by the molecular weight, it was measured by SEC-MALLS. 2 mg of each epimerized alginate was diluted in 2 ml MQ water and were left in room temperature for 24 hours to dissolve. The samples were processed and analyzed as described in (Aarstad, 2013). The Mark-Houwink-Sakurada equation was used to approximate the intrinsic viscosities of the epimerized alginates from the molecular weight (the intrinsic viscosity of SF60 earlier had been determined by a viscometer) in order to relate the data to other studies. The Mark-Houwink-Sakurada equation is defined as:

$$[\eta] = K * M^{\alpha} \qquad (2.1)$$

where η is the intrinsic viscosity [ml/g], M is the molecular weight [Da], and K and α are constants that depend on the particular polymer-solvent system. Two sets of constant (K, α) were used depending on the G content of the alginate. The constants that were used to estimate the intrinsic viscosity depend on the G-content of the alginate, however, due to the lack of constants for certain G-contents it should be noted that only the intrinsic viscosity of F_G=0,56 (MG) and F_G=0,60 were estimated by using a valid set of constants The constants (K=3,38*10^{-3}, α=1,06) is valid for G-contents of 50-55% and was used to estimate the intrinsic viscosity of F_G=0,48 (both batches) and F_G=0,56 (MG). The other set of constants was (K=1,71*10^{-1}, α=0,71) and it was used to estimate the intrinsic viscosity of F_G=0,60, F_G=0,62 (Ba), F_G=0,68 and F_G=0,85.

2.6 Preparation of gel cylinders

The epimerized alginates, as well as SF60, were used to make gel cylinders for the study of physical properties.

To make gel cylinders (n=8), 375 mg of epimerized alginate was dissolved in 25 ml MQ- water in a 250 ml flask with suction. 56.25 g calcium carbonate ($CaCO_3$) was dissolved in 5 ml MQ-water before it was added to the alginate solution. The mixture was degassed for 20-30 minutes, using vacuum suction to avoid air-bubbles in the cylinders. 200.36 mg D-glucono-δ-lactone (GDL) was mixed quickly in 7.5 ml MQ water and added to the solution. The solution was stirred carefully for 10 seconds to mix the components. The solution was poured into the 8 middle positions, on a 24-well-plate, making a positive meniscus. The lid was put on and the plate was left on a leveled bench for curing for at least 24 hours at room temperature. The well plate had a height of 18 mm and a diameter of 16 mm.

2.6.1 Saturation of Ca^{2+} alginate gels

Ca^{2+} saturated alginate gels were made by homogeneous gelling, as described in section (Section 1.1.4). The cylinders were removed from the 24-well plate and dialyzed against 800 ml of 50mM $CaCl_2$ in 0.2M NaCl for 48 hours at 4°C to saturate all G binding sites with Ca^{2+}. Please note that the alginate F_G=0,62 was saturated in 20 mM $BaCl_2$ 30mM $CaCl_2$ in 0.2M NaCl.

2.7 Physical properties of alginate gels

Weight (before and after compression), height and diameter of alginate gel cylinders were measured, and any characteristics in look or shape of the cylinders were noted before further measurements.

2.7.1 Syneresis

The degree of syneresis of non-saturated- and saturated gel cylinders was determined as weight reduction of the cylinders with respect to the initial weight, assuming a density value of 1. (Section 1.4.1) gives the equation (1.11) used in the calculations of syneresis.

2.7.2 Young's modulus, rupture strength and penetration-to-break

The gel cylinders of were gently dried with clinical wipes, before they were exposed to uniaxial compression to the point of rupture using a Stable Micro Systems TA.XTplus texture analyzer at 22± 1 °C. First was the Young´s modulus measured by with a load cell of 5 kg and a 50 mm diameter flat-ended probe. For the rupture strength measurements the 30 kg load cell was used. The compression speed was set to 0.1 mm/s, both pre- and during testing. Young's modulus (E) was calculated from the initial slope of the force/deformation curve ($F/A = E \times \Delta l / l$) obtained by the computer program "Texture Expert Exponent 32". Rupture strength was also determined by the same program.

2.7.3 Saline treatments of alginate gels

The stability of the alginate gels was measured as swelling in a saline solution. The cylinders (n=5) were kept in 0.15M NaCl at 4°C under gentle stirring for 24, 48, 72 or 96 hours prior to measurement. 20 mL NaCl solution was used per cylinder and the solution was changed every 24 hours. Swelling was determined as weight change since it was difficult to measure the gels when they had swelled.

Weight (before and after compression), height and diameter of the cylinders were measured after each saline treatment, before compression measurements were performed.

3 Results

3.1 Epimerization degree

Mannuronan with a molecular weight of 242 kDa was used as a start material in the epimerization reactions. The enzyme:alginate weight concentration was 1:100 in all epimerization reactions and by varying the incubation time different degrees of G-blocks were introduced and these are presented in (Section 3.2). A part of the sample of the alginate that had a G-content of 60% after the AlgE6 epimerization was incubated with AlgE4 in an attempt to introduce MG-blocks, however, as seen in (Section 3.2) AlgE6 was re-activated and the degree of alternating blocks did not change. Finally, a control alginate rich of G and MG-blocks was prepared by first performing a full epimerization of AlgE4 on mannuronan followed by a second epimerization with AlgE6.

3.2 Nuclear magnetic resonance spectra

To identify the degree of epimerization of the alginates, ^{1}H-NMR analyses were performed. The block composition of the epimerized alginates were calculated from the ^{1}H-NMR spectra, as explained by (Grasdalen, 1983b) and in (Section 1.3.1). A spectra of the AlgE6 epimerized alginates is presented in (Figure 8). A spectra of the control alginate, which was rich G and MG-blocks, and SF60 is seen in (Figure 9). The block composition of all examined alginates in the work are presented in (Table 2). The data used for the calculations is available in (Appendix A).

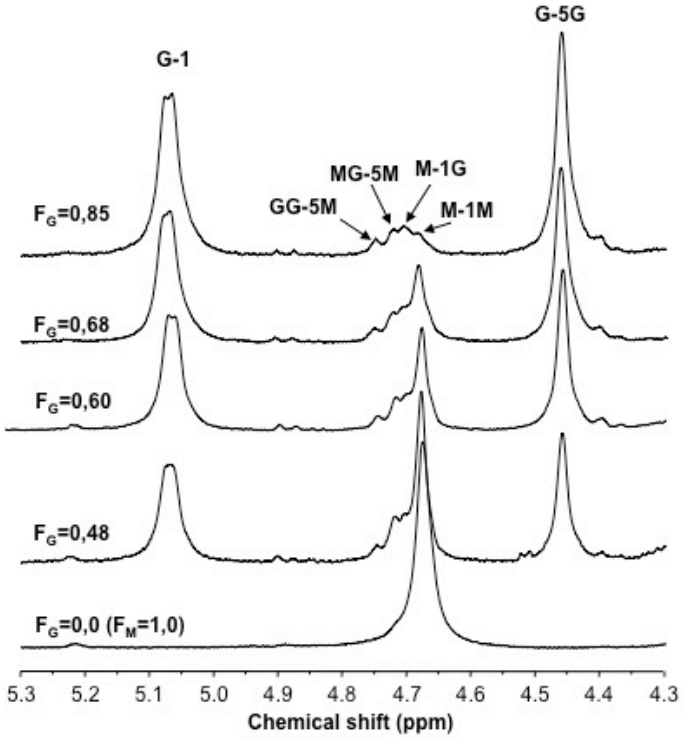

Figure 8. ^{1}H-NMR spectra of the AlgE6 epimerized alginates. The spectrum at the bottom shows a mannuronan sample, and the spectra of the epimerized samples are presented in an increasing order of their total G-content.

(Figure 8) demonstrates the introduction of G–blocks in the alginates, since they were lacking in the mannuronan spectrum before epimerization. The mannuronan spectrum showed very strong signals from the two adjacent M residues (M-1M). After epimerization a significant decrease in the M-residues signal were observed. As the incubation time in the samples increased, the M-block signals decreased correspondingly. Also, the intensity of the signals from the G residues G-1 and G-5G increased as the incubation time was increased. The spectra of the samples clearly showed that the incubation affected the degree of epimerization. Additionally, the rise of the G5-G and GG-5M signals in the spectra proved that AlgE6 introduced G-blocks. In this project there was an attempt to introduce alternating blocks in the alginate F_G=0,60 by epimerization with AlgE4 and

the result was the alginate F_G=0,85. As seen, the signal from the G-blocks G-1 and G-5G clearly increased as compared to F_G=0,60 and there was no increase of MG-5M which reveals presence of alternating sequences. Also, the M-1M signal had considerably decreased. Clearly, AlgE6 had been reactivated and dominated the epimerization over AlgE4 which resulted in an alginate with a significantly higher G-content than the original of F_G=0,60.

In this work a polyalternating alginate was made by performing a full epimerization of mannuronan with AlgE4 to F_G =0,45. This sample then was epimerized with AlgE6 using the same conditions as when the alginate F_G=0,48 (stirred) was prepared. The resulting alginate was F_G=0,56 (MG) and its NMR-spectrum, together with SF60, is shown in (Figure 9).

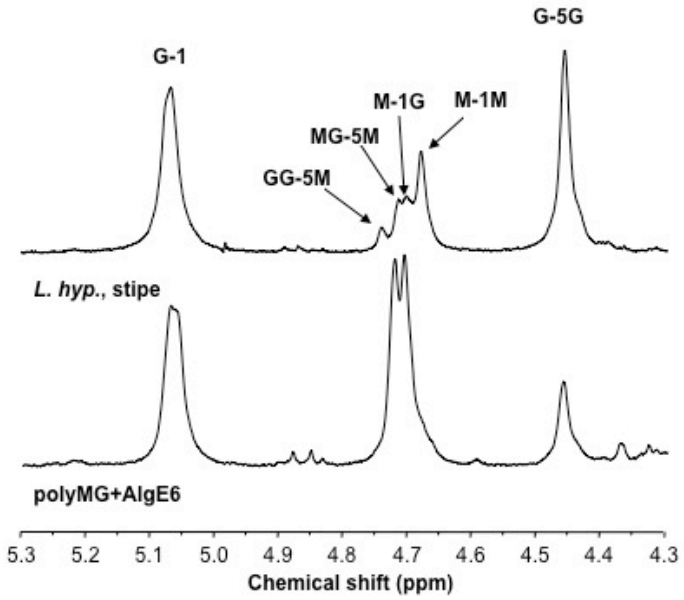

Figure 9. ^{1}H-NMR spectra of *L. hyp.,* stipe (SF60) and F_G=0,56 (MG) made by epimerization of mannuronan with AlgE4 and AlgE6.

As seen in (Figure 9, lower panel) the signal from M-1M was depleted and this was expected since the original polyalternating alginate consisted of about F_{GM}=0,45 and AlgE6 had a restrained time to convert the M-blocks to G-blocks. As expected, there were two signals from MG-5M and M-1G that indicated the presence of alternating blocks in the sample. The spectrum of *L. hyp.,* stipe (from a previous analyze by W. I. Strand) was sharp and there were distinctive signals. The intensity from the G sequences G-1 and G-5G were apparent, clearly, there was a high quantity of G-blocks in the alginate. Also, the M-1M signal was low, obviously, most M-blocks were put in between G-blocks and not next to each other. The signals from M-1G and MG-5M were clear, which showed existence of alternating sequences in the alginate due to AlgE6 had a restrained time to convert the MG-blocks to G-blocks.

Table 2. Description of epimerization process, abbreviation, block composition, molecular weight and estimated intrinsic viscosity of the alginates in this work. * The Mark-Houvink-Sakurada equation was used to approximate the intrinsic viscosities of the epimerized alginates. The intrinsic viscosity of SF60 was measured by a viscometer. * *No gel cylinders were made of PolyMG.

Type of alginate	Epimerization time [hours]	Abbreviation	F_G	F_M	F_{GG}	F_{GM}	F_{MM}	F_{GGM} F_{MGG}	F_{MGM}	F_{GGG}	$N_{G>1}$	M_w [kDa]	η * [ml/g]
PolyM + AlgE6	10,5	F_G=0,48 (not stirred)	0,48	0,52	0,38	0,10	0,42	-	-	-	-	155,0	1073
PolyM + AlgE6	8	F_G=0,48	0,48	0,53	0,38	0,10	0,43	0,03	0,09	0,35	13	242,2	1722
PolyM + AlgE6	15	F_G=0,60	0,60	0,40	0,51	0,09	0,31	0,03	0,08	0,48	18	256,9	1186
PolyM + AlgE6	15	F_G=0,62 (Ba)	0,62	0,38	0,54	0,08	0,30	0,03	0,07	0,52	21	225,3	1080
PolyM + AlgE6	26	F_G=0,68	0,68	0,32	0,61	0,08	0,24	0,03	0,06	0,58	20	226,5	1084
Fg=0,60 + AlgE4	8 + 48	F_G=0,85	0,85	0,15	0,77	0,08	0,07	0,03	0,06	0,74	24	213,7	1040
PolyMG+ AlgE6	8	F_G=0,56 (MG)	0,56	0,44	0,21	0,36	0,08	-	-	-	-	225,6	1598
PolyM + AlgE4	48	PolyMG **	0,45	0,55	-	0,45	0,10	0,00	0,45	-	-	-	-
L. Hyp., stipe	-	SF60	0,64	0,33	0,56	0,11	0,23	0,05	0,08	0,52	13	199,5	980

(Table 2) displays a clear increase in F_G, F_{GG} and F_{GGG} as the incubation time for the epimerization reaction of mannuronan with AlgE6 increased. Also, the average G-block length ($N_{G>1}$) was increasing with a longer incubation time except for F_G=0,68 that had a slightly shorter mean value than F_G=0,62 (Ba). The gel batches that were made from AlgE6 epimerized mannuronan, and which were saturated in Ca^{2+}, were given an abbreviation that corresponds to their total G-content. These gel batches consisted most of G and M-blocks, as can be seen in (Table 2), the content of MG-blocks were alike and between 8% and 10%. In this work gel batches F_G=0,48 (not stirred), F_G=0,48, F_G=0,60, F_G=0,68 and F_G=0,85 were denoted Ca-G-gels while the gel batch that was saturated in 20 mM $BaCl_2$ and 30 mM $CaCl_2$ was denoted F_G=0,62 (Ba). During the stability experiments the saline solution (0,15M NaCl) was stirred for all gel batches except for F_G=0,48 (not stirred) and SF60 (not stirred).

One of the goals of this project was to introduce alternating blocks in a gel rich of G and M-blocks. For this purpose a fraction of the sample F_G=0,60 was incubated with AlgE4, however, as seen when the block composition of

F_G=0,60 and F_G=0,85 are compared, the heating of the sample to 90° C did not not stop AlgE6 from introducing G-blocks and the content of alternating blocks was unchanged. The resulting alginate had the highest amount of G-blocks, as well as, the longest $N_{G>1}$ of the G-blocks.

A control alginate, F_G=0,56 (MG), consisting of a high content of MG-blocks as well as a G-blocks was made. This was achieved by first performing a full epimerization reaction of AlgE4 with polyM to create the alginate polyMG that mostly consisted of MG-blocks (F_{MG}=F_{MGM}=0,45). Finally, an epimerization with AlgE6 was performed to create the alginate. Noticeably, the content of MG-blocks was more than three times higher than in the other alginates. Importantly, the incubation time and reaction conditions of the last epimerization with AlgE6 were equal to when F_G=0,48 was formed from polyM. Thereby, it is possible to examine how the two substrates, polyM and polyMG, affected the activity of AlgE6.

As presented in (Table 2), there were few differences in the molecular weighs of the epimerized alginates except for F_G=0,48 (not stirred) that had a significantly lower molecular weight due to the longer treatment time in the water bath (95° C) after the AlgE6 epimerization. Also, it is noticeable that a longer incubation time during the epimerization seem to have resulted in a somewhat smaller molecular weight for the alginates, as seen for example when F_G=0,48 and F_G=0,85 are compared. As seen in (Table 2) the Mark-Houwink-Sakurada equation (2.1) was used to approximate the intrinsic viscosities of the epimerized alginates, not SF60, in order to relate the data to other studies. The constants that were used to estimate the intrinsic viscosity depend on the G-content of the alginate, however, due to the lack of constants for certain G-contents it should be noted that only the intrinsic viscosity of F_G=0,56 (MG) and F_G=0,60 were estimated by using a valid set of constants (Section 2.5). The viscosities of the examined gels in the work varied between 1000-1200 ml/g, excluding the viscosity of F_G=0,48 (not stirred). Finally, the intrinsic viscosity of SF60 was not estimated in this work since it earlier had been determined by a viscometer.

3.2.1 Examination of the possible re-activation of AlgE6 & AlgE4 epimerization of AlgE6 epimerized polyM

As described in (Section 2.2.2) epimerization reactions were performed to examine whether AlgE4 could introduce alternating blocks in polyM that had been epimerized with AlgE6, here denoted sample 1. Also, by incubating sample 0 in reaction buffer, without adding AlgE4, it was possible to check whether AlgE6 was re-activated. The NMR results from these experiments are presented below in (Table 3).

Table 3. NMR results from the initial experiments where the possible re-activation of AlgE6 was examined. Also, an AlgE4 epimerization of AlgE6 epimerized mannuronan was performed to test whether AlgE4 could introduce alternating block.

Alginate sample	F_G	F_M	F_{GG}	$F_{GM} = F_{MG}$	F_{MM}
0 = polyM + AlgE6	0,11	0,89	0,07	0,05	0,84
1 = sample 0 +AlgE4	0,49	0,51	0,11	0,38	0,14
2 = re-incubation of sample 0	0,16	0,84	0,09	0,07	0,76

As seen in (Table 3) both F_G and F_{GG} in sample 2 were higher than in sample 0. Clearly, the addition of EDTA, dialysis and freeze-drying had not stopped AlgE6 from being re-activated. From these results it was decided to try to denature AlgE6 by putting the AlgE6-epimiezied alginates in a warm water bath (95° C) after the addition of EDTA. Moreover, by comparing the block composition of sample 0 and 1 it is observed that the fractions F_{MG}, F_G and F_{GG} increased significantly when AlgE4 had been added to the epimerization reaction. Evidently, AlgE4 had introduced alternating blocks in the AlgE6 epimerized polyM.

3.2.2 Activity test of AlgE6

Before the full-scale epimerization reactions of AlgE6 had started, an activity test of AlgE6 was performed to examine how the incubation time affected the epimerization degree. In the test was a sample of alginate extracted from the reaction and analyzed by NMR according to the time points in (Table 4). The reaction concentrations and conditions were the same as in the full-scale epimerization, however, the amount of epimerized mannuronan and enzyme was far less. In a control the same amount of mannuronan was epimerized for 24 hours with the double amount of enzyme and it represented a positive control. The results from the experiments are presented below in (Table 4) and (Figure 10).

Table 4. Activity test of AlgE6 with mannuronan as substrate. The enzyme:mannuronan weight concentration was 1:100 in the activity test and the corresponding concentration was 1:50 in the control.

Incubation time [hour(s)]	Enzyme activity [epimerization degree/ time unit]	F_G	F_M	F_{GG}	F_{GM} F_{MG}	F_{MM}
Activity test (E:A = 1:100)						
1	0,08	0,08	0,92	0,04	0,04	0,88
2	0,01	0,09	0,91	0,04	0,05	0,86
3	0,05	0,14	0,86	0,08	0,06	0,79
5	0,10	0,34	0,66	0,24	0,10	0,57
8	0,03	0,42	0,58	0,36	0,05	0,53
24	0,02	0,69	0,31	0,58	0,11	0,20
Control (E:A = 1:50)						
24	0,03	0,71	0,29	0,62	0,10	0,19

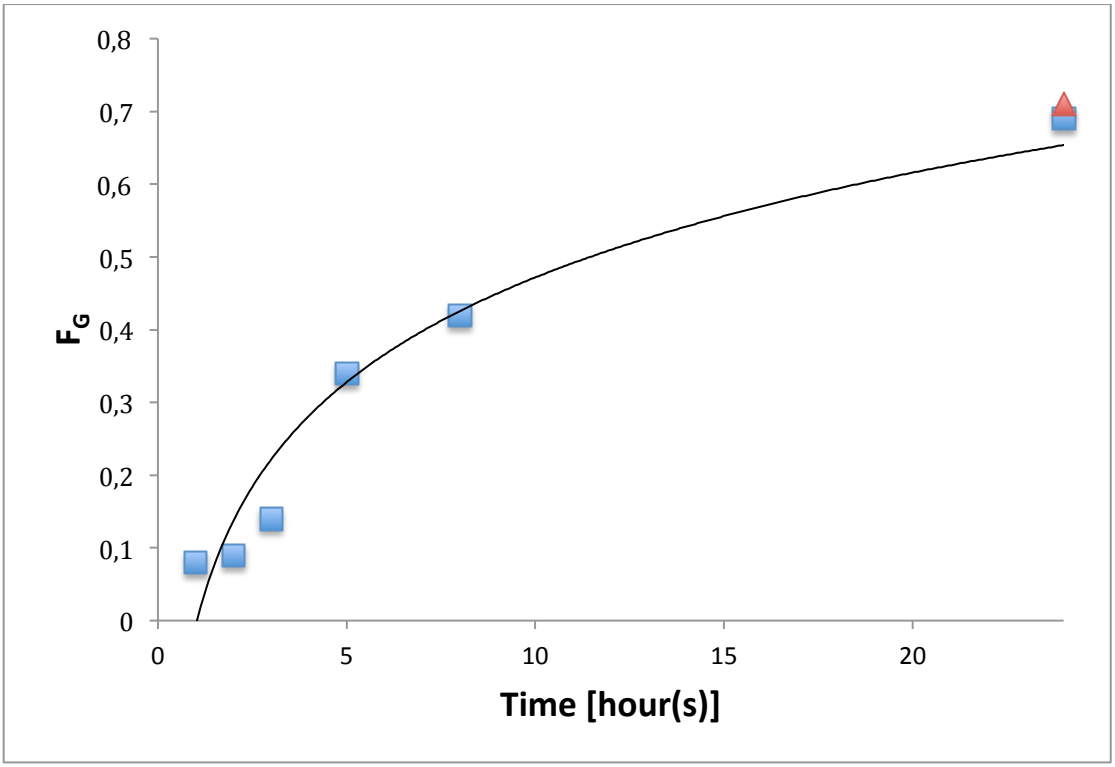

Figure 10. Activity test of AlgE6 with mannuronan as substrate. The blue squares are the activity test and the red triangle is the control. The enzyme:mannuronan weight concentration was 1:100 and corresponding concentration was 1:50 in the control. The line is drawn to guide the eye.

As seen, the enzyme was more efficient during the first hour compared to the second. However, between the third and fifth hour the activity increased again. Since there were only one data point after 8 hours the monitored activity was not as accurate as in the beginning, however, it is clear that the activity decreased as the reaction proceeded. The final epimerization degree of the control and the activity test was alike, hence, the concentration difference did not affect the epimerization degree after 24 hours.

3.3 Block structure analysis

To be able to study the block distribution of the alginates in more detail, they were degraded with M- and G-lyase, leaving G-blocks and M-blocks intact respectively, before analyzing the polymers by HPAEC-PAD. HPAEC-PAD is a chromatography technique used for separation of carbohydrates according to chain-length. (Figure 11) presents the polymers retention time for M-lyase degraded alginates.

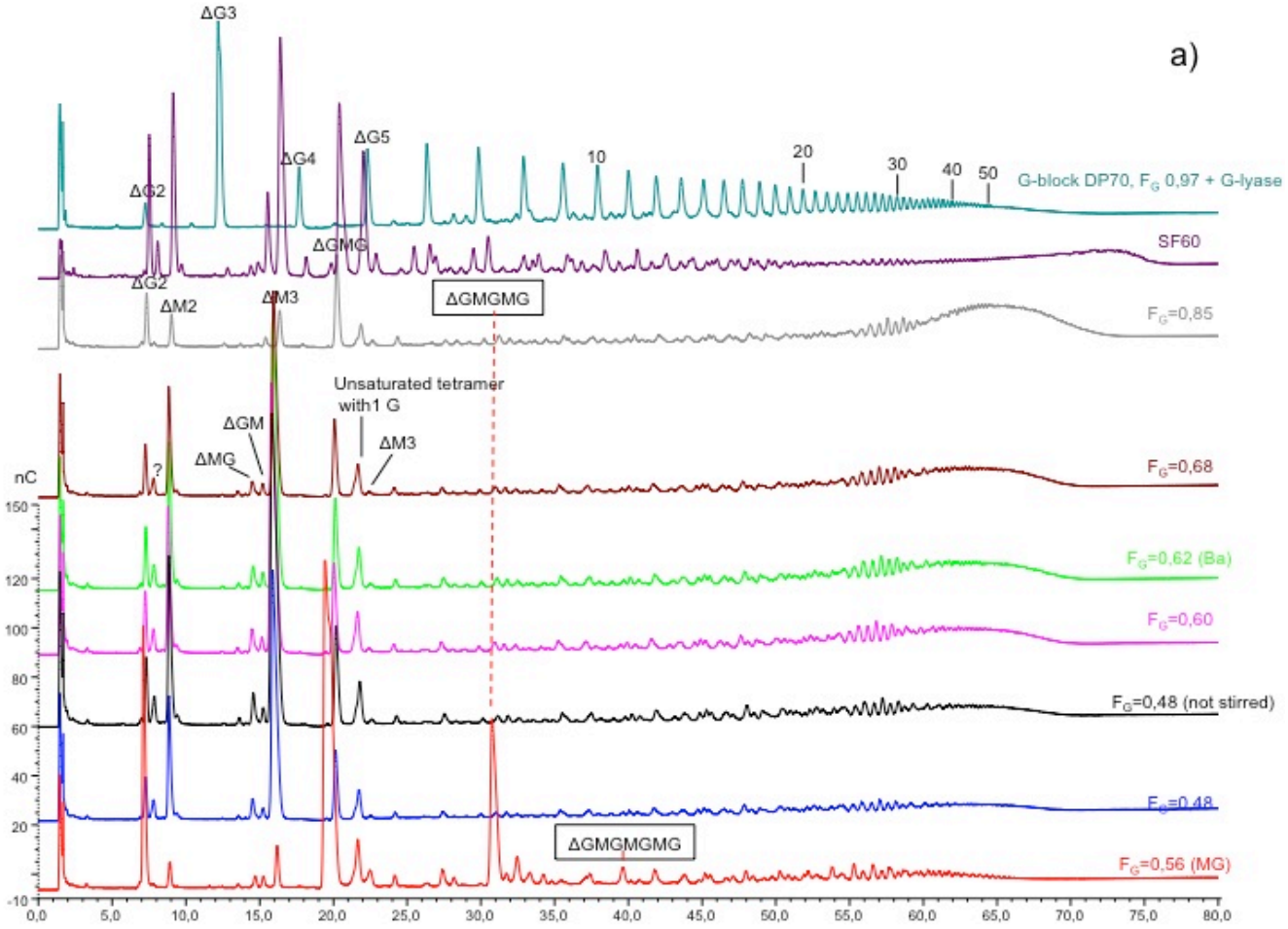

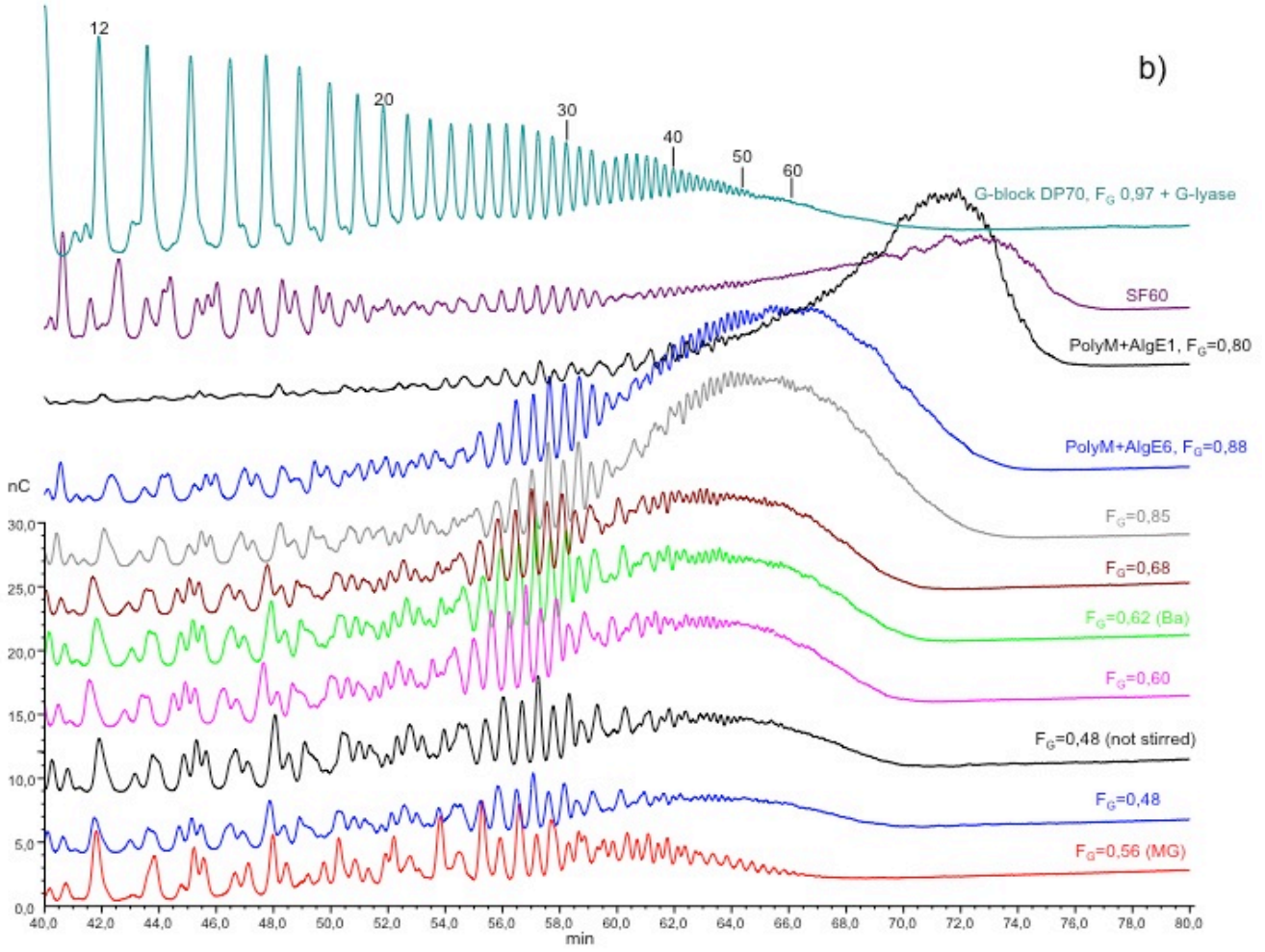

Figure 11. HPAEC-PAD chromatograms. a) HPAEC-PAD chromatograms of the epimerized alginates, SF60 and the reference alginates G-block DP70 F_G=0,97 (degraded with G-lyase), polyM+AlgE1 F_G=0,80 and polyM+AlgE6 F_G=0,88. All alginates were degraded with M-lyase except for the reference G-block DP70 F_G=0,97. The numbers above the reference alginate G-block DP70 corresponds to the DP. b) The same chromatograms as in a), during the retention times 40-80 min.

The chromatogram of SF60 and the reference alginates G-block DP70 (degraded with G-lyase) are from previous analyses (Aarstad et al., 2011) by O.A Aarstad. Each peak in the chromatograms, in (Figure 11), corresponds to a polymer with a specific chain-length. The shortest polymers have the lowest retention time and are eluted first. The first peak in the

chromatograms is salt, and is neglected in the analysis. The second peak represents the amount of G-block monomers (DP=1) and the third peak corresponds to the amount of G-block dimers (DP=2) and so on. As the chain-length increases, the polymers have longer retention times.

As (Figure 11) demonstrates, the chromatograms of the epimerized alginates were very alike up to the retention time 58 min. After this retention time, the oscillation pattern started to decrease while height of the chromatograms increased, especially for the alginates with a relative high G-content. This chromatogram shape was due to the difficulties of separating the longer polymers and as a result it was hard to know exactly how long the longest G-blocks were. Nevertheless, a qualitative analyze can be performed to compare the G-block distributions among the alginates. In addition, the reference G-block DP70 (F_G=0,97) can be used to more easily identify the chain-lengths.

As seen in (Figure 11), the height and length during the higher retention times in the chromatogram of F_G=0,56 (MG) was relative short and the alginate had the shortest G-blocks of all examined alginates. As expected, the two chromatograms of the alginates with a G-content of 48% were alike and there were longer G-blocks present than in F_G=0,56 (MG). Likewise, the chromatograms of F_G=0,60 and F_G=0,62 (Ba) were comparable, clearly, they consisted of longer G-blocks compared to the alginates with smaller G-contents. The chromatograms of F_G=0,68 implies that it consisted of somewhat longer G-blocks than F_G=0,60 and F_G=0,62 (Ba). Outstandingly, the high G alginate F_G=0,85 evidently contained longer G-blocks than the other epimerized alginates and it seems as a relative high part of the total G-blocks were longer compared to the other epimerized alginates. The chromatogram of the reference alginate (polyM + AlgE6, F_G=0,88) was very similar to the one of F_G=0,85 and the two alginates had a similar G-content. Interestingly, despite the somewhat lower G-content of the reference alginate (polyM + AlgE1, F_G=0,80) compared to F_G=0,85, undoubtedly, it contained the longest G-blocks of all examined epimerized alginates. In conclusion, among the AlgE6-epimierzed mannuronan alginates it was evident that a higher G-content lead to a G-distribution where a greater part of the blocks were longer. Lastly, the chromatogram of SF60 revealed that it contained G-blocks that were comprehensively longer than the ones present in the epimerized alginates. Since the area of the last part of the chromatogram, where the oscillations were small and the curve rose, was far

higher compared to the other alginates it seems as a great part of the G-blocks were comparatively long.

To analyse the G-block structure of the alginates more carefully, each peak in the chromatograms (given in Appendix B) were integrated and the relative areas (%) were calculated. The relative areas (%) of the oligosaccharides with DP ≤10, DP=11-20, DP=21-30, DP=31-40, DP=41-50 and DP>50 were summarized, and are presented in (Figure 12).

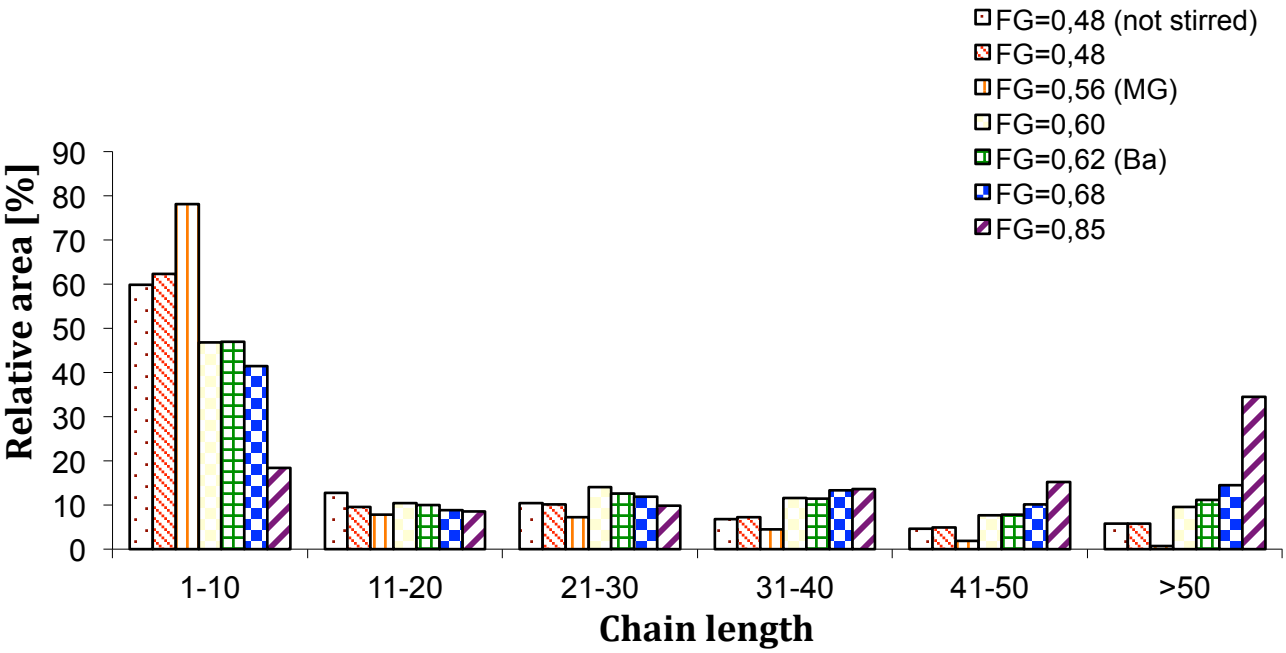

Figure 12. G-block distributions. The summarized relative areas [%] of the peaks in the chromatograms of the M-lyase degraded epimerized alginates. It is only possible to compare an individual G-block distribution and not the distributions among the alginates.

Importantly, due to different signal strength during the HPAEC-PAD analysis of the alginates it is only possible to compare an individual G-block distribution and not the distributions among the alginates. (Figure 12) confirms several of the findings from the chromatograms of the M-lyase degraded alginates (Figure 11). The G-block composition of F_G=0,48 and F_G=0,48 (not stirred) was similar and a majority of the G-blocks were not longer than 10 sequences. Furthermore, they contained some medium long G-blocks, although, the content of G-blocks over 30 residues was low. The G-block distribution of F_G=0,60, F_G=0,62 (Ba) and F_G=0,68 were alike and the majority of the G-blocks were less or equal to 20 sequences long. About 10% of the G-blocks were longer or equal to 50 residues. The average G-block length in F_G=0,85 was high, about half of the G-blocks were 40 residues or longer, specifically, around 34% of the G-blocks were at least 50 residues long. Finally, almost 90% of the G-blocks in F_G=0,56 (MG) were smaller or equal to 20 residues. A few percent of the blocks were between 30 and 40 sequences long, however, barely any of them were longer than 40 residues. Taken together, the data imply that amount of long G-blocks increased as the total G-content increased in AlgE6 epimerized mannuronan.

The epimerized alginates were also degraded with G-lyase, leaving the M-blocks complete, and the degraded polymers were analyzed by HPAEC-PAD. (Figure 13) shows the polymers retention time for G-lyase degraded samples.

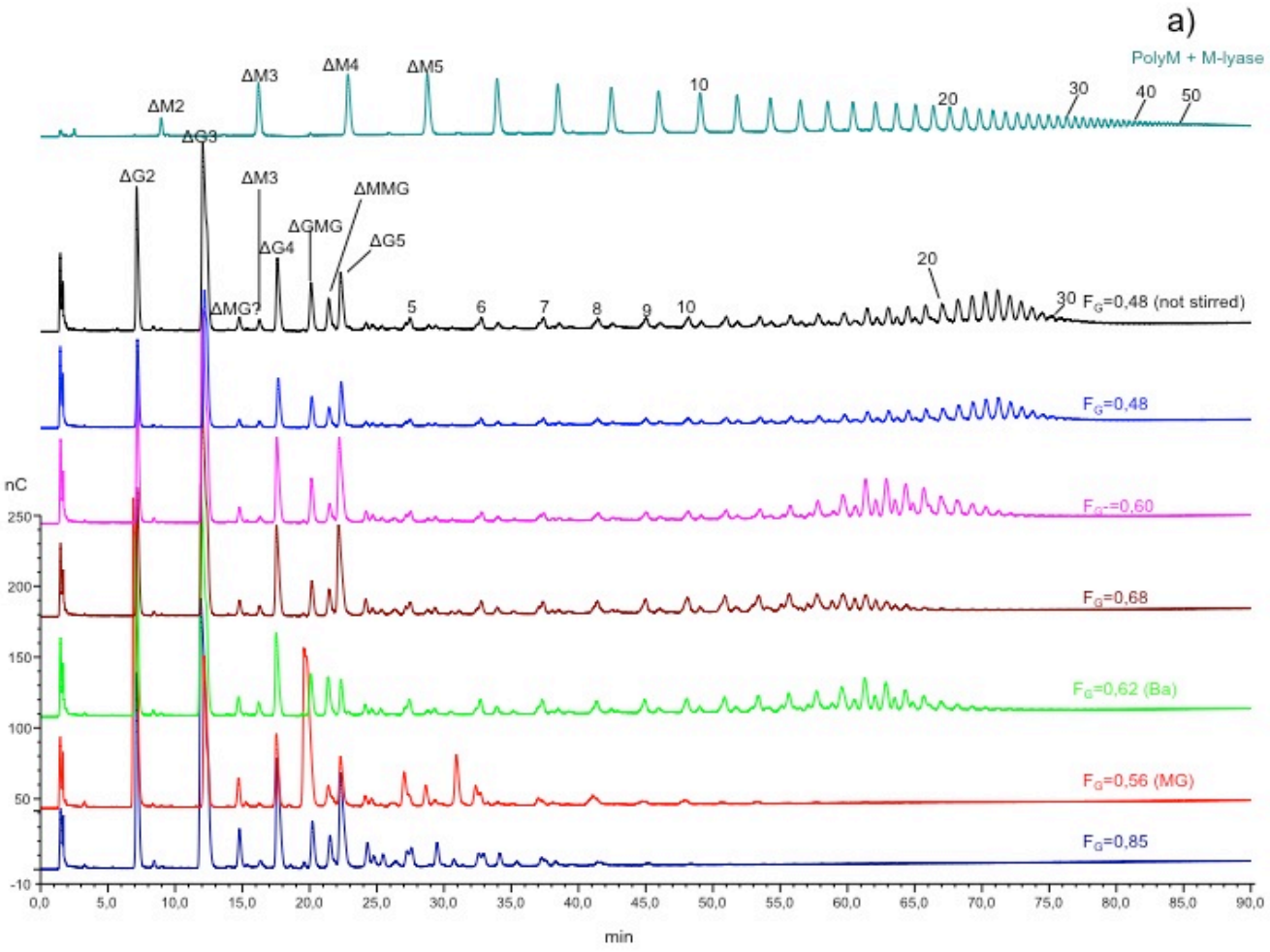
a)
PolyM + M-lyase
ΔM2
ΔG3
ΔM3
ΔM4
ΔM5
10
20
30
40
50
ΔG2
ΔM3
ΔMMG
ΔGMG
ΔG4
ΔG5
ΔMG?
5
6
7
8
9
10
20
30
F_G=0,48 (not stirred)
F_G=0,48
F_G=0,60
F_G=0,68
F_G=0,62 (Ba)
F_G=0,56 (MG)
F_G=0,85
nC
250
200
150
100
50
-10
0,0
5,0
10,0
15,0
20,0
25,0
30,0
35,0
40,0
45,0
50,0
55,0
60,0
65,0
70,0
75,0
80,0
85,0
90,0
min

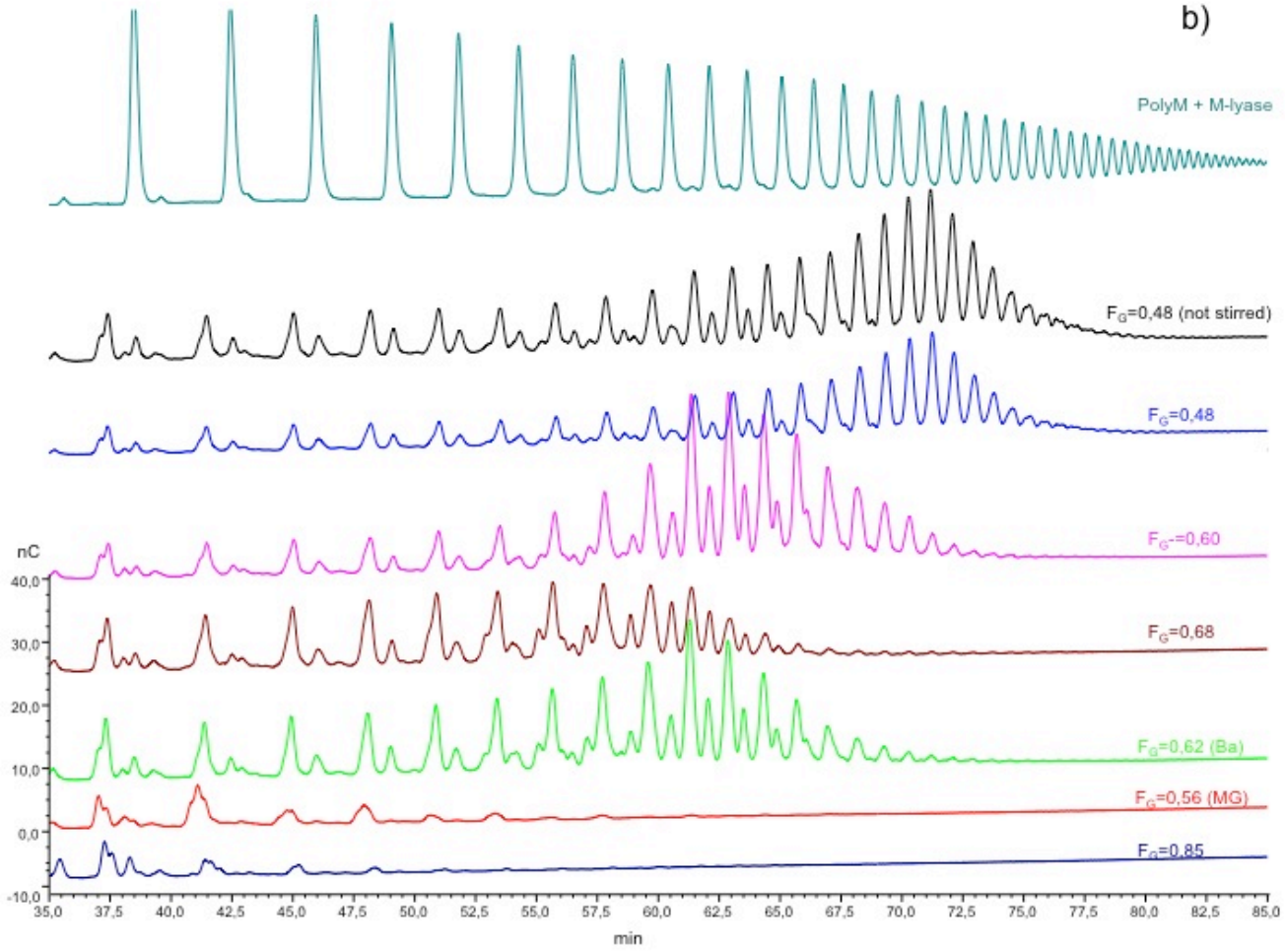

Figure 13. HPAEC-PAD chromatograms. a) HPAEC-PAD chromatograms of the epimerized alginates degraded with G-lyase, and the reference alginate polyM degraded with M-lyase. The numbers above polyM corresponds to the DP. b) The same chromatograms as in a) during the retention times 35-85 min.

The chromatogram of the reference alginate polyM (degraded with G-lyase) is from a previous analyze (Aarstad et al., 2011) by O.A Aarstad. Generally, G-lyase is not as specific as M-lyase and proves of this was seen in the chromatograms of polyM and F_G=0,48 (not stirred). In the chromatograms

were ΔM-blocks identified and as seen in (Section 1.3.2) these blocks normally are formed from a digestion-reaction by G-lyase. G-lyase can splint MG and MM-blocks to some extent and a consequence of this non-specificity is that the real M-block distribution is slightly longer than the presented by the chromatograms.

The oligomers that are marked by numbers are most likely unsaturated M-oligomers with a chain-length corresponding to the number. One end of the polymer is reduced, e.g. 5=ΔMMMG.

The chromatograms of F_G=0,85 and F_G=0,56 (MG), presented in (Figure 13), reveals that the two alginates lacked the long M-blocks that were present in the other alginates. As expected, the two chromatograms of F_G=0,60 and F_G=0,62 (Ba) were alike and after 72 min no significant signals were registered. The longest M-blocks of F_G=0,68 appeared to be shorter than the ones of F_G=0,60 and F_G=0,62 (Ba) since the last recorded signal occurred at 65 min. Unsurprisingly, the chromatograms of the both alginates with a G-content of 48% were similar and it was evident that these alginates contained the longest M-blocks. As seen, there was an obvious correlation between the G-content and length distribution of the M-blocks: the higher G-content, the shorter M-sequences.

To analyze the M-block structure of the oligosaccharides more carefully, each peak in the chromatograms (given in Appendix B) were integrated and the relative areas (%) were calculated. The relative areas (%) of the oligosaccharides with DP ≤10, DP=11-20, DP=21-30, DP=31-40, DP=41-50 and DP>50 were summarized, and are presented in (Figure 14).

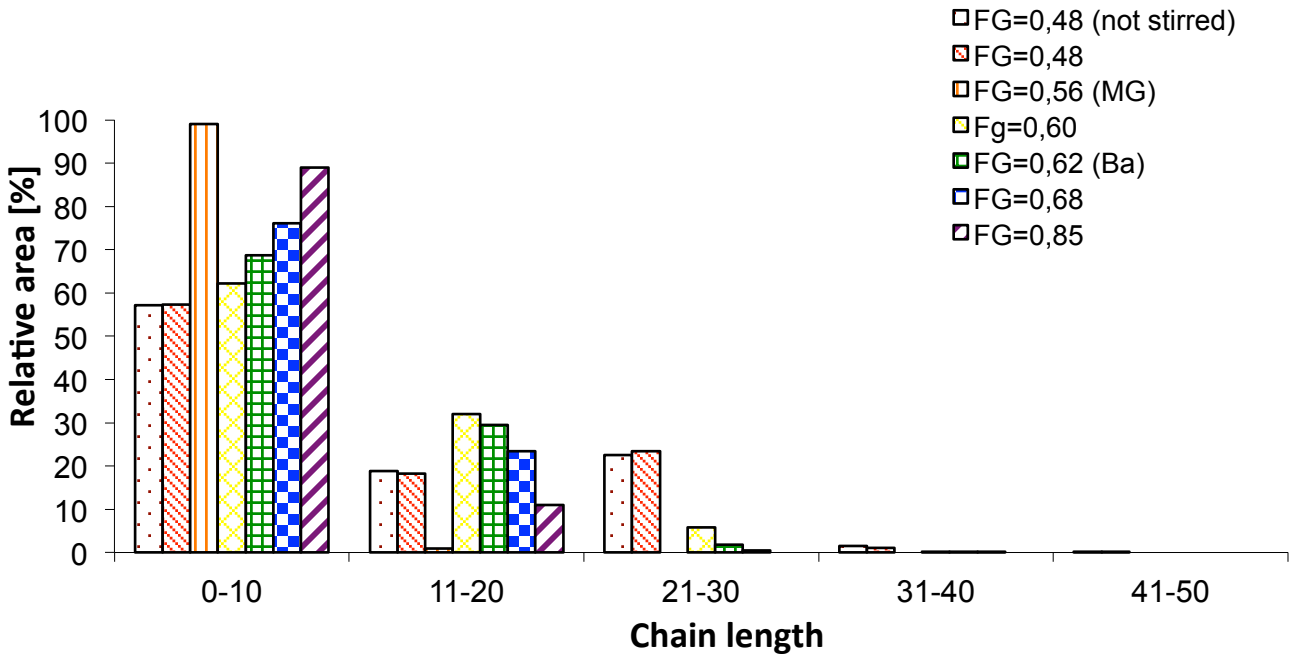

Figure 14. M-block distributions. The summarized relative areas [%] of the peaks in the chromatograms of the G-lyase degraded epimerized alginates. It is only possible to compare an individual G-block distribution and not the distributions among the alginates.

(Figure 14) shows that a majority of the M-blocks in the epimerized alginates were shorter or equal to ten residues. The M-distribution of the two alginates with a G-content of 48% was alike. Noticeably, in the two alginates the amount of M-residues between 21 to 30 residues was somewhat higher than the quantity of M-residues that were between 11 to 20

sequences. The M-block composition of F_G=0,60 and F_G=0,62 (Ba) were comparable and the amount of M-blocks that were up to ten residues was around 65%, lastly, most of the other M-blocks were between 11 and 20 sequences long. About 76% of the M-blocks in F_G=0,68 were up to ten residues long and the rest of the M-blocks were between 11 and 20 residues. Remarkably, almost 90% of the M-blocks in F_G=0,85 were not longer than ten residues and the other M-blocks were between 11 and 20 blocks long. In conclusion, the data suggested that for the AlgE6 epimerized mannuronan the amount of long M-residues was reduced as the total G-content increased. Finally, almost all M-blocks in F_G=0,56 (MG) were at most ten residues long.

3.4 Stability and appearance of alginate gels during the saline treatments

Alginates have higher affinity for the divalent cation Ca^{2+} than the non-gelling ion Na^{+} (Haug & Smidsrod, 1970), yet, during the saline treatments the great amount of Na^{+} ions are able to replace the Ca^{2+} ions in the gel network which leads to a less stable gel due to the inability of Na^{+} ions to form crosslinks. During the process the physical properties as well as the gel shape changes. The latter was documented by photographing the gels before the compression studies and representative photos are presented below in (Figure 15-21).

As seen in (Figure 15) the gels of F_G=0,48 (not stirred) had dissolved after four saline shifts.

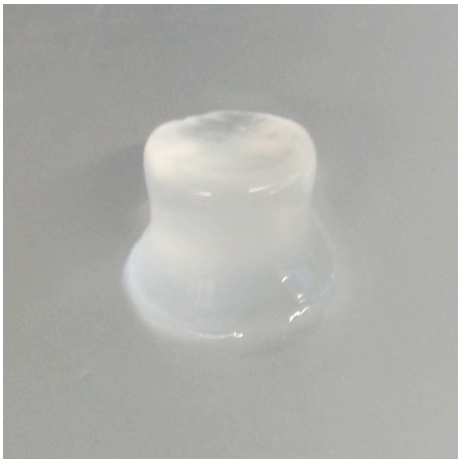

Figure 15. Representative photograph of F_G=0,48 (not stirred) after four saline treatments.

As seen in (Figure 16, 17) the gels of F_G=0,56 (MG) were stable and kept their gel form during all saline shifts. However, as presented in fig x the gels of F_G=0,48 and F_G=0,68 had lost their original gel shape after three saline shifts. Noticeably, when F_G=0,68 had been treated with four saline shifts there was only a small lump of alginate left.

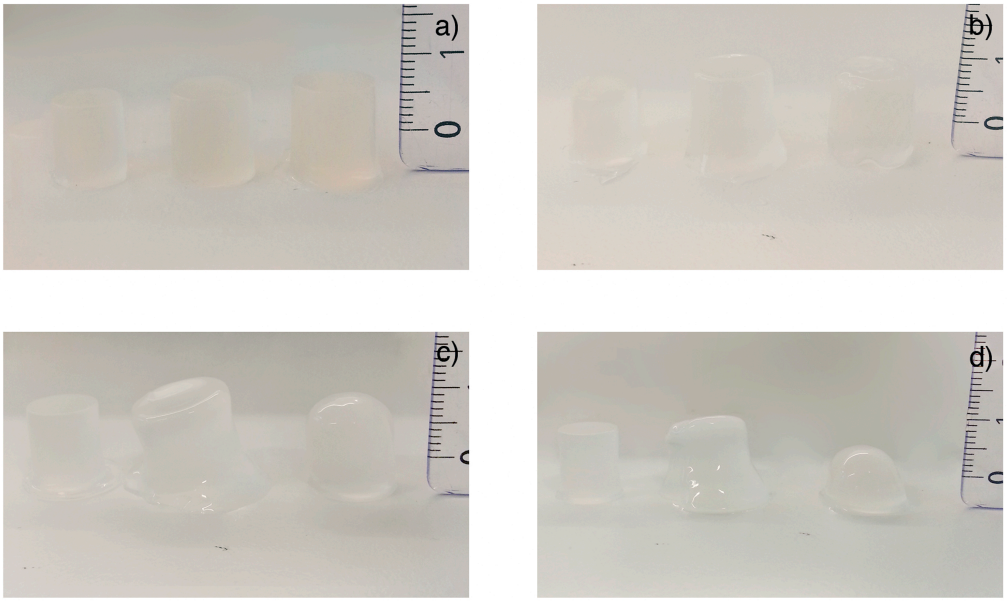

Figure 16. Representative photographs of the gel appearance of (from left to right) F_G=0,56 (MG), F_G=0,48 and F_G=0,68 during the saline treatments. a) The appearance of a saturated gel of F_G=0,56 (MG) and the appearance of F_G=0,48 and F_G=0,68 after one saline treatment. b) The appearance of F_G=0,56 (MG) after one saline treatment and the appearance of F_G=0,48 and F_G=0,68 after two saline treatments. c) The appearance of F_G=0,56 (MG) after two saline treatments and the appearance of F_G=0,48 and F_G=0,68 after three saline treatments. d) The appearance of F_G=0,56 (MG) after three saline treatments and the appearance of F_G=0,48 and F_G=0,68 after four saline treatments.

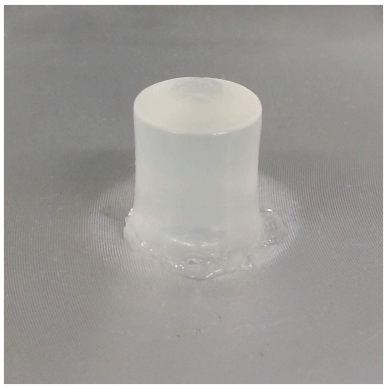

Figure 17. Representative photograph of F_G=0,56 (MG) after four saline treatments.

As observed in (Figure 18) the gels of F_G=0,60 were after four saline shifts easily formed by external forces.

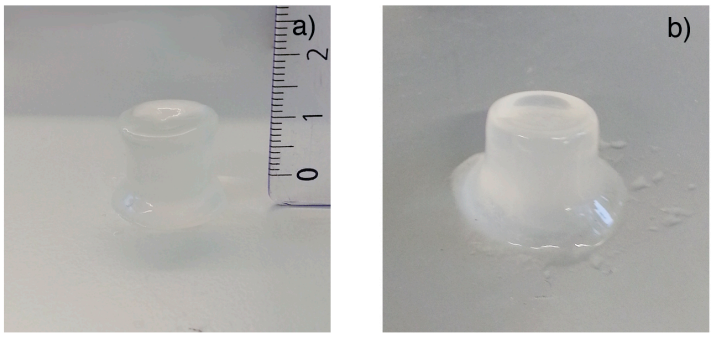

Figure 18. Representative photographs of F_G=0,60 during the saline treatments. a) After three saline treatments. b) After four saline treatments.

As seen in (Figure 19) the gel shape of F_G=0,62, which was saturated in Ba^{2+} and Ca^{2+}, was different from the form of SF60, as well as, all the other gel batches that were saturated only in Ca^{2+} (Figure 15-18, 20-21). The gel form of F_G=0,62 resembled the one of a bullet. The gel form of F_G=0,62 (Ba) was intact during all saline treatments.

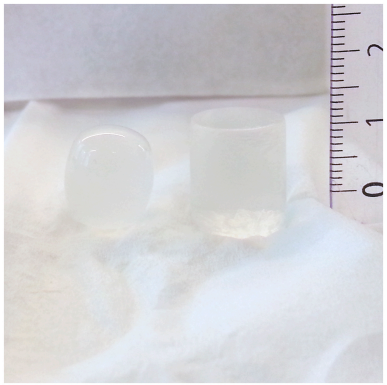

Figure 19. Representative photographs of the saturated gels (from left to right) of F_G=0,62 (Ba) and SF60.

(Figure 20) shows that the initial gel form of F_G=0,85 was changed after three saline shifts. Likewise with F_G=0,68 (Figure 16 d), after four saline treatments there was only a small lump of alginate left.

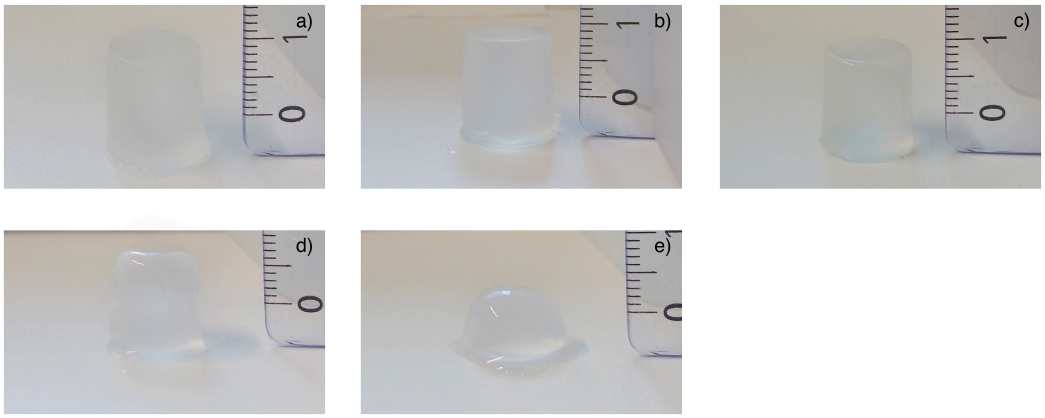

Figure 20. Representative photographs of F_G=0,85 during the saline treatments. a) The appearance of the saturated gels. b) The appearance after one saline shift. c) The appearance after two saline shifts. d) The appearance after three saline shifts. e) The appearance after four saline shifts.

In (Figure 21) the gel form of SF60 during the saline treatment is presented. As seen, after four saline shifts the gel had lost its initial form and could only lay on its long side. There are no presented photos of SF60 (not stirred), still, after four saline shifts the gels had swelled, however, the gels were still stable and it was possible to measure its physical properties.

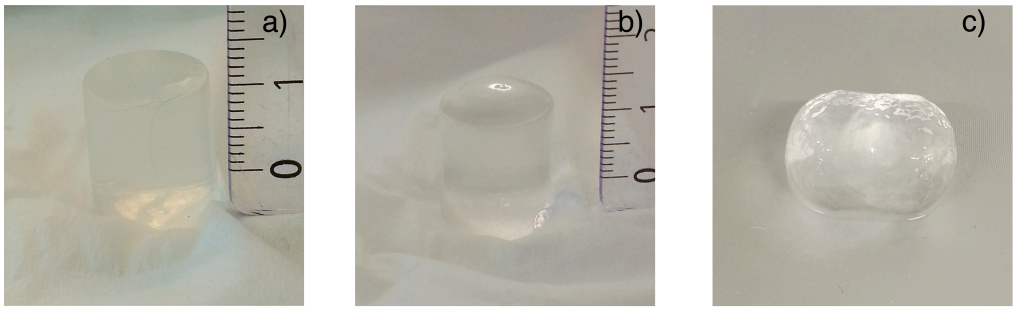

Figure 21. Representative photographs of SF60 during the saline treatments. a) The appearance of the saturated gels. b) The appearance after two saline shifts. c) The appearance after four saline shifts.

By qualitatively considering the shape and physical appearance, during all four saline shifts, the alginate gels were divided into three stability categories, which are defined below:

Stable:

- The gel has a well-defined structure.
- Normally a few gels have minor abnormalities such as air bubbles, most of which are located on the surface of the short sides.

Starting to dissolve & dissolving:

- The original cylindrical structure has changed considerably from the original one. Generally, there are fewer air bubbles likely due to gel-reorganization and filling of cavities with saline solution.
- The gel cannot uphold its own weight and the upper parts of the gel tends to lean downwards. Some gels lay on their long side instead of on one of the short sides.
- The gel is not stable and is shaped by external forces.

Dissolved:

- The gel has completely lost its original shape. Usually, only a lump of alginate is present in the saline solution.
- External forces easily penetrate the gel.

The stability of the gel batches during the saline treatments have been divided into one of the three categories and a scheme of it is found below in (Table 5).

Table 5. The stability of the gel batches during the saline treatments has been divided into three categories and the definitions are found above the table.

Alginate	**Saline shift**				
	Initial	**1st**	**2nd**	**3rd**	**4th**
SF60 (not stirred)	Stable	Stable	Stable	Stable	Stable
SF60	Stable	Stable	Starting to dissolve	Dissolving	Dissolved
F_G=0,56 (MG)	Stable	Stable	Stable	Stable	Stable
F_G=0,48 (not stirred)	Stable	Stable	Stable	Starting to dissolve	Dissolved
F_G=0,48	Stable	Stable	Starting to dissolve	Dissolved	Dissolved
F_G=0,60	Stable	Stable	Starting to dissolve	Dissolving	Dissolved
F_G=0,62 (Ba)	Stable	Stable	Stable	Stable	Stable
F_G= 0,68	Stable	Stable	Starting to dissolve	Dissolving	Dissolved
F_G=0,85	Stable	Stable	Stable	Starting to dissolve	Dissolved

As revealed by (Table 5) the stability of the alginate gels depends on the saline treatment method, the block composition, and gelling ions.

The effect of the two saline treatment methods can be studied by comparing the two batches of SF60 and F_G=0,48. The only difference between the two batches of SF60 was that one was treated in gently stirred saline solution and the other batch was just put in an unstirred saline solution. In an alike way, one of the batches of F_G=0,48 was put in gently stirred saline solution while the other batch was placed in saline solution that was not stirred. However, the molecular weight for one of these batches is noticeably smaller than the other. Also, the block composition differed between them, however, these

differences were very small and can be disregarded. By comparing the two batches of SF60 and F_G=0,48 with each other it is evident that the gentle stirring of the saline solution lead to that the gels dissolved faster. Specifically, the SF60 gels that were treated in saline solution with no stirring did not dissolve, whereas the SF60 gels that were treated in stirred saline solution started to dissolve after two saline shifts and finally dissolved after four shifts. In an analogous way, the gel batch F_G=0,48 (stirred) that was treated in stirred saline solution dissolved after three saline shifts while the other gel batch F_G=0,48 (not stirred) that was put in non-stirred saline solution dissolved after four saline shifts.

All the Ca-G-gels that were stirred in the saline treatment started to dissolve after two saline shifts, except for the high G-gel, F_G=0,85 which was stable longer and started to dissolve after three saline shifts. Furthermore, all the Ca-G-gels dissolved after four saline shifts, but the low G-content gel F_G=0,48 (stirred) was less stable and dissolved after three saline shifts. Taken together, of all the Ca-G-gels that were stirred during the saline treatment F_G=0.48 (not stirred) was the least stable gel and F_G=0,85 was the most stable gel, hence, the data indicated that a higher G-block content results in more stable alginate gels.

The gels prepared from F_G=0,56 (MG) were stable and kept the original cylindrical shape during all four saline treatments. Interestingly, this alginate had the third lowest G-content of all the tested gels but the content of alternating blocks was about three times higher (Table 2) than for all of the epimerized alginates in this work. These results suggest that the MG-blocks were important for the stability of the gel in saline solution.

The alginate gel F_G=0,62 (Ba) which was saturated in Ba^{2+} ions, had a similar block-distribution as F_G=0,60 (Table 2), yet, the stability of the two gels differed considerably, as well as between F_G=0,62 (Ba) and the other Ca-G-gels. In fact, of all the gels that were treated in stirred saline solution, only the gels prepared from F_G=0,56 (MG) and F_G=0,62 (Ba) were stable during all four saline shifts. Noticeably, the gels had a bullet-form like shape at every data point (Figure 19). Since the gel appearance was similar throughout the saline treatments it was defined as stable.

3.4.1 Gel shape after compression and water release

One of the main objectives of this thesis was to study how the stability of alginate gels was affected when treated with repeating saline shifts. Two of the used methods have been to document the appearance of the gels, as well as the water loss, after the compression studies. The gel shape after the compression studies changed accordingly to the gel stability that is presented in (Table 5). Specifically, there was one gel shape for each of the three gel states and representative photos of these are presented in (Figure 22) below. However the gel batch F_G=0,56 (MG) did not follow this pattern. Although it was considered to be stable during all saline shifts its gel appearance after two or more saline shifts was more alike that of an alginate gel that had started to dissolve, rather than a stable.

When a stable gel was fully compressed a comprehensive water loss occurred and the end result was a thin and transparent alginate film, usually a part of the gel edge was thicker than the rest of the film. The outcome after a full compression of a gel that had starting to dissolve was an aqueous mixture of alginate, typically there was one or two larger fragments. Furthermore, when a dissolved alginate lump was fully compressed an aqueous, "porridge-like" blend of small alginate pieces was formed, usually there were no larger fragments of alginate. Representative photographs of the gel appearance after a full compression for the three stability categories are presented below in (Figure 22).

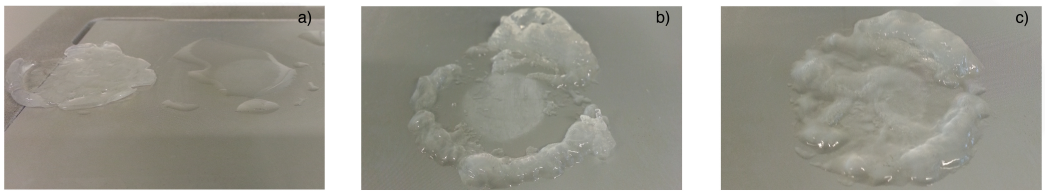

Figure 22. Representative photographs of the gel appearance after a full compression. a) The gel appearance after a full compression of a stable gel. b) The gel appearance after a full compression of a gel that has started to dissolve. c) The gel appearance after a full compression of a gel that has dissolved.

The weight of the alginate gel before and after the compression study was used to estimate the water loss. By using equation (1.11) the water loss was estimated and the data is presented below in (Table 6).

Table 6. The normalized water loss [%] of the alginate gels during the compression studies.

Alginate	**Water loss [%] ± SD (n=3-9)**				
		Saline shift			
	Initial	**1st**	**2nd**	**3rd**	**4th**
SF60 (not stirred)	19,51 ± 2,90	21,29 ± 3,76	8,33 ± 3,34	5,76 ± 2,82	4,80 ± 1,91
SF60	37,72 ± 13,69	12,31 ± 4,27	10,40 ± 5,69	21,52 ± 9,45	38,52 ± 4,07
FG=0,56 (MG)	31,50 ± 2,17	17,02 ± 4,65	16,99 ± 8,16	21,89 ± 4,38	28,34 ± 1,70
F_G=0,48 (not stirred)	22,86 ± 11,24	8,54 ± 5,93	11,01 ± 2,92	13,32 ± 3,66	17,22 ± 4,48
F_G=0,48	37,27 ± 14,53	12,80 ± 4,45	23,05 ± 4,96	15,92 ± 6,75	-
F_G=0,60	39,95 ± 11,02	13,14 ± 4,85	14,61 ± 5,26	37,10 ± 7,72	41,91 ± 8,39
F_G=0,62 (Ba)	48,94 ± 15,77	17,92 ± 11,91	12,85 ± 6,63	18,02 ± 9,41	15,53 ± 6,82
F_G=0,68	34,97 ± 7,33	11,70 ± 2,53	10,00 ± 0,44	34,37 ± 3,60	-
F_G=0,85	38,20 ± 10,08	36,67 ± 7,17	14,76 ± 5,09	-	-

In general, the water losses for the gels that had not been treated with saline solution were extensive, however, the standard deviations of some gel batches were high. For example, the gel batch F_G=0,62 (Ba) lost much weight after the compression, 48,94 ± 15,77%, and its standard deviation was high. As indicated by the other examined physical properties in this work all gel batches underwent broad re-organization at the first saline treatment that resulted in different physical properties and this effect was also seen for the estimated water loss. After one saline shift the water loss was far less compared to the non-saline treated gels. However, two gels, F_G=0,85 and SF60 (not stirred), were an exception and the characteristic drop of the water loss occurred after the second saline shift. Generally, after the first characteristic drop of the water loss the measured property was dependent of the gel state. As shown, the water loss increased for the Ca-G-gels and SF60 (not stirred) when the gels had started to dissolve. Furthermore, as seen for the gels with available data, the water loss increased even more when the gel had dissolved, in fact, it increased to values close to the original values of the non-saline treated gels. As seen in table (Table 6), after the first characteristic drop the water loss was

practically constant for the gel batches F_G=0,62 (Ba) and SF60 (not stirred) and these gels were also stable during all saline shifts. Finally, the water loss for F_G=0,56 (MG) started to increase slowly after two saline shifts and after four saline shifts the water loss had increased to a value similar to that of the non-saline treated gels.

It is important to be aware of that the reported water loss values were estimations. As mentioned, after a full compression of a dissolving gel an aqueous mixture of alginate pieces was formed and it was hard to collect and weight all the pieces. This was especially hard when collecting alginate pieces from a dissolved gel since the mixture normally just consisted of small pieces, and not a few larger ones, which was common in the formed mixture from an alginate gel that had started to dissolve. Since the estimator (1.11) for the water loss used the quotient of the weight before and after a full compression a smaller value than the true alginate weight after compression leads to an overestimation of the water loss. Therefore, the actual values for the dissolved gels, and to some extent the gels that had started to dissolve, were possibly slightly smaller.

3.5 Physical properties of the alginate gels

The functional properties of alginate gels have been shown to correlate strongly with the block distribution, the molecular weight and the ions present in the gel network. To be able to relate the physical properties of the epimerized alginates, as well as the natural alginate SF60, syneresis was measured, Young´s modulus, rupture strength and elasticity of the alginate gel cylinders were studied by compression of the gel cylinders.

The data of the non-saline treated alginate gels is first presented in each Section followed by the data from the saline treatment studies.

3.5.1 Syneresis of the saturated alginate gels

The initial volume of the different gel cylinders varied and representative photos are presented in (Figure 15-21). These differences are due to the distinctive shrinking behavior during the gel formation process. To determine the magnitude of the shrinkage the term syneresis is used. It is defined as the weight reduction of the gels with respect to the initial weight, assuming that the densities of the gels are the same, and identical to the one of water (Ý A Mørch et al., 2008). The results are given below in (Figure 23)

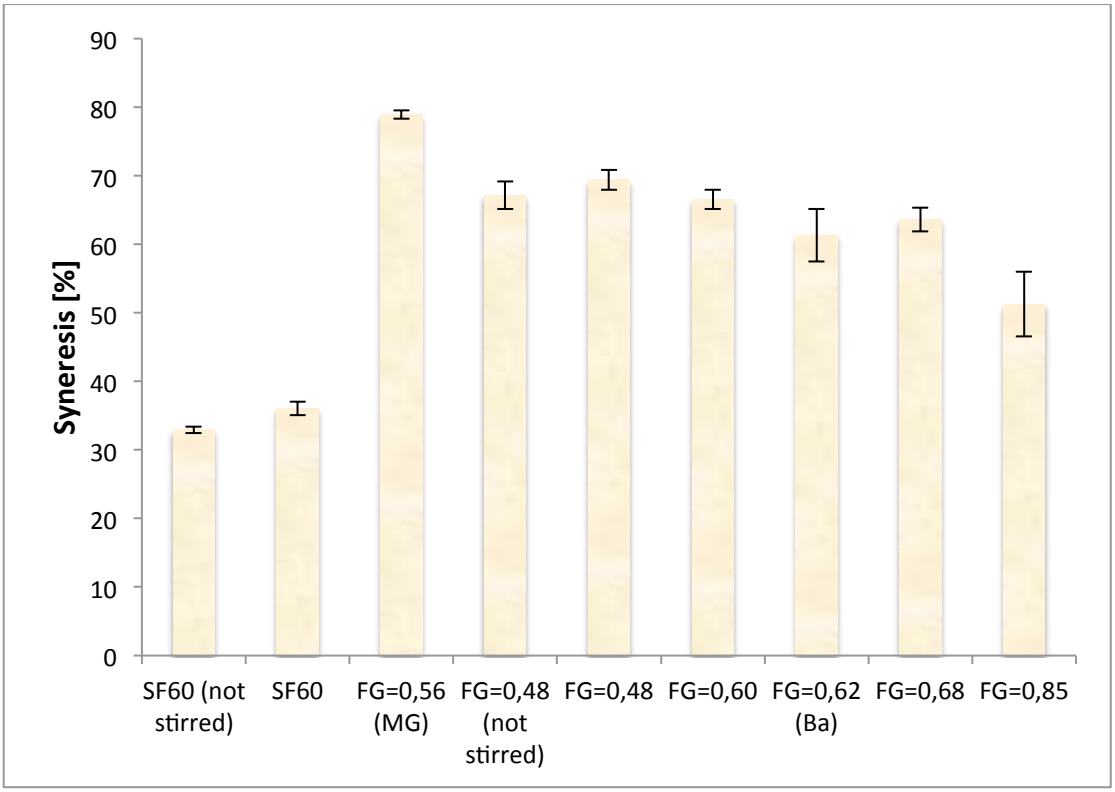

Figure 23.Initial syneresis of the saturated alginate gels, as reported in (Appendix D). Data is reported as mean values ± SD (n =3-7).

The syneresis of the epimerized alginates varied between about 50-80%. The syneresis of F_G=0,85 was statistically significantly (p=0,05) lower in relation to all other AlgE6 epimerized gels. Additionally, the syneresis of F_G=0,48 was statistically significantly (p=0,05) higher compared to F_G=0,62 (Ba) and F_G=0,68. Conclusively, the data of the AlgE6 epimerized gels suggested that a higher G-content resulted in lower syneresis.

Of all tested alginate gels F_G=0,56 (MG) undoubtedly experienced the highest degree of syneresis, which was about 79%. The syneresis of F_G=0,62 (Ba) was alike the one of F_G=0,60 and F_G=0,68, apparently, the presence of Ba^{2+} in the saturated gel did not affect the syneresis.

As shown in (Figure 23), the degree of syneresis was alike in the two gel batches of SF60, obviously, there was a small batch to batch difference. The syneresis of the natural alginates was about 32-36% and these gels experienced the lowest syneresis of all alginate gels. Compared to F_G=0,56 and F_G=0,48 the degree of syneresis was about the half.

It was not expected that the syneresis of the two alginate batches with a G-content of 48% would be alike since one of the batches had drastically lower molecular weight than the other.

3.5.2 Swelling of the alginate gels during the saline treatments

The swelling of the alginate gels was studied during the saline treatments (0.15 M NaCl, 0-4 shifts). In (Figure 24) below the swelling of the alginate gels is presented as the weight ratio of the gel weight at the measurement point, W, and the original weight, W_0, from when formed in a well (one of the wells of a 24-well-plate (Section 2.6).

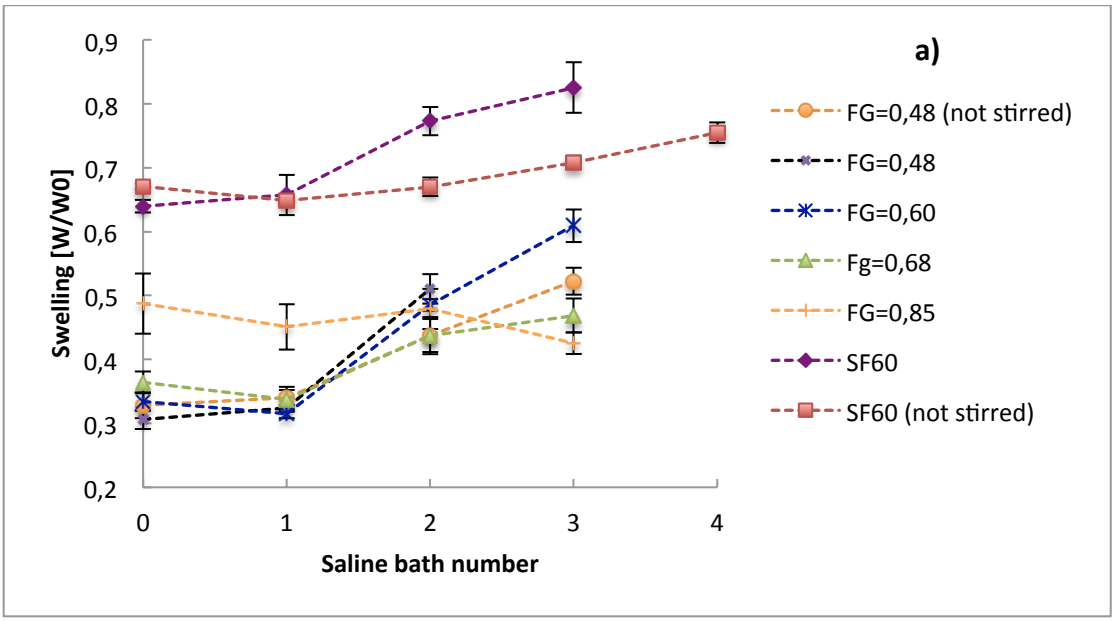

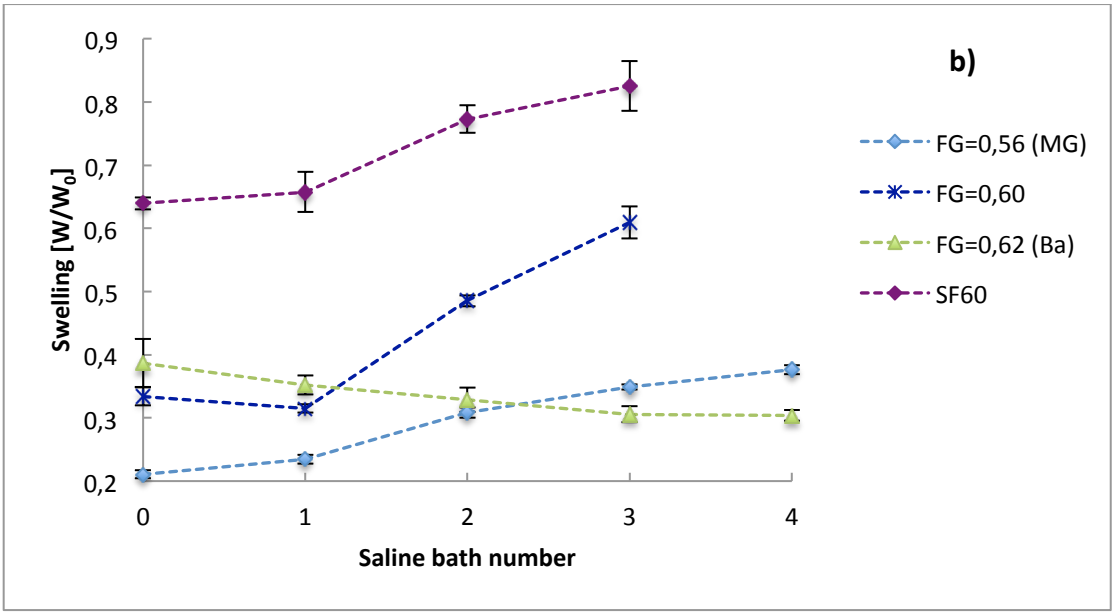

Figure 24. The swelling of the alginate gels during the saline treatment. The swelling is calculated as the weight ratio of the gel weight at the measurement point, W, and the original weight, W_0, from when formed in a well. a) The swelling of the Ca^{2+} saturated gels formed from AlgE6 epimerized mannuronan. The two batches of SF60 are included as controls. b) The swelling of F_G=0,56 (MG) and F_G=0,62 (Ba) during the saline treatments. SF60 and F_G=0,60 are included as references.

As seen in (Figure 24 a), the degree of swelling before the saline treatments had started were different among the gel batches, as presented in (Section 3.5.1). It is clear that the gels made of AlgE6 epimerized mannuronan were largely destabilized during the repeated saline treatments. However, after the first saline shift the swelling had not changed noticeably in any of the gel batches, including SF60. After the second saline shift F_G=0,48 and F_G=0,60 had swelled to a similar degree. Notably, after two saline shifts the volume of F_G=0,85 was alike the one of F_G=0,48 and F_G=0,60. After two saline treatments F_G=0,68 had swelled less than F_G=0,48 and F_G=0,60. After the third saline treatment the volume of F_G=0,85 decreased, this was due to the gels had started to loose alginate as seen in the photo (Figure 20). Surprisingly, the volume of F_G=0,68 did not change after the third saline change, however, this too was due to the gels had started to loose alginate, as seen in the photo (Figure 16). However, the gels of F_G=0,60 had not started to loose alginate, instead, the volume had increased from the third saline change. In fact, after the saline treatment it had almost doubled its volume.

As seen in (Figure 24 a) the gels of SF60 had not swollen after the first saline shift, however, during the two following shifts, the volume increased significantly. The initial value of the swelling for SF60 was 0,64 ± 0,03 and the value after the three saline changes was 0,83 ± 0,04. The corresponding values for F_G=0,60, which was the only gel batch prepared from AlgE6 epimerized mannuronan that had not started to loose alginate after three saline shifts, were 0,33 ± 0,01 and 0,61 ± 0,03. Apparently, SF60 swelled less than the gel batch prepared from AlgE6 epimerized mannuronan.

As presented in (Figure 24b) the initial swelling of F_G=0,56 (MG), before the saline treatments had started, was small an equal to 0,21 ± 0,01. After the first saline change the volume had not changed, however, after the second saline shift the volume increased. After the third saline change the swelling was equal to 0,35 ± 0,00. In conclusion, the gel batch had swelled less than both the natural alginate SF60 and the AlgE6 epimerized gel batch F_G=0,60. Surprisingly, the volume of F_G=0,62 (Ba) decreased during the saline shifts. There was no significantly differences between two subsequent saline shifts, however, after two saline shifts the gel batch had decreased statistically significantly (p=0,05) compared to the initial volume. During the last two last saline changes the volume was stable and did not change.

Interestingly, among the Ca-G-gels it was observed that the swelling difference before and after the saline treatment was decreasing with an increasing G-content. As seen, the difference of F_G=0,48 (both batches) was about 20% while the correspondingly number of F_G=0,68 was about 10%. However, the gel batch F_G=0,60 did not follow this pattern and the syneresis difference was around 25%.

The swelling behavior differed between the two SF60 gel batches. The gel that was treated in stirred saline solution dissolved after four saline shifts and experienced a more comprehensive syneresis reduction compared to the batch that did not dissolve and that was treated in non-stirred saline solution.

3.5.3 Dimensional stability of the alginate gels during the saline treatments

The dimensional stability of the alginate gels was studied during the saline treatments (0.15 M NaCl, 0-4 shifts). In (Figure 25) below the dimensional stability of the alginate gels is presented as the weight ratio of the gel weight at the measurement point, W, and the weight after saturation, $W_{saturated}$.

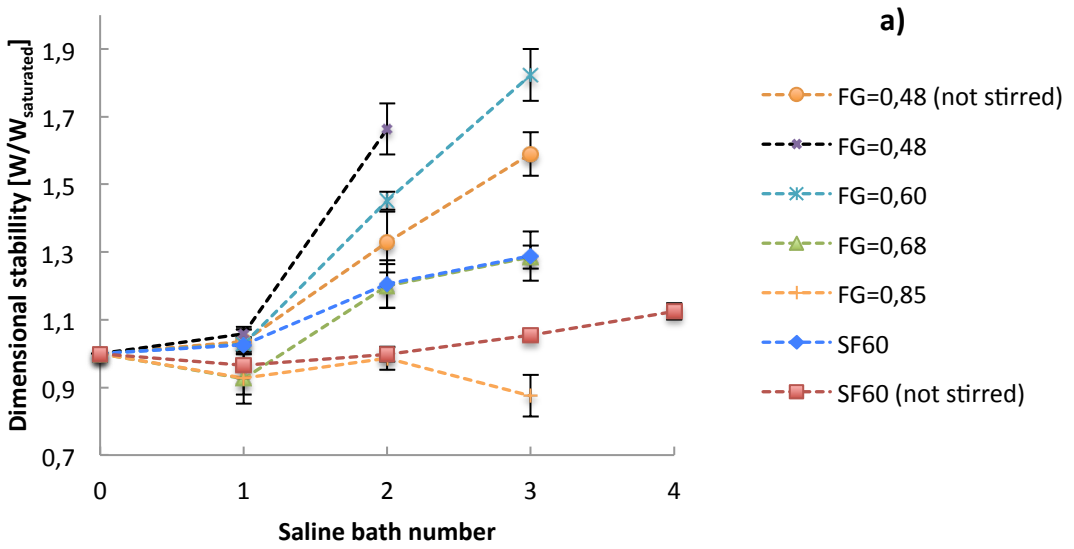

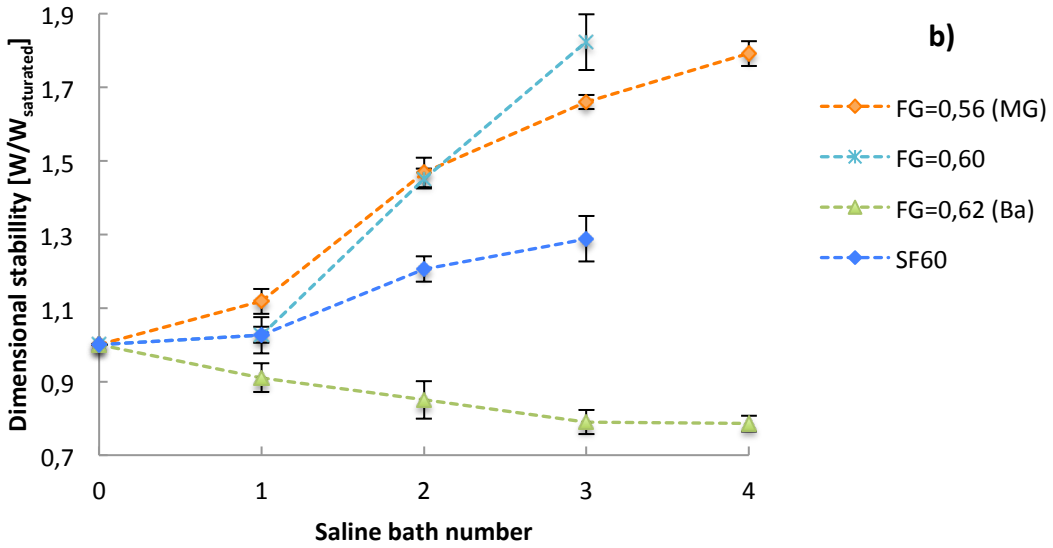

Figure 25. The dimensional stability of the alginate gels was studied during the saline treatments (0.15 M NaCl, 0-4 shifts). The dimensional stability is defined as the weight ratio of the gel weight at the measurement point, W, and the weight after saturation, $W_{saturated}$.

As seen in (Figure 25 a,b) after the third saline treatment it appears as F_G=0,85 had shrunk and that the volume of F_G=0,68 had not changed from the second saline shift. It is important to be aware of that these gel batches had lost their initial cylindrical form after three saline shifts, as seen in the photos (Figure 16,20) and they had as well started to loose alginate. Consequently, it seemed as F_G=0,85 had shrunk due to its lower weight. Furthermore, the dimensional stability of F_G=0,68 appeared not to have changed because the weight gain from the increase in volume, due to the saline shift, and the weight loss, due to the less amount of alginate in the gels, cancelled themselves out.

As revealed by (Figure 25 a), the swelling development of the Ca-G-gels that were stirred during the saline treatment clearly showed that the G-content and G-block length affected the volume change during the saline treatment. After the first saline shift the gel batches F_G=0,68 and F_G=0,85 had shrunk by a few percent while F_G=0,48 and F_G=0,60 had swollen slightly. All the mentioned changes in the dimensional stability after the first saline shift was statistically significantly (p=0,05) for all gel batches except F_G=0,85. After the second saline shift the relative volumes of the gel batches

F_G=0,48, F_G=0,60 and F_G=0,68 had increased by a decreasing G-content. As seen, the relative volume of F_G=0,48 was 1,66 ± 0,06 and the corresponding values of F_G=0,60 and F_G=0,68 were 1,45 ± 0,03 and 1,20 ± 0,07, respectively. Noticeably, after the second saline change it appeared as F_G=0,85 had swelled slightly so that the volume was close to the one of the saturated gels. As mentioned, after three saline shifts had the gels of F_G=0,68 and F_G=0,85 started to loose alginate so these values are not trustworthy. However, the measured relative volume of F_G=0,60 was trustworthy and as seen, the gel had swelled comprehensive.

As seen in (Figure 25 b) the relative volume change of F_G=0,56 (MG) and F_G=0,60, which had a similar G-content and molecular weight, was comparable during the first two saline shifts. However, after the third saline treatment the relative volume of F_G=0,56 (MG) was clearly lower than F_G=0,60. Finally, during the forth saline change the relative volume of F_G=0,56 (MG) increased and the last measured relative volume was 1,79 ± 0,03.

The gels that were saturated in Ba^{2+} and Ca^{2+} behaved differently from the gels that solely were saturated in Ca^2, as seen in (Figure 25 b), the saline treatments resulted in that the gels shrunk. In detail, it was during the first two saline treatments that the gels shrunk and during the last two saline treatments no significantly changes of the relative volume occurred. The final relative volume of the gel batch was 0,79 ± 0,02.

According to (Figure 25 b) the dimensional stability of SF60 was high and the relative volume increase was smaller compared to both F_G=0,60 and F_G=0,56 (MG) after the second and third saline treatment. The last measured relative volume of SF60 was 1,29 ± 0,06. Finally, as seen (Figure 25 b) the last measured volume change of the two gel batches with the G-content 48% was almost equal.

3.5.4 Young´s modulus of the saturated alginate gels

The gel strength of the Ca^{2+} saturated alginate gel batches, in addition to the Ba^{2+} saturated gel batch, were determined before the saline treatments had started by determining the Young´s modulus. The data is presented below in (Figure 26).

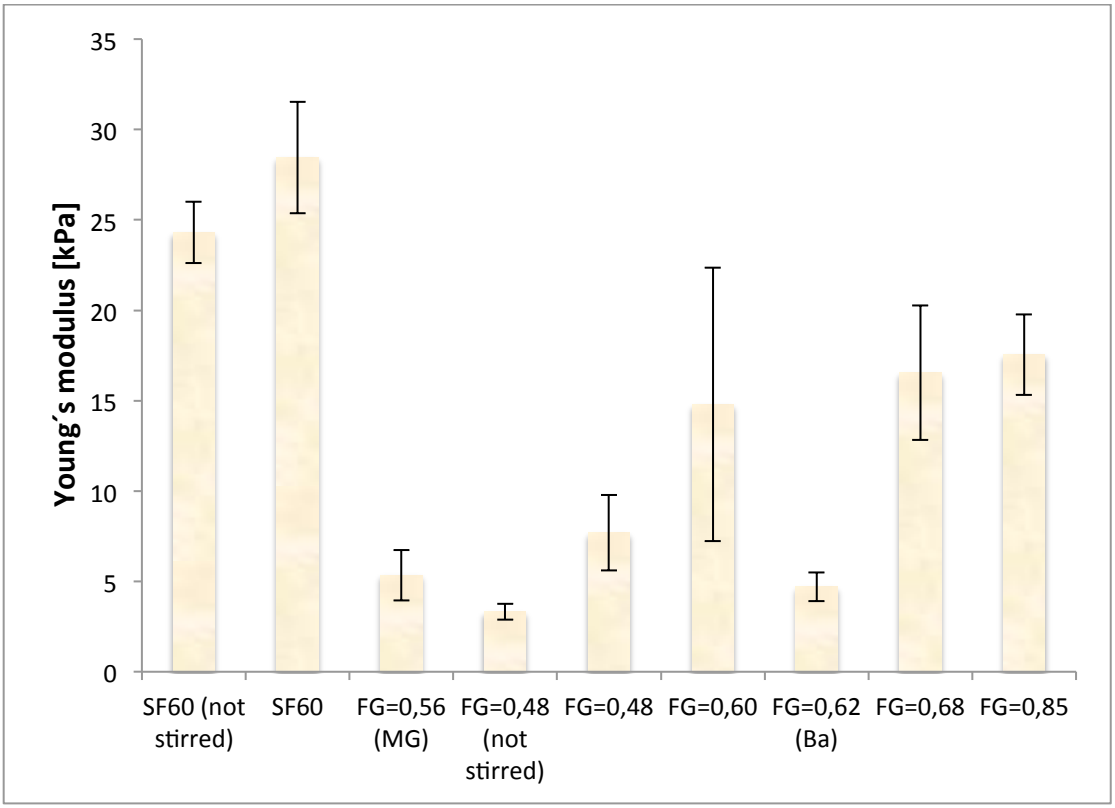

Figure 26. Young´s modulus [kPa] of the saturated alginate gels, as reported in (Appendix D). Data is reported as mean values ± SD (n =3-7).

From (Figure 26) it is noticeable that the standard deviation of F_G=0,68 was relatively high. This was due to that data from only three gels could be used and the Young´s modulus of one the gels were particularly higher than the other two.

The two gel batches F_G=0,85 and F_G=0,68 were statistically significantly (p=0,05) higher than both the gel batches that had a G-content of 48%. Interestingly, the Young´s modulus of the latter two mentioned gels differed substantially, in fact, the value of F_G=0,48 was more than the double of the other batch with a G-content of 48%. The standard deviation of F_G=0,60 was

high which made it hard to relate it to the other gel batches. Finally, despite the high standard deviations among the Ca-G-gels it appeared as a higher G-content resulted in a higher Young´s modulus.

While the block composition and molecular weight of the Ba^{2+} saturated gel resembled the one of F_G=0,60 and F_G=0,68 its Young´s modulus was, surprisingly, statistically significantly (p=0,05) smaller compared to them. Essentially, it was significantly smaller compared to all the Ca-G-gels except for F_G=0,48. The E value of F_G=0,56 (MG) was statistically significantly (p=0,05) smaller compared to the other epimerized and Ca^{2+} saturated batches F_G=0,60, F_G=0,68 and F_G=0,85.

The Young´s modulus of the two natural alginate batches was by far highest of all the gel batches. There was no significant difference between the two SF60 batches, yet, their mean values differed noticeably. Still, the difference can be regarded as batch-to-batch variability.

3.5.5 Young´s modulus during the saline treatments

As seen in (Figure 27), the Young´s modulus decreased or remained constant in all gel batches between subsequent saline shifts. Remarkably, after the first or second saline shift the value for each gel batch had decreased by at least 60% from the initial E value.

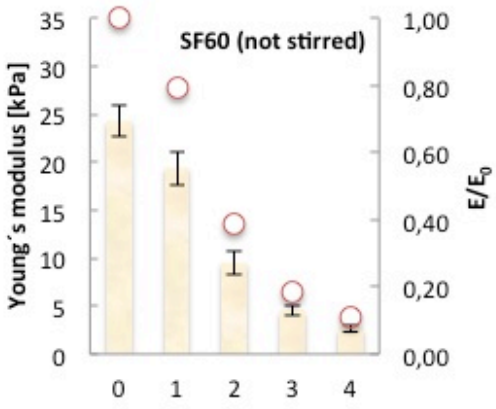
SF60 (not stirred)
Young´s modulus [kPa]
E/E0
0
5
10
15
20
25
30
35
0,00
0,20
0,40
0,60
0,80
1,00
0
1
2
3
4

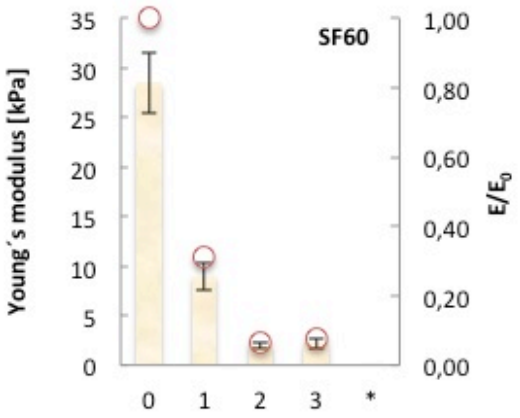
SF60
Young´s modulus [kPa]
E/E0
0
5
10
15
20
25
30
35
0,00
0,20
0,40
0,60
0,80
1,00
0
1
2
3
*

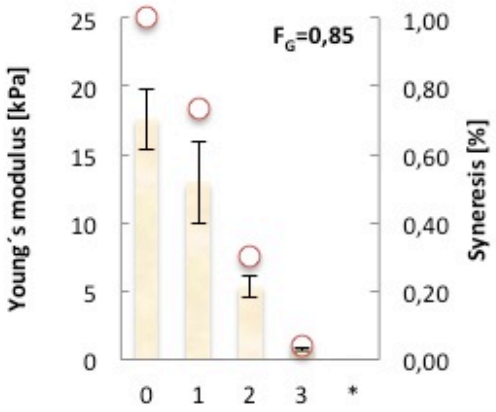
FG=0,85
Young´s modulus [kPa]
Syneresis [%]
0
5
10
15
20
25
0,00
0,20
0,40
0,60
0,80
1,00
0
1
2
3
*

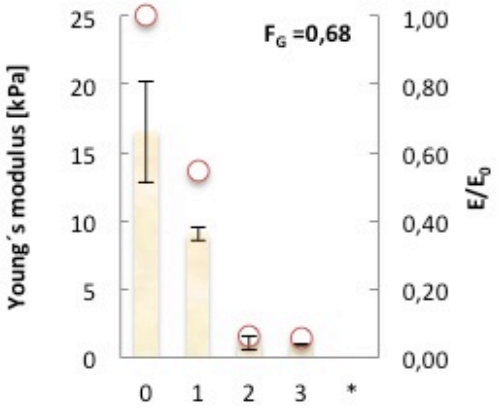
FG =0,68
Young´s modulus [kPa]
E/E0
0
5
10
15
20
25
0,00
0,20
0,40
0,60
0,80
1,00
0
1
2
3
*

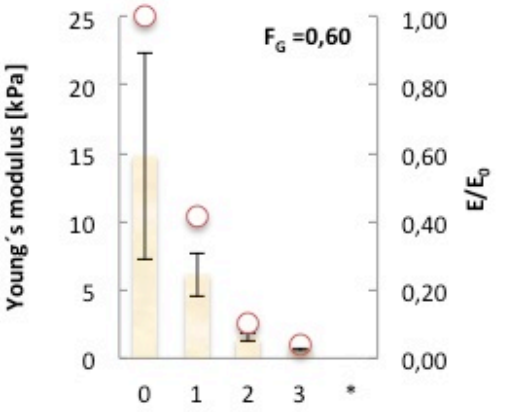
FG =0,60
Young´s modulus [kPa]
E/E0
0
5
10
15
20
25
0,00
0,20
0,40
0,60
0,80
1,00
0
1
2
3
*

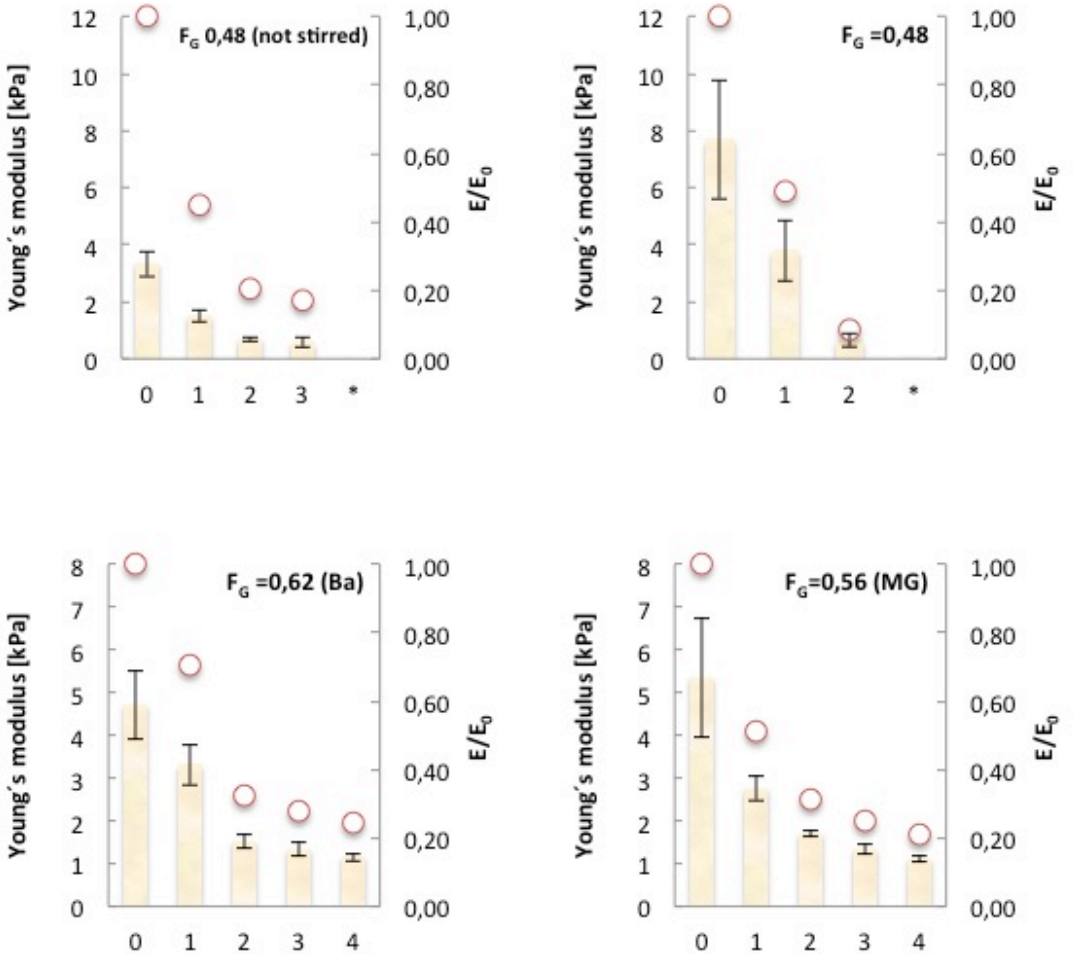

Figure 27. Young´s modulus of the saturated alginate gels [kPa] (columns), relative variation of the Young's modulus (circles) as reported in (Appendix D). Data is reported as mean values ± SD (n =3-7).

For all Ca-G-gels, except F_G=0,85, the original value of the Young´s modulus decreased by about 45- 55% after the first saline change. Furthermore, after the second saline shift the initial value of the gel batches F_G=0,48, F_G=0,60 and F_G=0,68 decreased by at least 90%. After the third saline change F_G=0,48 had dissolved and the Young´s modulus of F_G=0,60

and F_G=0,68 had not changed noticeably. After the Ca^{2+} saturation, the Young´s modulus of F_G=0,48 was about the double value of F_G=0,48 (not stirred), yet, after the first saline change the E value had decreased by over 50% for the both gel batches. After the second saline shift the Young´s modulus of F_G=0,48 (not stirred) was about 20% of the initial value, before the saline treatments had started. After the third saline shift the value had decreased by a few more percent.

After the saturation, the Young´s modulus of F_G=0,85 was among the highest of the epimerized gels. The gel batch resisted the first saline treatment comparatively well and the Young´s modulus was after the first treatment about 74% of the original value. However, after the next saline change the value decreased to only 30% of the initial one. After the third saline shift the value was only a few percent of the original value.

To summarize, after two saline shifts the Young´s modulus of the Ca-G-gels, which were stirred during the saline shifts, had decreased to only a tenth part or less, of the respectively gel batches initial values. However, the gel F_G=0,85 was an exception and its gel strength was more stable during the saline shifts, as seen in (Figure 27), it took three, not two, saline shifts before the E value had decreased to a few percent of the initial value. Additionally, the behavior of F_G=0,60 and F_G=0,68 after the first saline change also suggested that a higher content of G-blocks lead to a more stable gel strength during the saline treatment. Specifically, before the first saline shift the both gels had an alike E-value, however, after the shift the Young´s modulus of the gel with the higher G-content was 55% of the initial value while the corresponding value for the other gel batch was 42%. Finally, it should be noted that the Young´s modulus of F_G=0,48 after the first saline shift was 49% of its original value, and so, the relative decrease was similar as to the one of F_G=0,68. Yet, it is important to be aware of that the initial Young´s modulus of the latter mentioned gel batch was 16 ± 3 kPa while the corresponding value for F_G=0,48 was 7 ± 2 kPa, and so, the decreases in absolute values were not comparable.

The gel batches F_G=0,56 (MG) and F_G=0,62 (Ba) had similar and relativity low E-values, compared to the Ca-G-gels, before the saline treatments had begun. In regard of the gel strength, the two gels behaved equally during the saline shifts except after the first change where the Young's modulus of F_G=0,56 (MG) was smaller than the other gel batch. However, during the continuing saline shifts both the absolute and relative values of the two gel

batches were similar. As seen in (Figure 27) during the last two saline treatments the Young´s modulus only decreased marginally**.** In fact, after three saline shifts the E-values of the two discussed gel batches were higher compared to the correspondingly values of the Ca-G-gels.

The natural alginate that was stirred during the saline shifts, SF60, had the highest Young´s modulus after saturation of all gel batches, interestingly, after the first saline shift it had dropped by over 70%, this was the largest decrease recorded during all the saline shifts for the gels. After the following saline shift the Young´s modulus fell to 7% of the original value and during the last saline change, the value did not change. The Young´s modulus of the other SF60 batch, which was not stirred during the saline shifts, did not decline as considerably or as fast as the saline-stirred batch. After the first saline change the Young´s modulus was 80% of the original value and during each of the three succeeding saline changes the value was reduced by about half.

3.5.6 Rupture strength and elasticity of the saturated alginate gels

The rupture strength and elasticity of the saturated gel batches were measured by compression studies before the saline treatments started and the data is presented in (Figure 28) below.

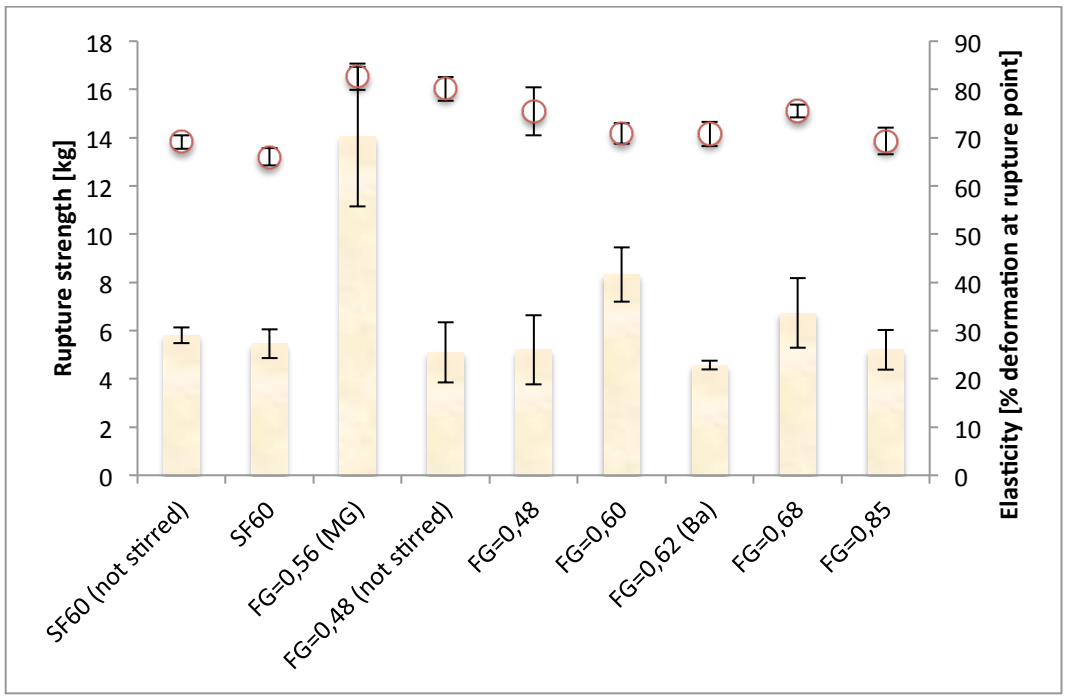

Figure 28. Measured rupture strength [kg] (columns) and elasticity [% deformation at rupture point] (circles) of the saturated alginate gels, as reported in (Appendix D). Data is reported as mean values ± SD (n =3-7).

During the compression measurements the alginate gels can break in many different ways and due to this complexity the standard deviations were rather high.

As revealed by (Figure 28), the rupture strength of the Ca-G-gels was around 5 kg, and there were few significant differences between them. However, the rupture strength of F_G=0,60 (8,32 ± 1,12 kg) was statistically significantly (p=0,05) higher than each of the Ca-G-gels except for F_G=0,68. The elasticity of the Ca-G-gels was similar and around 70%. The only statistically significant difference in elasticity between the Ca-G-gels was that F_G=0,68 had a higher elasticity compared to F_G=0,85.

The rupture strength of the gel batch F_G=0,56 (MG) was statistically significantly (p=0,05) higher than all the tested gel batches. Also, the elasticity of F_G=0,56 (MG) was statistically significantly (p=0,05) higher than all gel batches except for F_G=0,48 (not stirred).

The rupture strength of the Ba^{2+} saturated gel batch was comparatively small. In relation to the other gel batches, its rupture strength was statistically significantly (p=0,05) smaller than the one of SF60 (both batches), F_G=0,56 (MG), F_G=0,60 and F_G=0,68. The elasticity of the Ba^{2+} saturated gel batch was comparable to the one of F_G=0,60.

There was no noteworthy difference in rupture strength or elasticity between the two gels with a G-content of 48%, as well as, between the two batches of SF60. The elasticity of the both SF60 gel batches was statistically significantly (p=0,05) lower compared to all gel batches except F_G=0,60 and F_G=0,85. Moreover, the rupture strength of the two natural alginates were similar to the one of the Ca-G-gels, except that the ruptures strength of F_G=0,60 was statistically significantly (p=0,05) higher.

3.5.7 Rupture strength and elasticity during the saline treatments

The rupture strength and elasticity of the saturated gel batches were measured by compression studies during the saline treatments and the results are presented in (Figure 29) below.

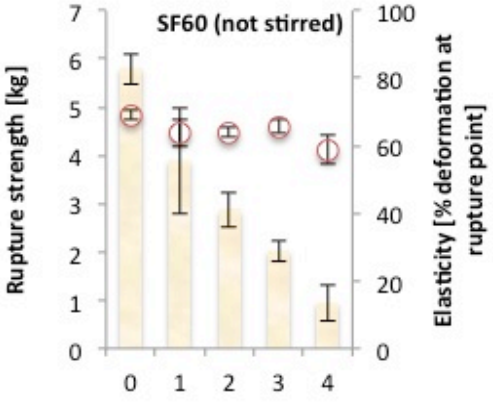
SF60 (not stirred)
Rupture strength [kg]
Elasticity [% deformation at rupture point]
0 1 2 3 4

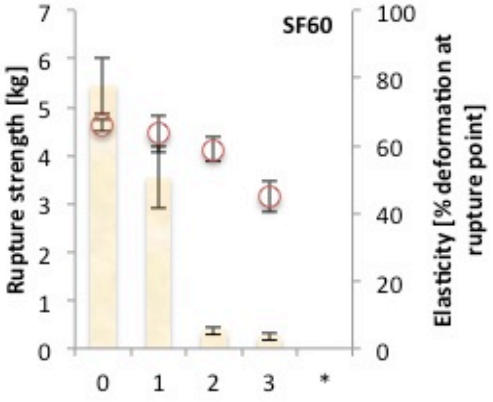
SF60
Rupture strength [kg]
Elasticity [% deformation at rupture point]
0 1 2 3 *

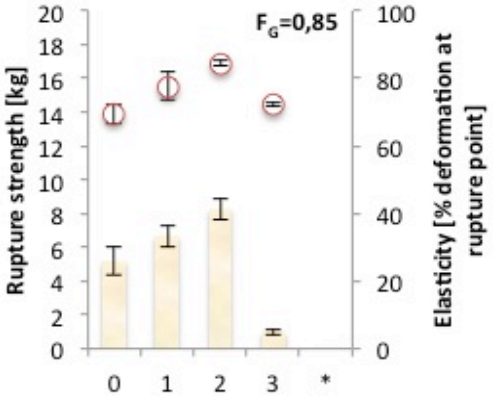
F_G=0,85
Rupture strength [kg]
Elasticity [% deformation at rupture point]
0 1 2 3 *

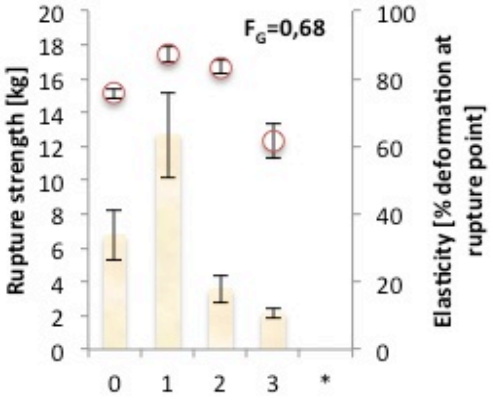
F_G=0,68
Rupture strength [kg]
Elasticity [% deformation at rupture point]
0 1 2 3 *

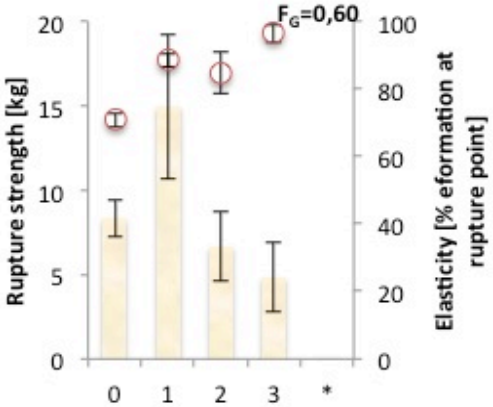
F_G=0,60
Rupture strength [kg]
Elasticity [% eformation at rupture point]
0 1 2 3 *

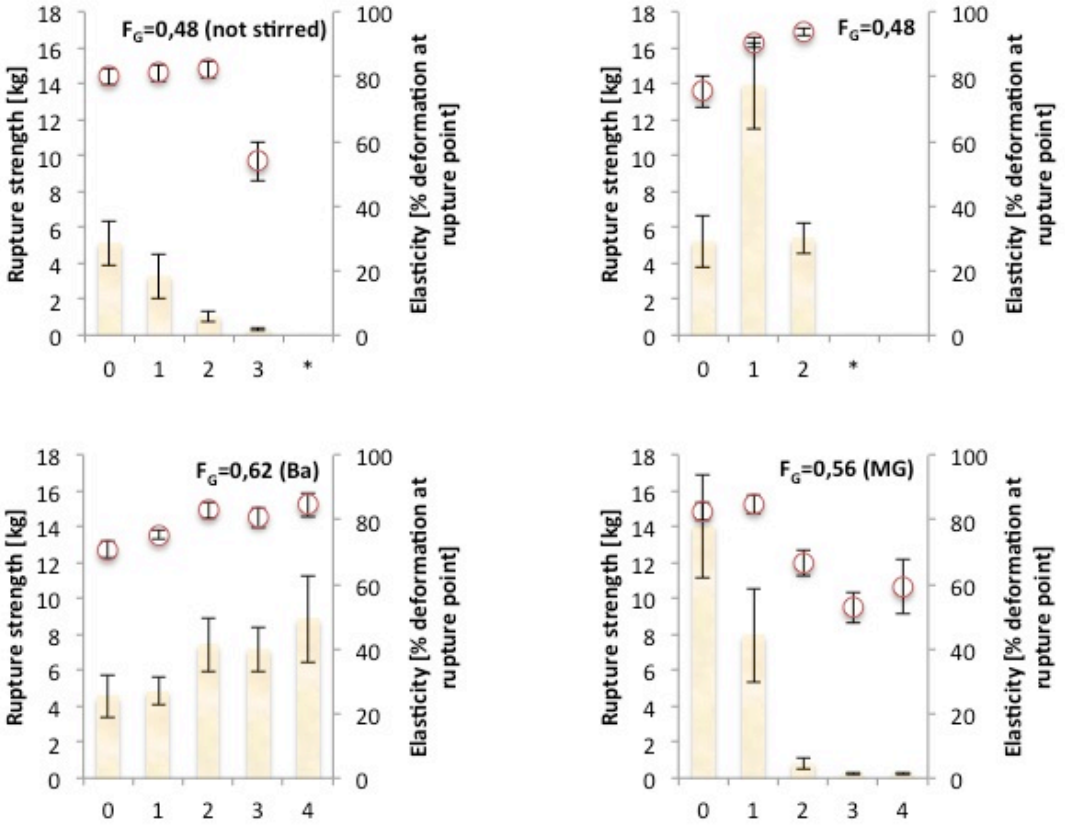

Figure 29. Measured rupture strength [kg] (columns) and elasticity [% deformation at rupture point] (circles) during the saline treatments, as reported in (Appendix D). Data is reported as mean values ± SD (n =3-7).

As reveled by (Figure 29) there were three different behavior patterns of the rupture strength and elasticity during the saline shifts for the alginate gel batches. For the following gel batches the rupture strength and elasticity decreased, or did not change considerably, between the subsequent saline

shifts: SF60 (both batches), F_G=0,48 (not stirred) and F_G=0,56 (MG). Furthermore, for all Ca-G-gels, except F_G=0,48 (not stirred), the rupture strength and elasticity increased considerably after the first saline or second saline shift to a maximum value, which then was followed by a profound decrease during the next saline treatment. This decrease was due to that the gels were not stable and had problems keeping up their own weight. Finally, the rupture strength and elasticity of the Ba^{2+} saturated gel increased after the second saline shift and during the subsequent saline shifts no significant changes occurred.

After the first saline change the respectively rupture strength of the gel batches F_G=0,48, F_G=0,60 and F_G=0,68 had increased to a maximum value that was about the double value of each saturated gel batch (before the first saline treatment). After the second saline shift the rupture strength for each of the batches decreased to values that were less than the values before the saline treatment had started. For F_G=0,60 the rupture strength did not change notably during the third saline change. However, the rupture strength of F_G=0,68 fell after the last saline shift. Finally, it is noticeable that during each of the saline shifts the rupture strength of F_G=0,60 was higher than the correspondingly values of the gel batches F_G=0,48, F_G=0,68 and F_G=0,85. Regarding the elasticity of the gel batches F_G=0,48, F_G=0,60 and F_G=0,68, it is observed that peak values were reached after the first saline change. During the following two saline shifts the elasticity decreased or did not change significantly for F_G=0,48 and F_G=0,68. Although, the elasticity of F_G=0,60 did not changed notably after the second saline treatment it increased considerably after the third saline treatment to a very high value; 96,48 ± 2,76%.

The rupture strength of the gel batch with the very high G-content, F_G=0,85, also increased during the saline shifts. Yet, it increased during the first two saline treatments, not just the first as it did for some of the other Ca-G-gels, before it reached its maximum value. The increase in rupture strength was also considerably smaller compared to the gel batches F_G=0,48, F_G=0,60 and F_G=0,68. The rupture strength before the saline treatments had started was comparatively small, 5,20 ± 0,82 kg, and after two saline shifts it had increased by about 3 kg. However, during the third saline treatment the value of the rupture strength fell and was only circa 1 kg. The elasticity followed the same pattern as the rupture strength, it first increased

statistically significantly (p=0,05) during the first two saline treatments, and then it decreased after the third saline change.

The initial rupture strength value of F_G=0,56 (MG) was 14,04 ± 2,89 kg, and it was the highest among the gel batches. Remarkably, after the first saline shift the value had been reduced to about 7,94 ± 2,60 kg. After the second saline change the decrease was even more profound and the value was about ten times smaller. However, the rupture strength did not change notably during the two last saline treatments. The elasticity of F_G=0,56 (MG) did not change significantly during the first saline changes, however, it decreased remarkably after the second one, from 84,70 ± 2,75% to 66,73 ± 4,05%. Finally, after the third saline change the elasticity had decreased to 52,70 ± 4,61% and during the last saline shift it did not change notably.

The rupture strength and elasticity of the Ba^{2+} saturated gel batch during the saline treatments changed in an unlike way in comparison to the other gel batches. The elasticity increased somewhat during the first two saline changes, however, the rupture strength only statistically significantly (p=0,05) changed after the second saline change. It was then increased by circa 2,5 kg which was about half of the value of its original rupture strength. During the last two saline changes the rupture strength and elasticity of the gel batch did not change significantly.

After the first saline treatment the elasticity of SF60 had decreased by around 20% while the elasticity of SF60 (not stirred) had been reduced by circa 10%. Additionally, the reduction of the rupture strength between the saline changes was larger for the stirred batch. For SF60 (not stirred) the most profound decline of the rupture strength occurred after the first saline shift, the original value of 5,80 ± 0,32 kg then was reduced by about 1,9 kg. During the following saline shifts the rupture strength decreased by about 1 kg. Regarding the other SF60 batch, after the first two saline treatments the rupture strength of SF60 had dropped from a value close to the one of the other SF60 batch to just a few percent of it. The rupture strength did not significantly change during the third saline shift. Also, the elasticity of SF60 did not notably change after the first saline shift, however, during the second, and especially the third saline change, the reductions were more substantial.

Even though the saline solution was not stirred the rupture strength of F_G=0,48 (not stirred) was heavily reduced during the first two saline shifts. Specifically, the initial rupture strength of 5,10 ± 1,25 kg decreased with approximately 4 kg during the first two saline shifts. Interestingly, the elasticity did not change considerably during the first two saline shifts, yet, it dropped during the third shift by about 30%.

4 Discussion

The aim of this work was to study the physical properties and stability of AlgE6 epimerized alginates. Mannuronan was used as a start material and by varying the incubation time with AlgE6 alginates with a different composition of G-and M-blocks, which had a similar degree of MG-blocks, were created. To study the effects of alternating blocks a control alginate rich of MG-blocks was formed by first performing an epimerization with AlgE4 in polyM, followed by an epimerization with AlgE6. Also, the effect of saturating an alginate rich of G-blocks in Ba^{2+} and Ca^{2+} , compared to solely Ca^{2+} , was examined.

4.1 Epimerization degree and block structure analysis

Mannuronan was epimerized with AlgE6 to compare the physical properties of alginates with different degree and length of G-blocks. This was achieved by using the same enzyme concentration and varying the epimerization time. The produced alginates had a G-content of 48% to 85%, where the number of long G-blocks increased by the G-content as seen from ^{1}H-NMR and $N_{G>1}$ (Table 2), as well as, the block structure analyses (Figure 12). Single G-residues were also established in the AlgE6 epimerized alginates and the MG-content was between 8% and 10% (Table 2). In conclusion, the G-content in epimerized mannuronan can effectively be adjusted by varying the incubation time.

The chromatogram of F_G=0,85 revealed that it consisted of long G-blocks that were not present in the other epimerized alginates (Figure 12). As further discussed in (Section 4.1.1), F_G=0,85 was formed when F_G=0,60 was epimerized with AlgE4 and this was most likely due to the re-activation of AlgE6 that made it dominate the epimerization reaction. Therefore, the end result was an alginate with a very high G-content, instead of an alginate rich in alternating sequences. Nor it is likely that G-blocks were introduced by AlgE4 as the enzyme is known to be introducing G in strict alternating manner and only minor increase in F_{GG} has been shown on natural alginates (Kurt Ingar Draget et al., 2001; Ý. Mørch et al., 2007; Ý A Mørch et al.,

2008; Strand, Mørch, Syvertsen, et al., 2003). Since the chromatogram of F_G=0,85 was very similar to the one of the reference alginate, which had been formed by AlgE6 epimerized polyM and that had a similar G-content, it seems as the final block composition of F_G=0,85, definitely, was not affected by AlgE4. Interestingly, when the chromatogram of F_G=0,85 was compared to the reference alginate that had a smaller G-content (80%), which had been formed by AlgE1 epimerization of polyM, it was clear that the reference alginate formed from AlgE1 contained some G-blocks that were even longer than in the other epimerized alginates. Even though the epimerization reaction had not reached as far in the AlgE1 reference as in F_G=0,85 and in the AlgE6 reference, revealed from the lower G-content, it had introduced longer G-block. In conclusion, AlgE1 could introduce longer G-blocks than AlgE6 in mannuronan.

From the M-block studies it was apparent that the epimerized alginates consisted of relatively short M-blocks, in relation to the G-block lengths (Figure 12,14). For example, the amount of M-blocks that were up to ten residues were about 57% in F_G=0,48 and around 89% in F_G=0,85. The presented example also reveals the trend that an increasing G-content resulted in a M-block distribution mostly consisting of short M-residues. Further on, the M-blocks of F_G=0,56 (MG) were short, about 90% were not longer than ten residues. This alginate also consisted of short G-blocks, as seen, circa 78% of the G-blocks were not longer than ten residues. This alginate was made by introducing G-blocks by AlgE6 epimerization in the alginate polyMG, which almost only consisted of alternating sequences (F_{MG}=F_{MGM}=0,45). Due to the relative short epimerization time, only approximately10% of the M-blocks were converted to G-blocks, due to this, the block composition of F_G=0,56 (MG) consisted of a large amount of alternating blocks (Table 2). As a result, most of the G and M -blocks were relatively short in F_G=0,56 (MG).

The Mark-Houwink-Sakurada equation was used to estimate the intrinsic viscosities of the epimerized alginates and as seen (Table 2), the viscosities of the examined gels varied between 1000-1200 ml/g, excluding the viscosity of F_G=0,48 (not stirred). Due to that only two parameter sets (chapt method) were used to approximate the intrinsic viscosities it is emphasized that the calculated numbers rather provide information of the magnitude of

the parameter than absolute values, especially since the used constant in several cases were to be used with alginates of another G-content, this was done due to the lack of constant for certain G-contents. In the work (Klepp-Andersen, 2010), where alginate gels made of AlgE4 and AlgE6 epimerized mannuronan were studied, the intrinsic viscosities were measured by a viscometer and varied around 1300-1450 ml/g. Although there was a small difference between the intrinsic viscosities of the two works, and thus the molecular weight, it should not affect a direct comparison of the alginates too severely.

The ^{1}H-NMR data of SF60 showed that the block composition resembled the one of F_G=0,68 as well as F_G=0,60 to some extent (Table 2). The G-content of the natural alginate was 64% and the M and MG-block composition was alike the one of F_G=0,68. According to the NMR data the average G-block length, $N_{G>1}$ was shorter compared to F_G=0,60 and F_G=0,68, however, the chromatogram of SF60 revealed that the there were a large amount of very long G-blocks in the alginate, which could not be found in the chromatograms of the epimerized alginates. There is no available chromatogram of SF60 treated with G-lyase in this work, however, studies has shown that it, surprisingly, has some very long M-blocks (Aarstad et al., 2011). Lastly, the physical properties of SF60 were in several aspects different from the epimerized alginates in this work. Despite its slightly lower molecular weight, these differences were likely due to the presence of very long G and M-blocks.

4.1.1 The re-activation of AlgE6

As seen in figure (Table 3), it was observed early in the work that the addition of EDTA followed by dialysis and freeze drying did not stop the activity of AlgE6 as introduction of epimerization buffer and temperature caused and increase in the G-blocks of the alginate. Likely, the enzyme had bound strongly to the alginate. Therefore, it was decided to use a warm water bath (95°) to denature and stop the enzyme after the AlgE6-epimeirzation. However, as seen in figure NMR when F_G=0,60 was epimerized with AlgE4 it was obvious that AlgE6 had not been stopped since the new alginate (F_G=0,85) had a very high content of G-blocks (85%) while the fraction of MG-blocks had not changed.

In general, an enzyme that is immobilized or bound to a substrate is more stable than the free and diluted enzyme, consequently, higher temperatures are required to denature them. In this work the alginates were put in a water bath (95°) for about 13 min, usually it took 3 minutes for the alginate temperature to rise to at least 85° C, so, the temperature of the alginate solution was at last 85° C for about 10 min. As stated earlier, perhaps the AlgE6 had bound so hard to the alginate that the treatment was not sufficient to denature it. However, if the protein had denatured it is possible that it could have renatured after the water bath, when the temperature was normal again. Since the molecular weight of AlgE6 is 90,2 kDa (Holtan et al., 2006) and the cutoff weight for the used dialysis filter was smaller (12-14 kDa) any intact AlgE6 (both enzyme that had not denatured and enzyme that could have renatured) would not have been separated from the alginate during the dialysis and had been able to bind the alginate again. Consequently, during the AlgE4-epimerization when Ca^{2+} was added and the temperature rose the enzyme was activated again. Another explanation to the low enzyme activity of AlgE4 could be due to its substrate preference. It has been shown that a hexameric oligomer of M-blocks is the minimum length required for enzyme activity (Campa et al., 2004) and due to that a majority of the M-blocks of F_G=0,60 were between one and ten sequences long (Figure 14) there was a risk for decreased enzyme activity. An additional argument for the last hypothesis is that the AlgE4 activity obviously was higher in the AlgE6 epimerized polyM alginate that had had a M-content of about 89% (Table 3). Also, it has been shown that AlgE4 readily could epimerize several natural alginates (Kurt Ingar Draget et al., 2001), which likely consisted of long M-blocks as it has been shown that these longer blocks seems to be characteristic for several natural alginates (Aarstad et al., 2011). Finally, a third reason to why no new alternating blocks were formed could be that AlgE6 processed most of the MG-blocks that were formed by AlgE4 to GG-blocks. So, is there a way to introduce alternating blocks by AlgE4 in AlgE6 epimerized mannuronan? As discussed, there are two reasons behind the low activity of AlgE4. Firstly, it is due to the re-activation of AlgE6 and secondly, it seems as it is hard for AlgE4 to process the substrate. The first problem could possibly be solved by using acid precipitation to separate the alginate from AlgE6 before the AlgE4-epimerization. However, the yield of the technique usually is low, and so, a large amount of alginate should be epimerized in the first step so there is a sufficient quantity of alginate for the second epimerization with AlgE4. The second problem is harder to deal with

but one strategy could be to use a higher concentration of the AlgE4 to increase the activity of it.

4.1.2 Kinetics and substrate preference of AlgE6

In this study the same reaction parameters and enzymes were used when polyM was epimerized with AlgE6 to form F_G=0,48, as well as, when polyMG was epimerized to F_G=0,57 (MG) (Table 2). As seen, the increase of the G-content was much higher when mannuronan was used as substrate. This result agrees well with the findings of (Holtan et al., 2006) where it was shown that AlgE6 most efficiently introduced G-blocks in mannuronan followed by *L., hyp* leaves and polyMG. Also, in this article it was obvious that the AlgE6 epimerization of mannuronan was as fastest when some G-blocks had formed and there were many available M-blocks. This trend was also seen in the performed activity test (Section 3.2.2) where the epimerization activity of AlgE6, with polyM as substrate, was documented over time. An important observation from the experiment was that 24 hours after the reactions had started the epimerization degree of the activity test and the control, where a double amount of AlgE6 was used, were alike. Since the last measured F_G was alike a less amount of enzyme could be used to reach the desired epimerization degrees in reasonable incubation times.

4.2 Physical properties of alginate gel cylinders

In the following sections the physical properties of the gel batches are discussed.

4.2.1 Gel appearance and water release after compression

There was a correlation between the stability state of an alginate gel and its behavior and appearance after a full compression. In this work three different gel states were defined –stable, starting to dissolve/dissolving, dissolved –and used to characterize gels. As shown, there was a relationship between the gel appearance after a full compression and the weight-normalized water release. When an alginate gel started to dissolve the water release increased and when the gel had dissolved, the water release was close to the original value of the non-saline treated gel. However, as stated in (Section 3.4.1) the calculated values were likely overestimated for unstable gels. Also, the standard deviations were quite high for most data points for each gel due to the relatively heterogeneous compression pattern of the gels as well as the difficulties of collecting the alginate after the compression. To my best knowledge, there are no publications that study the gel appearance and water loss in alginate gels after a full compression, so, much can be done in future work to improve the measuring method. For example, a water-absorbing napkin, placed under the gel to capture the water, could be tried for the weight difference measurements.

The hypothesis that the normalized water release increase as an alginate gel becomes more unstable was confirmed by the behavior of the gels F_G=0,62 (Ba) and SF60 (not stirred). These gels were stable during all saline shifts, so, the water release should not have increased during the saline shifts. This was also observed; after the first characteristic decrease in water release, which all gel batches experienced, it did not change considerably throughout the saline shifts. The water release behavior of the stable gel batch F_G=0,56 (MG) started to increase at a regular pace after two saline shifts and after four saline changes the value was close to the one of the non-saline treated gels. Since the gel appearance after two or more saline shifts were alike the one of an alginate gel that had started to dissolve it seems as the suggested model, which connect gel stability with gel appearance after full

compression studies, cannot be applied to gels containing a large amount of alternating sequences, in this case about 36%.

4.2.2 Syneresis of the alginate gels

An increasing content of G-blocks in Ca^{2+} saturated alginate gels usually results in lower syneresis (Moe et al., 1995) and this pattern was also seen for the Ca-G-block gels and F_G=0,62 (Ba).

The two gel batches of the natural alginate SF60 underwent the smallest syneresis followed by F_G=0,85. As seen in the chromatogram of the M-lyase treated alginates (Figure 11) SF60 consisted of large fractions of long G-blocks that were not present in the epimerized alginates. However, there was a substantial fraction of relatively long G-blocks (not as long as in SF60) in F_G=0,85, in relation to the other epimerized alginates. Additionally, as determined by ^{1}H-NMR, F_G=0,85 had the longest average G-block length of all examined alginates (Table 2). Taken together, since SF60 clearly experienced the lowest syneresis and there were longer G-blocks in the alginate compared to the high G alginate F_G=0,85, the data suggested that the G-length, rather than the G-content, determined the syneresis. Finally, studies (Aarstad, 2013; Klepp-Andersen, 2010) have as well revealed that long G-blocks lower the syneresis of alginate gels.

Despite that the total G-content and molecular weight of F_G=0,56 (MG) and F_G=0,60 were comparable, the degree of syneresis was much higher for gels prepared from F_G=0,56 (MG). In fact, the gel clearly experienced the highest degree of syneresis of all the examined gels. As seen in (Table 2) the content of alternating blocks in F_G=0,56 (MG) was about three times higher in relation to the other AlgE6 epimerized alginates, which were dominated by M-blocks in between the G-blocks. Moreover, in the literature there are examples of that higher degrees of alternating blocks lead to higher syneresis in Ca^{2+} saturated alginate gels (Kurt Ingar Draget et al., 2001; Kurt I. Draget et al., 2000; Ý A Mørch et al., 2008; Strand, Mørch, Syvertsen, et al., 2003). Definitely, the high degree of syneresis in F_G=0,56 (MG) was caused by the relatively high content of MG-blocks.

There was no significant difference in syneresis between the gel batch F_G=0,62 (Ba), which was saturated in Ba^{2+} and the two gel batches F_G=0,60 and F_G=0,68, which were saturated in Ca^{2+}, and had a similar block

composition and weight compared to F_G=0,62 (Ba). Apparently, the Ba^{2+} saturation did not affect the initial syneresis since similar alginate gels saturated in Ca^{2+} experienced a similar degree of syneresis. Nevertheless, it should be noted that F_G=0,62 (Ba) was saturated in 20 mM $BaCl_2$ and 30 mM $CaCl_2$, consequently, there were Ca^{2+} ions present in the gel network that likely contributed to the outcome that the gel properties were similar between the three discussed alginates.

The two alginates with a total G-content of 48% had a similar block distribution. However, the molecular weight of F_G=0,48 (not stirred) was considerably less than the one of F_G=0,48. Since it has been reported that increasing molecular weights result in higher syneresis (Kurt Ingar Draget et al., 2001) it was anticipated that the syneresis of the gel batches would differ. But, there was no significant difference between the gels and apparently the molecular weight difference did not affect the gel batches in this aspect.

4.2.3 Swelling of the alginate gels during the saline treatments

During the saline shifts the gelling ion Ca^{2+} is replaced in the alginate-network by the non-gelling ion Na+ and this leads to a weaker gel. Due to the increasing concentration of Na+ water flow into the gel and this results in osmotic swelling (Thu et al., 1996). In this work increasing gel stability against swelling was observed in alginate gels that had the following structural features: G- and M-blocks (stability increased with an increasing G-content) < long G-blocks < MG-blocks < saturation with the high affinity ion Ba^{2+}.

In regard of swelling all gel batches handled the first saline shift well and the respectively volumes had not changed noticeably after it. However, during the second saline shift it was obvious that the swelling was depending of the chemical structure of the alginate. Among the gel batches that were formed from AlgE6 epimerized mannuronan it was seen that F_G=0,68 had swelled less than F_G=0,48 and F_G=0,60. After the third saline shift it was not possible to compare these three gels since F_G=0,48 had dissolved after two saline shifts and the gels of F_G=0,68 had started to lose alginate, which resulted in that the measured volume did not change. It seems as the increase in volume due to the saline shift and the less amount of alginate in the gels, cancelled

themselves out. The gels of F_G=0,85 had as well begun to lose alginate after three saline shifts, and so, a decrease in the volume was also detected. In conclusion, the data from the second saline shift made it possible to compare how the G-content in alginate gels, which mostly consists of G- and M-blocks, affects the swelling and it was then observed that a higher G-content lead to more stable gels against swelling. In addition, the study (Klepp-Andersen, 2010) observed how an increasing G-content in alginate gels, which mostly comprised of G- and M-residues, resulted in gels that swelled less.

After the saline treatment the swelling had increased with about 20% in the both gel batches with a G-content of 48%. Therefore, it seems as there was a defined limit for how much the gels could swell before they dissolved. Remarkably, among the Ca-G-gels this so called "swelling limit" decreased with an increasing G-content except for the gel batch F_G=0,60 that experienced the highest swelling. However, as stated earlier the volume of F_G=0,68 did not change after the third saline shift due to the gels had started to lose alginate, and so, the swelling of F_G=0,60 appeared to be relatively higher compared to F_G=0,68 than it had been if F_G=0,68 had not started lose alginate. In the study (Klepp-Andersen, 2010), where the swelling behavior of gels made from AlgE6 epimerized polyM was examined, the swelling limit was also decreasing with a rising G-content. Unfortunately, in this work the limit could not be compared between the batches of SF60 since the batch that was treated in saline solution that was not stirred did not dissolve, in contrast to the other. Most likely, the slower exchange of Ca^{2+} ions with Na^{+} ions in the gel network where the saline solution was not stirred, compared to the stirred, was the main reason why the last measured syneresis values of the gel batches differed so substantially.

When the swelling behavior of SF60 and F_G=0,60 during the three saline shifts were compared it was concluded that SF60 was more stable (fig x b). Since the G-content of the two gels were similar, 60% respectively 64%, and SF60 consisted of some very long G-blocks that was not found in the epimerized alginates (Figure 12) it seems as long G-blocks give more stability against swelling. Furthermore, when the swelling development of F_G=0,56 (MG) and SF60 were compared it was clear that the first mentioned alginate had swelled less (fig x b). Since the G-content in F_G=0,56 (MG) was less than in SF60 (Table 2) and the most G-blocks of F_G=0,56 (MG) were relatively short (Figre 12), it is certain that the great amount of alternating blocks lead to more stable gels. Also, in the study (Ý. Mørch et al., 2007)

where alginate beads were prepared from AlgE1 epimerized polyMG, it was observerd that the MG-rich beads swelled less than the beads prepared from *L.hyp.,* stipe. Furthermore, in the literature there are examples of how AlgE4 epimerization of natural alginates results in more stable gels (Donati et al., 2009) and microcapsules (Strand, Mørch, Syvertsen, et al., 2003).
The concentrations and type of gelling ions used to saturate alginate gels have shown to alter the swelling behavior (Ý. A. Mørch et al., 2006), likewise, this was observed in this study. Even though the block distribution (Table 2, Figure 12,14) and molecular weight (Table 2) of the Ba^{2+} saturated gel resembled the one of F_G=0,60 and F_G=0,68, it behaved very differently from them, clearly, the Ba^{2+} ions in the network gave the gel different properties compared to the other G-block rich and Ca^{2+} saturated alginate gels. After the first two saline shifts the volume of F_G=0,62 (Ba) had decreased and throughout the last two saline changes the volume did not change noticeably. It is important to remember that both Ca^{2+} and Ba^{2+} ions were present in the gel network since the gels were saturated in 20 mM $BaCl_2$, 30 mM $CaCl_2$ and 0,2 M NaCl. Additionally, alginates affinity of Ba^{2+} is higher compared to Ca^{2+} and Na^{+} (Haug & Smidsrod, 1970). Taken together, it is tempting to suggest that during the first two saline shifts, when the volume decreased, the Ca^{2+} -ions in the gel network were outrivaled and replaced by the Na^{+} ions, due to the vast abundance of them. However, since the volume did not change particularly during the last saline changes it looks as despite that there were many Na^{+} ions present in the solution the alginates affinity towards the Ba^{2+} ions was so strong that they could not be replaced.

4.2.4 Dimensional stability

During the saline treatments the dimensional stability of the gel batches depended on the block composition and gelling ion. However, it seems as the molecular weight did not affect the final relative volume since the two gels batches with the G-content 48%, which had a comparable block composition but two considerably different molecular weights (242 kDa and 155 kDa,) had swelled equally after the saline treatments.

To study the effect of the total G-content it is appropriate to compare the three alginates F_G=0,48, F_G=0,60 and F_G=0,68 since they had a similar molecular weight and content of MG-blocks (Table 2). However, the

changes in their respectively relative volumes were low after one saline shift. Moreover, after three shifts, F_G=0,48 had dissolved and alginate from gels of F_G=0,68 had started to detach. Consequently, only the relative volumes after two saline shifts could be evaluated to examine the dimensional stability. As seen in (Figure 25 a), the relative volume of F_G=0,48 was 1,66 ± 0,06 and the respectively corresponding values of F_G=0,60 and F_G=0,68 were 1,45 ± 0,03 and 1,20 ± 0,07. Evidently, a higher G-content resulted in more stable alginate gels and this trend has been observed before (Martinsen et al., 1989; Strand, Mørch, Syvertsen, et al., 2003; Thu et al., 1996). Regarding F_G=0,85 it was obvious that the high G-content and relatively long G-blocks affected the dimensional stability. During the first two saline shifts the relative volume did not change noticeably compared to the other Ca-G-gels. However, after the third shift alginate had started to come off from the gels and the gels clearly had been affected by the saline treatments. The appearance of F_G=0,68 was alike after three saline shifts, noticeably, the two Ca-G-gels with the highest G-content had started to lose alginate. It seems as most of the Ca^{2+} in the alginates was washed out during the three saline shifts since all the Ca-G-gels had dissolved after four saline shifts. The two highlighted alginates likely had the highest number of crosslinks in the network before the saline treatments had started, this means that the re-organization of the alginate was very intense when the crosslinks were broken down, possibly this comprehensive alteration of the gel network lead to the detaching of alginate from the gels.

The relative volume increase of F_G=0,56 (MG) was comparable to F_G=0,60 during the first two saline shifts, though, after the third saline shift F_G=0,56 (MG) had a lower relative volume than F_G=0,60. This pattern was expected since the articles (Donati et al., 2009; Strand, Mørch, Syvertsen, et al., 2003) showed that the insertion and elongation of alternating blocks by AlgE4 resulted in more stable alginate gels. However, the actual dimensional stability of F_G=0,56 (MG) cannot solely be described by its relative volume change. As seen in fig (Figure 25), it is clear that the dimensional stability of F_G=0,56 (MG) was superior to the one of F_G=0,48 and F_G=0,68. Also, when the appearance of F_G=0,56 (MG) and SF60 after four saline shifts are compared (Figure 17,21) and fig X) it is clear that F_G=0,56 (MG) better handled the saline treatments. Furthermore, the gel batch F_G=0,56 (MG) had a considerably lower weight, 0,76 ± 0,02g, after the saturation process in relation to the other gels (Appendix D). The dimensional stability was defined as the quotient between the weight of the saline treated gel and its

initial weight after saturation. Therefore, the relative volume change of F_G=0,56 (MG) was more sensitive towards small absolute weight differences.

In this work an attempt was made to create an alginate that both consisted of longer G-blocks and MG-blocks. This was done by first performing an AlgE6 epimerization with polyM, followed by a warm water bath and a final epimerization by AlgE4. As discussed in (Section 4.1.1), the warm water bath did not stop the re-activation of AlgE6 and the end result was the alginate F_G=0,85. If AlgE6 had been stopped and AlgE4 had converted the majority of the M-blocks to MG-blocks, the alginate likely had been one of the most stable since it would had both consisted of long G-blocks, which have been shown to improve the stability (Martinsen et al., 1989; Thu et al., 1996), as well as alternating blocks. Consequently, the discussed alginate likely had been more stable than F_G=0,56 (MG) since the alginate lacked longer G-blocks (Figure 12). This was due to that the first epimerization with AlgE4 created an alginate almost only consisting of alternating blocks (Table 2), which then were converted to G-blocks. This reaction was different to the one that would have occurred in the other discussed alginate, where M-blocks would have been converted to MG-blocks.

The two different gelling ions used in the work indeed affected the dimensional stability. The Ba^{2+} saturated gel batch shrunk during the first two saline treatments and after the final two treatments the relative volume had not changed noticeably. It was during the two first shifts that the volume changed and it appears as the majority of the Ca^{2+} ions were washed out from the gel network during these shifts. It should be noted that the gels were saturated in a solution where the concentration of Ca^{2+} ions was 50% higher than the one of Ba^{2+} ions. If a higher part of Ba^{2+} ions had been used then perhaps the gels had shrink less due to that the saline shifts had been less effective in re-organizing the gel network.

As shown in (Figure 25) the gel batch SF60 undoubtedly was more stable than the Ca-G-gels. Noticeably, the gels of SF60 and F_G=0,85 had a similar dimensional stability during the first two saline shifts. Taken together, it is evident that the long G-blocks (Figure 12) of SF60 improved its stability.

Additionally, the study (Klepp-Andersen, 2010) also showed that AlgE6 epimerized polyM was more stable than SF60 during saline treatments.

In conclusion, when dimensional stability is examined it is important not to only consider the relative weight difference. In this work it was shown that an alginate gel with a rich content of alternating blocks better handled a stressful saline treatment than gels prepared from AlgE6-epimerized mannuronan and the natural alginate *L.hyp., stipe*. Evidently, the alginate gel stability was more dependent of the order of G and M-blocks than the G-content and G-block lengths. However, since the gels formed from *L.hyp.,* stipe were more stable than the ones prepared from AlgE6 epimerized mannuronan the G-block lengths also were important. Also, among the gels prepared from AlgE6 epimerized it was evident that a higher G-content lead to better stability. Finally, the choice of gelling ions as well significantly affected the gel stability as presented.

4.2.5 Young´s modulus of the saturated gels

As seen in (Figure 26), the AlgE6 epimerized gel batches that had the highest G-content, F_G=0,85 and F_G=0,68, had statistically significantly (p=0,05) higher E values than both the gel batches that had a G-content of 48%. Due to the very large standard deviation of F_G=0,60 it is difficult to compare it to other gels, nonetheless, earlier work has shown (Ý. A. Mørch et al., 2006) that higher G-content in alginate gels leads to higher gel strength and this trend could as well be anticipated in this works data.

As revealed by fig xx, the Young´s modulus of SF60 was undoubtedly the highest among the studied gels. Interestingly, in the study (Ý A Mørch et al., 2008) the Young´s modulus of SF60 was about 26 kPa, which is close to the values in this study. Although the molecular weight of SF60 was lower compared to F_G=0,68, which had a similar G-content, the Young´s modulus of SF60 was considerably higher. In the literature (Ingar Draget et al., 1990; Moe et al., 1995; Skják-Bræk et al., 1986) it has been shown that long G-blocks tend to increase the Young´s modulus of alginate gels, clearly, this trend was also observed in this study. Furthermore, F_G=0,85 had a relatively

high E, although not statistically significantly (p=0,05) higher compared to F_G=0,60 and F_G=0,68. Despite the non-significant result it appears as the long G-blocks in F_G=0,85 as well increased its Young´s modulus, however, not to the same extent as the natural alginate. Finally, in the article (Ý A Mørch et al., 2008) Ca^{2+} saturated gel cylinders were prepared from AlgE6 epimerized mannuronan, which had a G-content of 88% and a similar block distribution as F_G=0,85 in this study according to (Table 2). The Young´s modulus of the alginate with the G-content 88% was higher than F_G=0,85, the respectively values were about 26 kPa and 18 kPa. The difference could partly be due to the somewhat higher G-content.

Even though the alginate F_G=0,56 (MG) had a similar molecular weight and G-content similar to F_G=0,60 its Young´s modulus was statistically significantly (p=0,05) smaller compared to it. In a study (Ý A Mørch et al., 2008) where G-blocks were introduced by AlgE1 or AlgE6 on a polyalternating alginate (F_{MG}=F_{GM}=F_{MGM}=0,46) it was evident that the gels prepared from the MG-rich alginate had a considerably lower Young´s modulus than the gels where G-blocks had been inserted, specifically, the more introduced G-blocks the higher Young´s modulus. In this context, possibly, it is not so extraordinary that the gels prepared from F_G=0,56 (MG) were rather weak since few G-blocks had been introduced. Although, it should be noted that gels made, according to the same protocols as used in this work, of the alginate "polyMG + AlgE6, F_G=0,55", which had a comparable block composition, in the article (Ý A Mørch et al., 2008), had an Young´s modulus of 13 ± 0,5 kPa which was notably larger than the measured value in this work. Likely, the most probable explanation to the relatively low E value was the lack of long G-blocks as revealed by the G block studies (Figure 12). The G-block study displayed that a great part of the G-blocks in the alginate were quite short, while the content of longer G-blocks were very low.

The Young´s modulus in alginate gels has shown to increase when a high affinity crosslinking ion is used (Haug & Smidsrod, 1970), however, the opposite effect was seen for the Ba^{2+} saturate gel batch. Specifically, the Young´s modulus was statistically significantly (p=0,05) smaller in relation to the Ca-G-gels. However, as discussed (Section discussion on E and saline shift) the Young´s modulus of the Ba^{2+} saturated gels were relatively stable during the saline shifts, compared to the Ca-G-gels. As seen in (Figure 19)

the gels were formed as small bullets after the Ba^{2+} saturation, as well as, during the saline treatments. The distinctive geometry might have affected the measured Young´s modulus since the areas of the other gel batches were larger and more defined. Conclusively, the smaller and more irregular area of the Ba^{2+} saturated gels could have resulted in that a higher pressure, due to a lower contact surface in relation to the other gel batches, was applied during the compression studies that resulted in underestimated values. However, it is striking that the standard deviation of the batch was low, and so, the Ba^{2+} saturated gels behaved alike during the compression studies.

The Young´s modulus of the two gels with the G-content 48%, which had a comparable block distribution but considerably different molecular weights (Table 2), differed extensively and the value of F_G=0,48 was more than the double of the other gel batch. This difference was likely due to the difference in molecular weight since it has been shown (Martinsen et al., 1989) that Young's modulus increases with a higher molecular weight, up to a certain threshold.

4.2.6 Young´s modulus during the repeated saline treatments

During the saline shifts crosslinks are broken down when Ca^{2+} ions are replaced by the non-gelling ion Na^{+}. The fewer crosslinks in the gel network lead to a decrease of the gel strength as reflected by the lower Young´s modulus. In general, a high G-content in an alginate gel is crucial for high gel strength due to the enhanced potential of crosslinks to form. In this work, the Ca^{2+} saturated alginate gels were sensitive towards the saline treatments. As seen in (Figure 27) the Young´s modulus for the Ca-G-gels (except F_G=0,85) and SF60, had after two saline shifts, resulted in a comprehensive reduction of the gel strength, specifically, the Young´s modulus had decreased by 90% or more for all the mentioned gel batches. Furthermore, after another saline change the mean values of Young´s modulus was reduced to less than 1 kPa (mostly low standard deviations) for each of the Ca-G-gels. In the work (Klepp-Andersen, 2010) where alginate gels, made from AlgE6 epimerized mannuronan of different epimerization degrees as well as SF60, were treated in saline solution the Young´s modulus generally decreased less than in this study. Since the gels were prepared using the same methods and alike materials the differences should be due to that the saline solution treatment was gentler, as compared to the one in this thesis.

Apparently, the exchange of Ca^{2+} with Na^{+} was slower which lead to slower destabilization of the gels. This effect was seen in this work as the E-value of the SF60 batch, which was stirred during the saline treatments, decreased more during the corresponding saline shifts compared to the batch that was treated in saline solution, which was not stirred.

The E-values of the Ca-G-gels, except the two gel batches with a G-content of 48%, were statistically significantly (p=0,05) higher after saturation compared to F_G=0,56 (MG) and F_G=0,62 (Ba) (Figure 26). However, after two saline shifts (three for F_G=0,85) the Young´s modulus of each Ca-G-gel was considerably smaller compared to F_G=0,56 (MG) and F_G=0,62 (Ba). The E-values of F_G=0,62 (Ba) and F_G=0,56 (MG) were alike before and after the saline treatments. The absolute and relative gel strength were alike during the saline changes, except for the Young´s modulus of F_G=0,56 (MG) decreased more after the first saline shift compared to F_G=0,62 (Ba). After two saline changes the Young´s modulus for each of the gels was about 30% of the initial value. Since the relative gel strength only decreased slightly after the two last saline changes it seems as most of the Ca^{2+} ions were exchanged during the first two saline treatments.

Despite that the saline solution was not stirred in F_G=0,48 (not stirred) the Young´s modulus decreased in a similar way as F_G=0,48 during the first two saline changes. After the third and last change, the gel strength barely had changed, most likely due to that the gel already had lost most of its strength and that the saline was not stirred. As discussed in (Section 4.2.5) the difference in molecular weight between the two gel batches seem to have resulted in a substantially lower Young´s modulus for the gel that was not stirred during the saline treatment. Taken together, the data suggests that the lower molecular weight made the gel strength of the alginate gel more sensitive towards saline treatments.

4.2.6.1 Berg hypothesis – a proposal for the gel strength behavior of SF60 and F_G=0,85 during the saline treatments

An analyze explaining why the gel strength of SF60 decreased as quickly as it did during the saline changes is proposed in in this part. SF60 had longer G-blocks than F_G=0,85 (Figure 12) and its Young´s modulus after saturation

was by far the highest of all examined gels (Figure 26). However, it was less stable than F_G=0,85 since it took two, and not three saline treatments as it did for F_G=0,85, to reduce the gel strength to only a few percent of the original one. In detail, as seen in fig (Figure 27) the respectively absolute Young´s modulus values of F_G=0,85 was higher than SF60 after one and two saline shifts. So, why was F_G=0,85 more stable? An important difference was that the G-content of SF60 was 64% (Table 2), and so, the total fraction of G-blocks was considerably higher in F_G=0,85. In this work it was showed that the reduction of Young´s modulus during the first saline treatment was less in alginate gels that had higher G-content. Specifically, the Young´s modulus of the two gel batches F_G=0,68 and F_G=0,60 were similar before the saline treatments had started, however, after the first saline shift the gel batch with the higher G-content had a statistically significantly (p=0,05) higher Young´s modulus, which was about 55% of the original value, while the value of the other gel batch was circa 42% of the initial E value. Also, as emphasized previously (Ý. A. Mørch et al., 2006) alginates with a high G-content have more possibilities to bind divalent ions, thereby, more crosslinks are formed which ultimately results in stronger gels. Moving on, the gel batch of SF60, which was not stirred during the saline shifts, behaved differently from the other SF60 batch due to the smaller exchange rate of Ca^{2+} ions with Na^{+} ions in the gel network. After the first saline treatment the gel strength decreased by about 20%, while the gel strength of the saline-stirred batch decreased by around 70%. However, after the second saline shift the gel strength of the non- stirred gel batch was about the half, obviously, the great reduction in gel strength, which was observed during the first or second saline shift for all gel batches, occurred then. This delay of the drop in gel strength for SF60 was also seen in the study (Klepp-Andersen, 2010) since the Young´s modulus did not change meaningfully during the first saline change, instead, the reduction occurred after the second change. In the report an alginate gel, formed from an epimerization of polyM with AlgE6 and AlgE4 (just as F_G=0,85 in this thesis work) with a total G-content of 77%, also was examined. There was no lyase-block study performed on it, however, it is safe to assume that the alginate contained a substantial amount of long G-blocks, like the alginate F_G=0,85 in this work, which were longer than the longest in the other epimerized alginates, but at the same time, not as long as the longest in SF60. Additionally, the NMR-data in (Klepp-Andersen, 2010) showed that the mean average length in F_G=0,77 of the G-blocks was the longest of all examined alginates, analogous to F_G=0,85 in this study. Finally, the alginates relative high Young´s modulus leads to the conclusion that it had longer G-blocks

compared to the other epimerized gels, however, not as long as the longest in SF60. Interestingly, the Young´s modulus of F_G=0,77 in (Klepp-Andersen, 2010) was reduced to around 67% of the initial value after the first saline change, evidently, there was no delay for the drop in gel strength. Moving on, an important observation in the described work (Klepp-Andersen, 2010) was that the gel the gel strength of F_G=0,77 and SF60 was about the same before and after the four saline treatments. Specifically, after the final saline treatment the Young´s modulus of F_G=0,77 was 1,23 ±0,09 kPa, which corresponded to about 9% of the original value and after the last saline shift the Young´s modulus of SF60 was 1,99 ± 0,18 kPa which was equal to around 14% of the initial value. This data revealed that, in regards of the gel strength, F_G=0,77 and SF60 were equally stable. To conclude so far it seems as long G-blocks in alginate gels can delay the first big decrease in Yong´s modulus that generally occurs during reoccurring saline treatments. Also, due to the stirring of the saline solution in this work the mass transport and exchange of Ca^{2+} ions with Na^{+} ions in the gel network increased. Because of this condition, there was no delay in the decrease of Young´s modulus in the gel batch SF60, however, there was a delay for the other gel batch SF60 (not stirred). Additionally, due to a relative gentle saline treatment process in the work (Klepp-Andersen, 2010) it took two saline treatments to comprehensively lower the Young´s modulus of the SF60.

In this part of the analysis a hypothesis is made by reflecting over the summary above. Since the longer G-block seem to postpone the drop in gel strength during saline shifts it is likely to assume that it takes a relatively long time for the Na^{+} ions to break as many stabilizing crosslinks in the long G-blocks so that the gel strength is largely disrupted. Apparently, the longer G-blocks seem to work like a mountain (or “berg” in Swedish and Norwegian) that protects and shields a valley. A consequence of this hypothesis is that alginate gels that lack longer G-blocks do not have this protection, and as seen in this work and the report (Klepp-Andersen, 2010), each of the AlgE6 epimerized mannuronan gels, except F_G=0,85 in this study, have a substantial smaller gel strength after the first saline shift. If we again consider the alginate SF60 or any other alginate containing long G-blocks, how does the physical properties change when the junctions that are formed from the long G-blocks break? As presented in (Aarstad, 2013) the long G-blocks affect the gel properties significantly, for example the presence of them seem to lower the syneresis, increase the gel strength and lower the rupture strength. Thus, when the mentioned blocks disappears the gel properties drastically change and this is likely the main reason for the

large decrease in gel strength that SF60 experience. But, is there a way for the gel properties to stand strong when the protection falls? It seems so, as shown, the relative gel strength of F_G=0,85 (which comprised of long G-blocks, although, shorter than the longest in SF60) was higher than the one of SF60 after the first saline change. If we return to the first question, was there a significant structural difference between SF60 and F_G=0,85? The answer was that the G-content of F_G=0,85 was substantially higher. As shown earlier (Table 1) a higher G-content in alginate gels often results in gel properties similar to those three earlier mentioned (lower syneresis and rupture strength, increased gel strength). In conclusion, due to the comparatively low G-content in the SF60 alginate the gel properties changed extensively after the junctions, which were formed by the long G-blocks, had been ruptured during the first saline shift. Moreover, the high G-content in F_G=0,85 protected the gel properties after the junctions, formed by the long G-blocks (which were shorter than the longest in SF60), had been ruptured. Likely, these longer crosslinks were dissolved already during the first saline change since it appears as the junctions, formed from the long G-blocks in SF60, broke during the first saline shift. During the second saline shift the gel strength of F_G=0,85 decreased comprehensively, just as the other epimerized gel batches and SF60 did in this work during the first saline treatment. Finally, during the third and last saline shift the remaining intact crosslinks were easily broken down by the Na^+ ions, which ultimately lowered the gel strength to only a few percent of the original one.

To conclude, the Berg hypothesis predicts that long G-blocks in an alginate network works as a protecting mountain that up-keeps the gel properties. However, when the long crosslinks are broken the G-content of the alginate needs to be high in order to avoid a chock in the gel network, which otherwise leads to a drastically change of the gel properties.

4.2.7 Rupture strength and elasticity of the saturated alginate gels

During the compression studies there are many factors that decide when an alginate gel breaks. Due to the complicated system, as compared to other measurements, for example the syneresis, the standard deviations typically are rather high.

The elasticity of the Ca-G-gels was similar, the only statistical significant difference was that the elasticity of F_G=0,68 was higher than the one of F_G=0,85. In the literature(Aarstad, 2013; Klepp-Andersen, 2010) it has been shown that the elasticity of Ca^{2+} saturated alginate gels tends to be decreasing with an increasing G-content, obviously , this relationship was also valid for the two mentioned alginate gels. Moreover, the rupture strength of the Ca-G-gels was, like the elasticity, similar between the gels. The only statistically significant (p=0,05) difference was that the rupture strength of F_G=0,60 was higher than the other Ca-G-gels, except for F_G=0,68. Likewise with the elasticity of alginate gels, the rupture strength of alginate gels has been shown to be decreasing with an increasing G-content (Aarstad, 2013; Klepp-Andersen, 2010) as well as increasing G-block length (Ý A Mørch et al., 2008), likely, this explains why the rupture strength of F_G=0,60 was higher compared to F_G=0,85. It is harder to explain why the rupture strength of F_G=0,60 was higher than the both gel batches with a G-content of 48%. Moreover, since the molecular weight of F_G=0,48 was considerably higher than the one of F_G=0,48 (not stirred) (Table 2), and as rupture strength increases with increasing molecular weight (Moe et al., 1995), it was surprising that the rupture strength of the two gel batches was alike.

In the article (Ý A Mørch et al., 2008) G-blocks were introduced in polyMG by epimerization with AlgE1 or AlgE6. When the AlgE6 epimerized gels, which had the G-content 55%, 63% and 72% are compared to the gel batches F_G=0,48, F_G=0,60 and F_G=0,68 from this study it is seen that the elasticity of the corresponding gel batches were similar. This observation is surprising since the higher amount of alternating blocks in the alginates from the study (Ý A Mørch et al., 2008), compared to the alginates in this study (Table 2), should have resulted in even more elastic gels. When the rupture strengths of the discussed alginate gels are compared it is observed that the gels in this thesis tend to have slightly higher rupture strengths. As mentioned, the alginates in the study (Ý A Mørch et al., 2008) comprised of more MG-blocks and these alginates apparently was more fragile than the alginates in this study , which mostly consisted of G- and M-blocks (Table 2). Furthermore, when the AlgE1 and AlgE6 epimerized alginate gels in (Ý A Mørch et al., 2008) are related to each other it is clear that the elasticity and rupture strength was higher in the AlgE6 epimerized gels. This observation is expected since AlgE1 can introduce longer G-blocks than

AlgE6 (Figure 12) and alginate gels with longer G-blocks tend to be less elastic and have less rupture strength (Aarstad, 2013; Donati et al., 2009).

The elasticity of the two SF60 gel batches were relatively small and statistically significantly (p=0,05) smaller than all gel batches except for F_G=0,60 and F_G=0,85. The result is expected since studies (Klepp-Andersen, 2010; Ý. Mørch et al., 2007; Ý A Mørch et al., 2008) have shown that Ca^{2+} saturated alginates of *L.hyp.,* stipe have lower elasticity than AlgE6 epimerized polyMG. There was no important difference in the rupture strength of the two SF60 gel batches, or between them and the Ca-G-gels, except for F_G=0,60, which had a higher rupture strength. Since gels (Klepp-Andersen, 2010; Ý A Mørch et al., 2008), or microbeads (Ý. Mørch et al., 2007), prepared from *L.hyp.,* stipe often have lower rupture strengths, compared to gels formed from epimerized mannuronan, it was expected that the rupture strength of the two SF60 gel batches to be lower than most of the Ca-G-gel batches. In the earlier presented study (Aarstad, 2013), the rupture strength of AlgE6 epimerized polyM clearly was lowered by the addition of long G-blocks, and so, it is tempting to suggest that the long G-blocks that are present in natural alginates was the reason behind their lower rupture strength compared to epimerized mannuronan. Additionally, the previously discussed articles (Donati et al., 2009; Ý A Mørch et al., 2008) have shown that longer G-blocks (although not as long as the longest in natural alginates), which were introduced by epimerization reactions, in Ca^{2+} saturated alginate gels appeared to lower the rupture strength. These results add credibility to the hypothesis that the relatively low rupture strength of some natural alginate gels are due to their content of long G-sequences.

Despite the rather high standard deviation the rupture strength of F_G=0,56 (MG) clearly was the highest of the tested gel batches. Moreover, the elasticity of the gel was statistically significantly (p=0,05) higher than all gel batches excluding F_G=0,48 (not stirred). The total G-content and molecular weight was comparable to the one of F_G=0,60 but the gel acted very different from it, undoubtedly, the high gel strength was due to the relatively high content of alternating blocks. It is believed that when a crosslink under high pressure breaks the released energy speeds up the rupture of close junctions in a chain-reaction way (Zhang et al., 2007). Alternating blocks add elastic properties to an alginate gel network (Donati et al., 2009) and the high elasticity of the gel, 82,67% ± 2,76% , revealed this property. The crosslinks between alternating blocks are believed to work as reels that slides when force is applied (Donati et al., 2009). The described mechanism spreads out

stress in the gel network, thereby, prolonging the maximum compression point to which the gel can be contracted before the first junction breaks that starts the rupture cascade. In conclusion, the rupture strength and elasticity of the gel batch F_G=0,56 (MG) was high due to the alginates high content of MG-blocks.

The gel batch that was saturated in $BaCl_2$ and $CaCl_2$, had a comparable block composition and molecular weight as F_G=0,68, but its rupture strength was clearly lower. Evidently, the ion mix of the two mentioned divalent ions in the gel network resulted in a gel, which more easily than the other gel batches, broke when an increasing force was applied. As seen in figure (Figure 19) the gel shape differed from the other gel batches and the gels were formed as small bullets. Since Ba^{2+} can crosslink shorter G-blocks than Ca^{2+} (Bjørn T. Stokke et al., 1993) it is likely that the formed junctions in the alginate, in large, were different compared to the junctions in F_G=0,68, which only was saturated in Ca^{2+}. Additionally, Ba^{2+} can crosslink with M-blocks while Ca^{2+} cannot (Ý. A. Mørch et al., 2006), so, the structure of the two gels likely differ fundamentally. Possibly, these differences contributed to the asymmetrical gel form. Many factors are important for the rupture strength and the irregular gel form could have caused an earlier rupture. Maybe the asymmetrical form resulted in that some parts of the gel network experienced higher pressures than others during the compression, which ultimately lead to an en earlier ignition of the chain-reaction as compared to the symmetrical gel cylinders.

4.2.8 Rupture strength and elasticity during the saline treatments

As seen in (Figure 29) there were, in general, two modes of how the rupture strength and elasticity of the Ca^{2+} saturated alginate gels developed during the saline treatments. The AlgE6 epimerized gel batches F_G=48 (stirred), F_G=60, F_G=68 and F_G=85 behaved according to the first mode. In this mode, the rupture strength and elasticity of the gels reached a maximum after one (two for F_G=0,85) saline shift and during the subsequent saline treatments the rupture strength and elasticity declined extensively. The gel batches SF60 (both), F_G=0,48 (not stirred) and F_G=0,56 (MG) behaved according to the second mode. In this mode, the rupture strength and elasticity of the gels declined steadily during all saline treatments.

A gel network requires elastic segments and crosslinks and it seems as when some of the crosslinks in a gel, which behaves as a "first mode gel", are broken by the first saline treatment, due to the replacement of Ca^{2+} ions with Na^{+} ions, there is a shift of the gel-properties and the elastic properties increase, as seen by the higher elasticity of the gels. Due to this, the gels are far more compressible which results in higher rupture strengths during the compression before gel breakage. Another example of that a highly elastic alginate gel can be compressed to a high degree without breaking is F_G=0,56 (MG). This gel had the highest rupture strength of the gel batches before the saline treatments had started and as discussed in (Section 4.2.7) the high content of alternating blocks in the gel, most likely, was the most important reason behind it. Coming back to the first mode behavior, after the peak of the elasticity and rupture strength the both mentioned gel-properties changed considerably and the measured values decreased heavily. Likely, when even more crosslinks were broken it was hard to upkeep the gel network and this lead to that the gel started to have problems keeping up its own weight. Moreover, the high concentration of Na^{+} ions made water flow into the gel that caused osmotic swelling. At this point the gels had started to dissolve (Table 5) and the drastically re-organization of the gel network lead to a collapse that resulted in lower elastic properties and rupture strength. The described process explains the behavior of F_G=0,68 and F_G=0,85 during the saline shifts. Due to the Berg hypothesis (Section 4.2.6.1) the gel properties of F_G=0,85 did not change significantly during the first saline treatment, instead, it was after the second saline change that the gel was as most elastic. Moreover, the elasticity of F_G=0,48 (not stirred) increased by a few percent after the second saline shift, which also was the last saline shift before the alginate gels dissolved. Even though the elasticity had increased slightly after the second saline change the rupture strength still decreased. As seen in (Table 5) the gel had started to dissolve and was unstable, in fact, it dissolved after three saline shifts and not two as for the other Ca-G-gels. Due to the unstable state of the gel it was difficult to measure the elasticity. Although, it should be noted that it is also hard to measure the absolute elasticity values of stable gels that are highly compressible. When the elasticity of a gel is over 90%, as it was for F_G=0,48 (not stirred) during the first two saline shifts, the gel system is complex and many factors affect the rupture point, which makes it hard to compare two mean values that both are over 90%. Regarding the gel batch F_G=0,60 the same explanation can be applied to describe why the elasticity increased again after the last saline

shift. The unstable gel network made the gel sensitive and external forces easily shaped it. Lastly, during the saline shifts the rupture strength of F_G=0,60 was higher than the corresponding values of F_G=0,48, F_G=0,68 and F_G=0,85. Probably, this was due to its somewhat higher molecular weight compared to the other gels.

To emphasize, when the rupture strength of one of the AlgE6 epimerized gels had reached the maximum point the gel was still stable, but after the next saline treatment, when the rupture strength was extremely reduced, the gels had started to dissolve (Table 5). Furthermore, when the gel had started to dissolve and the rupture strength had fallen, the Young´s modulus also had declined heavily and was only 10% or less of the original value (Figure 29). In the study (Klepp-Andersen, 2010) where alginate gels of AlgE6 epimerized mannuronan was examined during saline shifts most of the gels behaved like the stable, not dissolving, AlgE6 epimerized polyM gels in this work. Therefore, it is possible to relate the results from (Klepp-Andersen, 2010) to the ones in this work. As seen in the report (Klepp-Andersen, 2010) the elasticity, and thereby the rupture strength, of the gels increased for every saline shifts until the point where the gels did not break upon 100% compression. As already discussed, the saline treatments in the work (Klepp-Andersen, 2010) was not as extreme as in this work, therefore, the gels were stable throughout the saline shifts and did not start to dissolve, they just became more and more elastic of the repeated saline treatments. In the discussed report, the elasticity of the gels with a low G-content increased more during the first saline shifts compared to the gels with a higher G-content. This trend was harder to observe in this work due to the very effective saline changes, however, the fact that F_G=0,85 could manage one more saline shift than the other AlgE6-gels demonstrates this tendency. The probable explanation behind this development was that a higher G-content in the Ca^{2+} saturated gels, lead to the formation of more crosslinks in the gel network, consequently, more saline shifts were required to break the crosslinks that increased the elasticity of the gels. Interestingly, the gel F_G=0,77 in the work (Klepp-Andersen, 2010) behaved like most the Ca-G-gels in this work, after two saline shifts the rupture strength had reached a maximum value and during the two final saline shifts the elasticity clearly decreased. Possibly, the high G-content of the gel, and the long G-blocks (not as long as the longest in SF60) that likely were present in the alginate as discussed in (Section 4.2.6) made the gel behave differentially from the other gel batches in the study. The control gel, SF60, in the work (Klepp-Andersen, 2010) behaved like the both SF60 gel batches in this thesis,

specifically, the repeated saline shifts lowered the elasticity and rupture strength of the gels. Taken together, it seems as the gel F_G=0,77 during the first saline treatments behaved like the AlgE6 epimerized gels but after the peak in elasticity it behaved more like the natural alginate SF60.

In this work, during the first saline shift the gel-properties of SF60 changed drastically. As discussed in (Section 4.2.6) the extreme decrease of Young´s modulus probably was due to its relatively low G-content. During the first saline treatment the junctions, which were formed from the long G-blocks, likely were disrupted and the gel could not uphold its properties, as predicted by the Berg theorem (Section 4.2.6.1). This could be why the rupture strength decreased during the first saline shift, while the elasticity did not change. During the following saline treatments both the elasticity and rupture strength of the both SF60 gel batches were reduced. The two highlighted gel properties decrease faster in the SF60 gel batch that was stirred during the saline treatments compared to the other batch. Obviously, this was due to more efficient mass transport of Na^+ ions.

As discussed (Section 4.2.6) the gel batch F_G=0,48 (not stirred) appeared to be more sensitive towards the saline treatment due to its lower molecular weight. Also, it is remarkable how different the two gels with a G-content of 48% behaved during the saline treatments. The rupture strength of F_G=0,48, which had a higher molecular weight, was higher at each correspondingly saline change, however, the gel batch dissolved after three saline shifts, and not four as the other batch, due to the more efficient saline treatment. Moving on, the elasticity of F_G=0,48 (not stirred) did not change during the first two saline changes, however, during the third change it decreased largely. The gels had then started to dissolve (Table 5), and so, the gels were very elastic and were simply shaped by external forces. Since the elasticity did not change during the first two saline treatments it seems as the less crosslinks did not shift the overall gel-properties towards a more elastic mode, as happened for the other AlgE6 epimerized alginates in the work. Again, the molecular weight of F_G=0,48 (not stirred) was much lower compared to the other alginate gels and likely this was one of the reasons behind the diverse behavior.

Just like the gels made of AlgE6 epimerized polyM, which were stirred during the saline shifts, the rupture strength of the gel batch F_G=0,56 (MG) decreased comprehensively during the first two saline shifts. However, the elasticity of the gels profoundly decreased after the second and third saline shift and this development was the opposite of the other epimerized gels where the elasticity, generally, increased during the saline shifts. Circular dichroism studies have shown that Ca^{2+} has higher affinity for G-blocks than MG-blocks (Donati et al., 2005). Since Na^{+} ions in this study were able to replace Ca^{2+} -ions, which formed junctions between the G-blocks, the Ca^{2+} ions, which formed the crosslinks between MG-blocks, also must have been replaced by Na^{+} ions during the saline treatments. As stated earlier (4.2.2, 4.2.6), alternating blocks work as elastic segments and when these are disrupted by the saline treatment the elasticity of the gel is reduced. Probably, the decrease of the rupture strength during the saline treatment was a result of the disruption of the reeling properties as well as due to the fewer crosslinks, which lowered the overall gel strength. Finally, the elasticity and rupture strength did not statistically significantly (p=0,05) change during the third and fourth saline shift. Likely, the introduction of alternating blocks by AlgE4 created a more stable gel than when AlgE6 introduced G-blocks on a polyM backbone.

The elasticity and rupture strength development during the saline treatments of the Ba^{2+} saturated gel batch differed considerably from the other Ca^{2+} saturated gel batches. Like most of the Ca-G-gels the elasticity and rupture strength increased, however, the only statistically significant (p=0,05) increase of the elasticity occurred during the first two saline shifts and the only statistically significant (p=0,05) increase in rupture strength occurred during the second saline change. Likely, most of the Ca^{2+} ions were replaced by Na^{+} ions during the first two saline changes, yet, the Ba^{2+} ions were not replaced since the gel continued to be stable during the following saline treatments. In regard of the rupture strength and elasticity, the Ba^{2+} saturated gel batch was stable during the last two saline treatments unlike the Ca-G-gels and two gel batches of SF60.

4.3 Summary of the gel behavior during the saline treatments

In this project there were four main groups of alginate gels that were examined and their behavior during the saline treatments is reviewed here.

4.3.1 G and M-block rich alginates saturated in Ca^{2+}

Overall, the gel properties of the Ca^{2+} saturated alginates that most consisted of G and M-blocks varied well accordingly to the summary of the correlation of structural and physical properties (Table 1). When the physical properties of alginates with higher and lower G-content and G-block lengths were compared, substantial differences were observed. For example, when the saturated gels of F_G=0,48 and F_G=0,85 were compared it was observed that the Young´s modulus of the gel batch with the higher G-content was about the double size of the other alginate. Also, during the first saline shift the relative decrease of the gel strength was drastically higher for the alginate with a lower G-content. Furthermore, F_G=0,48 dissolved after three saline shifts and not four as the other gel batches in this group. Overall, these alginate gels were less stable and swelled more compared to the other three examined alginate groups. In general, the initial syneresis was high and it appeared to be a distinct limit for how much the gels could swell before they dissolved. This limit seemed to decrease with an increasing G-content. Finally, during the initial saline treatments the reduction of the crosslinks in the gel network resulted in that the gels became more elastic and as a result the rupture strength increased to a maximum after one (two for F_G=0,85) saline shift. During the succeeding saline treatments the gels collapsed and the rupture strength and elasticity declined comprehensively.

4.3.2 Alginate with a high content of MG-blocks

The gel batch with a high content of alternating blocks was more stable than the gels prepared from the natural high-G alginate *L. hyp.,* stipe as well as the epimerized gels that had different content of G and M-blocks and a low and similar content of MG-blocks. Together with the gel batch that was saturated in Ba^{2+}, it was the only gel batch that did not start to dissolve during the saline treatments. After the Ca^{2+} saturation the gel batch had undergone the highest syneresis of all alginates and it was very compressible as seen by the by the high elasticity and rupture strength. The initial

Young´s modulus was low but after the four saline treatments its rupture strength was the second highest, after F_G=0,62 (Ba). During the first two saline changes most of the significant changes of the gel properties occurred. Interestingly, the elasticity decreased comprehensive during the second saline change, and it was probably due to the lost of the elastic junctions, which the alternating blocks formed.

4.3.3 G and M-block rich alginate saturated in Ba^{2+} and Ca^{2+}

The gel properties and behavior during the saline treatments of the gel batch, which was saturated in Ba^{2+} and Ca^{2+}-ions, was different from the other gel batches that were saturated in solely Ca^{2+}-ions. The initial Young´s modulus and rupture strength was comparatively low, however, the gels were stable during all saline shifts and its relative decrease in gel strength was the smallest of all gel batches. The gels, which were formed as small bullets, had shrunk by about 20% after the saline treatments. When the gel properties were studied one by one it was evident that most of the Ca^{2+} ions were washed out from the gel during the first two saline shifts, however, due to the alginates high affinity towards Ba^{2+}, these ions remained and upheld the gel network. Also, in a study where microbeads of *L. hyp.,* stipe were saturated in Ca^{2+} and/or Ba^{2+} the leakage of Ba^{2+} from the beads was low (Yrr A Mørch et al., 2012). Regarding the gel stability, it has been showed that high affinity ions requires smaller G-block lengths for junction formation, therefore, these alginate gels have a higher density of stable crosslinks in the gel network (Bjørn T. Stokke et al., 1993). Because of this, it is likely that a few Ba^{2+} ions could be replaced without that it affected the stability of the junctions (Bjoern T Stokke, Smidsroed, Bruheim, & Skjaak-Braek, 1991). The volume of the gels did not change during the last two saline shifts, in fact, during the last two saline shifts there were no significant differences of the syneresis, Young´s modulus, water loss, rupture strength or elasticity. To my best knowledge, there are no previous studies where gels formed from AlgE6 epimerized mannuronan has been saturated in Ba^{2+}, so, it is hard to compare and check the presented data to earlier findings. However, since Ba^{2+} can bind both G and M-blocks (Ý. A. Mørch et al., 2006), while Ca^{2+} only can bind G-blocks, it is likely that the differing physical properties of the discussed gel batch could be due to its different potential to form gel networks.

4.3.4 The natural high-G alginate *L. hyp.,* stipe

After the Ca^{2+} saturation the gel batch that was prepared from *L. hyp.,* stipe had undergone the least syneresis of all batches due to the long G-blocks that the alginate consisted of. The Young´s modulus of SF60 was definitely the highest among the studied gels before the saline treatments had started. However, during the first two saline shifts it decreased to less than 10% of the original value. Notably, the G and M-block rich alginates also experienced this rapid fall. The rupture strength and elasticity of the gel batch declined steadily during the saline treatments.

The gels made from the natural alginate *L. hyp.,* stipe swelled less and were more stable against the saline treatments than the gels prepared from the AlgE6 epimerized mannuronan. However, the alginate gel batch that was rich in MG-blocks, as well as the G-and M-block rich batch that was saturated in Ba^{2+}, swelled less (or even slightly shrunk as F_G=0,62 (Ba)) during the saline shifts. Also, these last two mentioned gel batches were more stable and they did not dissolve during the saline treatments, in contrast to the gels prepared from *L. hyp.,* stipe and AlgE6 epimerized polyM.

4.4 Further work

This thesis demonstrates how the block structure and choice of gelling ions affects the physical properties of alginates based on syneresis, gel strength, water loss, elasticity and rupture strength measurements of alginate gel cylinders. The epimerized alginates were analyzed by both ^{1}H-NMR and HPAEC-PAD to acquire information about the chemical compositions and block structures, in order to compare the alginates.

In an attempt to introduce alternating blocks in F_G=0,60 by AlgE4 epimerization it was observed that AlgE6 was reactivated. As discussed in (Section 4.1.1) the activity of AlgE6 was not stopped by the warm water bath. Another method to separate the alginate from AlgE6 is by acid precipitation. After the submission of this thesis it is planned to use this method on a smaller fraction of the alginate F_G=0,48 and F_G=0,68, which was not epimerized in this work. The rest of the alginate will be used to form Ba^{2+} saturated gel cylinders as mentioned in the next part. After the acid precipitation the alginates will be epimerized by AlgE4. As discussed in (Section 4.1.1) it is possible that the activity of AlgE4 was low due to the short M-blocks of F_G=0,60, and since the M-block distribution of F_G=0,48 and F_G=0,68 are different the hypothesis can be evaluated.

The physical properties of the gels that were saturated in Ba^{2+} and Ca^{2+} were in many aspects different from the other gels that were only saturated in Ca^{2+}. Especially, the Young´s modulus, elasticity and rupture strength of F_G=0,62 (Ba) was surprisingly low. To my best knowledge there are no other studies where AlgE6 epimerized mannuronan alginate gels have been saturated in Ba^{2+}. Therefore, it is planned to prepare gel cylinders from F_G=0,48 and F_G=0,68 and saturate the gels in equal solutions to those used to saturate F_G=0,62 (Ba). Since Ba^{2+} can bind to both G and M-blocks it would be interesting to visualize the alginate by the developed methods from (Strand, Mørch, Espevik, & Skjåk‐Bræk, 2003). The visualization might be able to provide answers to why the gel properties and shape of G- and M-block rich alginates saturated in Ba^{2+} and Ca^{2+} are different in comparison to similar alginates that only are saturated in Ca^{2+}.

AlgE1 can introduce longer G-blocks than AlgE6 in mannuronan and the longer G-blocks could increase the stability of the alginate. It would be interesting to compare the stability and physical properties of AlgE1

epimerized polyM to AlgE6 epimerized polyM during saline treatments. The data would contribute more to the understanding of how the block distribution in alginates affects the physical properties of alginate gels.

5 Conclusions

The physical properties of alginates correlate strongly with their structure, which depends on the block distribution, molecular weight and the ions present in the network. In this report it was demonstrated that alginates consisting of mostly G and M- blocks, with a similar degree of MG-blocks, effectively could be made by AlgE6 epimerization of mannuronan. The G-block content was controlled by using the same enzyme concentration and varying the epimerization time. The AlgE6 epimerization of mannuronan was as fastest when some G-blocks had formed and there were many available M-blocks.

In this work increasing gel stability against swelling was observed in alginate gels that had the following structural features: G- and M-blocks (stability increased with an increasing G-content) < long G-blocks < MG-blocks < saturation with the high affinity ion Ba^{2+}.

Three different gel states were defined –stable, starting to dissolve/dissolving, dissolved –and used to characterize the alginate gels. There was a relationship between the gel appearance after a full compression and the weight-normalized water release. When an alginate gel started to dissolve the water release increased and when the gel had dissolved, the water release was close to the original value of the non-saline treated gel.

The HPAEC-PAD analyses showed that the number of long G-blocks (DP>40) increased by the G-content among the AlgE6 epimerized mannuronan. The natural alginate *L. hyp.,* stipe consisted of a large quantity of very long G-blocks that was not present in the epimerized alginates. The epimerized alginates contained relatively short M-blocks, compared to the G-block lengths, and an increasing G-content resulted in M distribution mostly consisting of short M blocks.

There was an attempt to create an alginate that both consisted of longer G-blocks and MG-blocks, This was done by first performing an AlgE6 epimerization with polyM, followed by a warm water bath to denature AlgE6, and a final epimerization by AlgE4. During the second incubation AlgE6 was re-activated and it dominated the epimerization reaction over

AlgE4. Likely, the activity of AlgE4 was low due to it at least requires a hexameric oligomer of M-blocks to be active and a majority of the M-blocks of the starting alginate was between one and ten residues long.

Among the G and M-block rich alginates, the G-content and G-block lengths, significantly affected the physical properties. For example, after Ca^{2+} saturation the Young´s modulus of the alginate with the highest G-content (85%) was about the double strength in relation to the alginate with the smallest G-content (48%). The syneresis of the Ca^{2+} saturated gels was high and it appeared to be a distinct limit for how much the gels could swell before they dissolved. This limit seemed to decrease with an increasing G-content. During the initial saline treatments the reduction of the crosslinks in the gel network resulted in that the gels became more elastic and as a result the rupture strength increased to a maximum after one or two saline treatments. During the following saline treatments the gels collapsed and the rupture strength and elasticity decreased significantly.

A control alginate rich of MG-blocks and relative short G-blocks was formed by first performing an AlgE4 epimerization with polyM, followed by an AlgE6 epimerization. After the Ca^{2+} saturation the alginate had undergone the highest syneresis of all alginates, it had a relatively low Young´s modulus and it was very compressible as the high elasticity and rupture strength revealed. It was the only alginate, together with the one that was saturated in Ba^{2+}, which did not start to dissolve during the saline treatments. The elasticity decreased comprehensive during the second saline change, and it was probably due to the lost of the elastic junctions, which the alternating blocks formed.

The effect of saturating an alginate rich of G and M-block in Ba^{2+} and Ca^{2+}, compared to solely Ca^{2+}, was studied. The initial Young´s modulus and rupture strength was surprisingly low, however, the relative decrease in gel strength was the smallest of all gel batches. The gels were formed as small bullets and the volume had shrunk by about 20% after the saline treatments. Most of the Ca^{2+} ions were washed out during the first two saline shifts and due to the alginates high affinity towards Ba^{2+} these ions remained and maintained the gel. During the last two saline shifts the alginate was stable and there were no significantly differences of the volume, syneresis, Young´s modulus, water loss, rupture strength or elasticity. Finally, the appearance and properties of these gels were different in several aspects

compared to the other G and M-block rich alginates, which were only saturated in Ca^{2+}. Since Ba^{2+} can bind both G and M-blocks, while Ca^{2+} only bind G-blocks, it is likely that the differing physical properties were due to its different potential to form gel networks.

After the Ca^{2+} saturation the control batch that was prepared from *L. hyp.,* stipe had undergone the smallest syneresis of all alginates and it had the highest Young´s modulus due to the long G-blocks that it contained. After the first two saline shifts had Young´s modulus decreased to less than 10% of the original value. The G and M-block rich alginates also experienced a similar fall in the gel strength. The rupture strength and elasticity of the gel batch declined steadily during the saline treatments.

In conclusion, this thesis demonstrates that the physical properties of alginate can be designed to meet requirements in different applications. The modifications of alginate are readily done by performing epimerization with mannuronan C-5 epimerases from *A. vinelandii* as well as by wisely choosing ions for the gel formation. Finally, a guide for the correlations between the structure of alginates and the physical properties of alginate gels is presented in the thesis.

6 References

Aarstad, O. A. (2013). *Alginate sequencing: Block distribution in alginates and its impact on macroscopic properties.* Norwegian University of Science and Technology.

Aarstad, O. A., Tøndervik, A., Sletta, H., & Skjåk-Bræk, G. (2011). Alginate Sequencing: An Analysis of Block Distribution in Alginates Using Specific Alginate Degrading Enzymes. *Biomacromolecules, 13*(1), 106-116. doi: 10.1021/bm2013026

Bernkop-Schnürch, A., Kast, C. E., & Richter, M. F. (2001). Improvement in the mucoadhesive properties of alginate by the covalent attachment of cysteine. *Journal of Controlled Release, 71*(3), 277-285. doi: http://dx.doi.org/10.1016/S0168-3659(01)00227-9

Campa, C., Holtan, S., Nilsen, N., Bjerkan, T., Stokke, B., & Skjak-braek, G. (2004). Biochemical analysis of the processive mechanism for epimerization of alginate by mannuronan C-5 epimerase AlgE4. *Biochem. J, 381*, 155-164.

Christensena, B. E. (2011). Alginates as biomaterials in tissue engineering. *Carbohydrate Chemistry: Chemical and Biological Approaches, 37*, 227-258.

Darquy, S., Pueyo, M. E., Capron, F., & Reach, G. (1994). Complement activation by alginate–polylysine microcapsules used for islet transplantation. *Artificial organs, 18*(12), 898-903.

Dionex. (2004). Technial note: Analysis of Carbohydrates by High-Performance Anion-Exchange chromatography with Pulsed Amperometric Detection (HPAE-PAD), from http://www.dionex.com/en-us/webdocs/5023-TN20_LPN032857-04.pdf

Donati, I., Holtan, S., Mørch, Y. A., Borgogna, M., Dentini, M., & Skjåk-Bræk, G. (2005). New hypothesis on the role of alternating sequences in calcium-alginate gels. *Biomacromolecules, 6*(2), 1031-1040.

Donati, I., Mørch, Y. A., Strand, B. L., Skjåk-Bræk, G., & Paoletti, S. (2009). Effect of elongation of alternating sequences on swelling behavior and large deformation properties of natural alginate gels. *The Journal of Physical Chemistry B, 113*(39), 12916-12922.

Dornish, M., Kaplan, D., & Skaugrud, Ø. (2001). Standards and Guidelines for Biopolymers in Tissue‐Engineered Medical Products. *Annals of the New York Academy of Sciences, 944*(1), 388-397.

Draget, K., Simensen, M., Onsøyen, E., & Smidsrød, O. (1993). *Gel strength of Ca-limited alginate gels made in situ.* Paper presented at the Fourteenth International Seaweed Symposium.

Draget, K. I., Gåserød, O., Aune, I., Andersen, P. O., Storbakken, B., Stokke, B. T., & Smidsrød, O. (2001). Effects of molecular weight and elastic segment flexibility on syneresis in Ca-alginate gels. *Food Hydrocolloids, 15*(4), 485-490.

Draget, K. I., Strand, B., Hartmann, M., Valla, S., Smidsrød, O., & Skjåk-Bræk, G. (2000). Ionic and acid gel formation of epimerised alginates; the effect of AlgE4. *International Journal of Biological Macromolecules, 27*(2), 117-122. doi: http://dx.doi.org/10.1016/S0141-8130(00)00115-X

Ertesvåg, H., Doseth, B., Larsen, B., Skjåk-Bræk, G., & Valla, S. (1994). Cloning and expression of an Azotobacter vinelandii mannuronan C-5-epimerase gene. *Journal of bacteriology, 176*(10), 2846-2853.

Ertesvåg, H., Høidal, H. K., Schjerven, H., Svanem, B. I. G., & Valla, S. (1999). Mannuronan C-5-Epimerases and Their Application for< i> in Vitro</i> and< i> in Vivo</i> Design of New Alginates Useful in Biotechnology. *Metabolic engineering, 1*(3), 262-269.

Ertesvåg, H., & Valla, S. (1999). The A modules of the Azotobacter vinelandii mannuronan-C-5-epimerase AlgE1 are sufficient for both epimerization and binding of Ca2+. *Journal of bacteriology, 181*(10), 3033-3038.

George, M., & Abraham, T. E. (2006). Polyionic hydrocolloids for the intestinal delivery of protein drugs: Alginate and chitosan — a review. *Journal of Controlled Release, 114*(1), 1-14. doi: http://dx.doi.org/10.1016/j.jconrel.2006.04.017

Grasdalen, H. (1983a). High-field,1H-NMR spectroscopy of alginate: sequential structure and linkage conformations. *Carbohydrate Research, 118*, 255-260.

Grasdalen, H. (1983b). High-field, 1H-n.m.r. spectroscopy of alginate: sequential structure and linkage conformations. *Carbohydrate Research, 118*(0), 255-260. doi: http://dx.doi.org/10.1016/0008-6215(83)88053-7

Grasdalen, H., Larsen, B., & Smidsrød, O. (1979). A pmr study of the composition and sequence of uronate residues in alginates. *Carbohydrate Research, 68*(1), 23-31.

Haug, A., & Smidsrod, O. (1970). Selectivity of some anionic polymers for divalent metal ions. *Acta Chem Scand, 24*(3), 843-854.

Holtan, S., Bruheim, P., & Skjak-Braek, G. (2006). Mode of action and subsite studies of the guluronan block-forming mannuronan C-5 epimerases AlgE1 and AlgE6. *Biochem J, 395*(2), 319-329. doi: 10.1042/bj20051804

Huebsch, N., Arany, P. R., Mao, A. S., Shvartsman, D., Ali, O. A., Bencherif, S. A., . . . Mooney, D. J. (2010). Harnessing traction-mediated manipulation of the cell/matrix interface to control stem-cell fate. *Nature materials, 9*(6), 518-526.

Ingar Draget, K., Østgaard, K., & Smidsrød, O. (1990). Homogeneous alginate gels: a technical approach. *Carbohydrate polymers, 14*(2), 159-178.

King, A., Strand, B., Rokstad, A. M., Kulseng, B., Andersson, A., Skjåk‐Bræk, G., & Sandler, S. (2003). Improvement of the biocompatibility of alginate/poly‐L‐lysine/alginate microcapsules by the use of epimerized alginate as a coating. *Journal of Biomedical Materials Research Part A, 64*(3), 533-539.

Klepp-Andersen, L. M. (2010). *Master thesis.* (Master), Norwegian University of Science and Technology.

Kong, H. J., Lee, K. Y., & Mooney, D. J. (2003). Nondestructively Probing the Cross-Linking Density of Polymeric Hydrogels. *Macromolecules, 36*(20), 7887-7890. doi: 10.1021/ma034865j

Lee, K. Y., & Mooney, D. J. (2012). Alginate: Properties and biomedical applications. *Progress in Polymer Science, 37*(1), 106-126. doi: http://dx.doi.org/10.1016/j.progpolymsci.2011.06.003

Mancini, M., Moresi, M., & Rancini, R. (1999). Mechanical properties of alginate gels: empirical characterisation. *Journal of food engineering, 39*(4), 369-378. doi: http://dx.doi.org/10.1016/S0260-8774(99)00022-9

Martinsen, A., Skjåk‐Bræk, G., & Smidsrød, O. (1989). Alginate as immobilization material: I. Correlation between chemical and physical properties of alginate gel beads. *Biotechnology and bioengineering, 33*(1), 79-89.

Mitchell, J. (1980). The rheology of gels. *Journal of Texture Studies, 11*(4), 315-337.

Mitchell, J., & Blanshard, J. (1976). Rheological properties of alginate gels. *Journal of Texture Studies, 7*(2), 219-234.

Moe, S., Draget, K., Skjåk-Bræk, G., & Smidsrød, O. (1995). Alginates. *Food polysaccharides and their applications*, 245-245.

Mørch, Ý., Donati, I., Strand, B. L., & Skjåk-Bræk, G. (2007). Molecular engineering as an approach to design new functional properties of alginate. *Biomacromolecules, 8*(9), 2809-2814.

Mørch, Y. A. (2008). *Novel Alginate Microcapsules for Cell Therapy–A study of the structure-function relationships in native and structurally engineered alginates.* Norwegian University of Science and Technology.

Mørch, Ý. A., Donati, I., Berit, L., & Skjåk-Bræk, G. (2006). Effect of Ca2+, Ba2+, and Sr2+ on alginate microbeads. *Biomacromolecules, 7*(5), 1471-1480.

Mørch, Y. A., Holtan, S., Donati, I., Strand, B. L., & Skjåk-Bræk, G. (2008). Mechanical properties of C-5 epimerized alginates. *Biomacromolecules, 9*(9), 2360-2368.

Mørch, Y. A., Qi, M., Gundersen, P. O. M., Formo, K., Lacik, I., Skjåk‐Bræk, G., . . . Strand, B. L. (2012). Binding and leakage of barium in alginate microbeads. *Journal of Biomedical Materials Research Part A, 100*(11), 2939-2947.

Saitoh, S., Araki, Y., Kon, R., Katsura, H., & Taira, M. (2000). Swelling/deswelling mechanism of calcium alginate gel in aqueous solutions. *Dental materials journal, 19*(4), 396.

Sandoval. (2010). Young´s modulus.

Sikorski, P., Mo, F., Skjåk-Bræk, G., & Stokke, B. T. (2007). Evidence for Egg-Box-Compatible Interactions in Calcium−Alginate Gels from Fiber X-ray Diffraction. *Biomacromolecules, 8*(7), 2098-2103. doi: 10.1021/bm0701503

Simsek-Ege, F. A., Bond, G. M., & Stringer, J. (2003). Polyelectrolyte complex formation between alginate and chitosan as a function of pH. *Journal of Applied Polymer Science, 88*(2), 346-351. doi: 10.1002/app.11989

Skják-Bræk, G., Smidsrød, O., & Larsen, B. (1986). Tailoring of alginates by enzymatic modification< i> in vitro</i>. *International Journal of Biological Macromolecules, 8*(6), 330-336.

Sletmoen, M., Skjåk-Bræk, G., & Stokke, B. T. (2005). Mapping enzymatic functionalities of mannuronan C-5 epimerases and their modular units by dynamic force spectroscopy. *Carbohydrate Research, 340*(18), 2782-2795.

Smidsrød, O. (1974). Molecular basis for some physical properties of alginates in the gel state. *Faraday Discuss. Chem. Soc., 57*, 263-274.

Smidsrød, O. (1990). Alginate as immobilization matrix for cells. *Trends in biotechnology, 8*, 71-78.

Smidsrød, O., Glover, R., & Whittington, S. G. (1973). The relative extension of alginates having different chemical composition. *Carbohydrate Research, 27*(1), 107-118.

Smidsrød, O., & Haug, A. (1972). Properties of poly (1, 4-hexuronates) in the gel state. II. Comparison of gels of different chemical composition. *Acta Chem Scand, 26*, 79-88.

Smidsrød, O., Haug, A., & Lian, B. (1972). Properties of poly (1, 4-hexuronates) in the gel state. I. Evaluation of a method for the determination of stiffness. *Acta Chemica Scandinavica, 26*(1), 71-78.

Stokke, B. T., Smidsroed, O., Bruheim, P., & Skjaak-Braek, G. (1991). Distribution of uronate residues in alginate chains in relation to alginate gelling properties. *Macromolecules, 24*(16), 4637-4645.

Stokke, B. T., Smidsrød, O., Zanetti, F., Strand, W., & Skjåk-Bræk, G. (1993). Distribution of uronate residues in alginate chains in relation to alginate gelling properties — 2: Enrichment of β-d-mannuronic acid and depletion of α-l-guluronic acid in sol fraction. *Carbohydrate polymers, 21*(1), 39-46. doi: http://dx.doi.org/10.1016/0144-8617(93)90115-K

Strand, B. L., Mørch, Y. A., Espevik, T., & Skjåk‐Bræk, G. (2003). Visualization of alginate‐poly‐L‐lysine‐alginate microcapsules by confocal laser scanning microscopy. *Biotechnology and bioengineering, 82*(4), 386-394.

Strand, B. L., Mørch, Y. A., Syvertsen, K. R., Espevik, T., & Skjåk‐Bræk, G. (2003). Microcapsules made by enzymatically tailored alginate. *Journal of Biomedical Materials Research Part A, 64*(3), 540-550.

Strand, B. L., Ryan, L., Veld, P. I. t., Kulseng, B., Rokstad, A. M., Skjak-Braek, G., & Espevik, T. (2001). Poly-L-lysine induces fibrosis on alginate microcapsules via the induction of cytokines. *Cell transplantation, 10*(3), 263-275.

Tam, S. K., Bilodeau, S., Dusseault, J., Langlois, G., Hallé, J. P., & Yahia, L. H. (2011). Biocompatibility and physicochemical characteristics of alginate–polycation microcapsules. *Acta Biomaterialia, 7*(4), 1683-1692. doi: http://dx.doi.org/10.1016/j.actbio.2010.12.006

Technology, W. (2013). Understanding Light Scattering and Chromatography, from http://www.wyatt.com/theory/theory/understanding-light-scattering-and-chromatography-mode.html

Thu, B., Bruheim, P., Espevik, T., Smidsrød, O., Soon-Shiong, P., & Skjåk-Bræk, G. (1996). Alginate polycation microcapsules: II. Some functional properties. *Biomaterials, 17*(11), 1069-1079. doi: http://dx.doi.org/10.1016/0142-9612(96)85907-2

Tøndervik, A., Klinkenberg, G., Aarstad, O. A., Drabløs, F., Ertesvåg, H., Ellingsen, T. E., . . . Sletta, H. (2010). Isolation of mutant alginate lyases with cleavage specificity for di-guluronic acid linkages. *Journal of Biological Chemistry, 285*(46), 35284-35292.

Vandenbossche, G. M., Bracke, M. E., Cuvelier, C. A., Bortier, H. E., Mareel, M. M., & Remon, J. P. (1993). Host Reaction against Empty Alginate‐polylysine Microcapsules. Influence of Preparation Procedure. *Journal of pharmacy and pharmacology, 45*(2), 115-120.

Wong, T. Y., Preston, L. A., & Schiller, N. L. (2000). Alginate lyase: review of major sources and enzyme characteristics, structure-function analysis, biological roles, and applications. *Annual Reviews in Microbiology, 54*(1), 289-340.

Zhang, J., Daubert, C. R., & Allen Foegeding, E. (2007). A proposed strain-hardening mechanism for alginate gels. *Journal of food engineering, 80*(1), 157-165.

Appendices

7 Appendix A - Alginate composition

The chemical composition and structure of the epimerized alginates were determined with ^{1}H-NMR. The areas under each of the peaks in the resulting chromatograms were integrated (A, B1, B2, B3, B4 and C in Table A.1). From these areas all sequence parameters were calculated, hence the monad-, diad- and triad frequencies were determined. The calculations are shown in Table A.1.

Table A7. Chemical composition of the epimerized alginates. A, B1, B2, B3, B4 and C correlates to the peaks in the ^{1}H-NMR spectra (Figure 8).

Alginate	**F_G=0,48**	**F_G=0,60**	**F_G=0,62 (Ba)**	**F_G=0,68**	**F_G=0,85**	**polyMG**
Peak (ppm)	Area	Area	Area	Area	Area	Area
A=5.05 (G-1)	1,000	1,000	1,000	1,000	1,000	1,000
B1=4.75 (GGM-5)	0,064	0,048	0,042	0,044	0,038	0,000
B2=4.72 (MGM-5)	0,183	0,125	0,103	0,084	0,064	1,000
B3=4.70 (GM-1)	0,170	0,120	0,112	0,095	0,083	1,000
B4=4.67 (MM-1)	0,896	0,518	0,470	0,344	0,076	0,215
C=4.45 (GG-5)	0,786	0,847	0,853	0,860	0,880	0,000
I(G)	0,997	0,996	0,991	0,986	0,986	1,000
I(M)	1,104	0,664	0,599	0,455	0,169	1,215
I(GG)	0,789	0,850	0,862	0,874	0,894	0,000
I(MG)=I(GM)	0,208	0,146	0,129	0,112	0,093	1,000
I(MM)	0,896	0,518	0,470	0,344	0,076	0,215
I(GGM)=I(MGG)	0,064	0,048	0,042	0,044	0,038	0,000
I(MGM)	0,183	0,125	0,103	0,084	0,064	1,000
I(GGG)	0,725	0,802	0,820	0,830	0,855	0,000
F(G)	0,475	0,600	0,623	0,684	0,854	0,451
F(M)	0,525	0,400	0,377	0,316	0,146	0,549
F(GG)	0,375	0,512	0,542	0,607	0,774	0,000
F(GM)=F(MG)	0,099	0,088	0,081	0,077	0,080	0,451
F(MM)	0,426	0,312	0,295	0,238	0,066	0,097
F(GGM)=F(MGG)	0,030	0,029	0,027	0,031	0,033	0,000
(F(MGM)	0,087	0,075	0,065	0,058	0,055	0,451
F(GGG)	0,345	0,483	0,516	0,576	0,740	0,000
N($G_{>1}$)	12,812	18,194	20,982	20,322	24,030	0,000

8 Appendix B – Block structure analysis

The AlgE6 epimerized alginates were degraded with M- and G-lyase, before separating and characterizing the oligosaccharides by HPAEC-PAD. The various oligosaccharides were separated according to chain-length. For each top, the area is given as retention- time (min) x signal (nC).

The chromatograms and data tables provided by the HPAEC-PAD analyses of the epimerized alginates degraded with M-lyase are given in the following figures:

- F_G=0,48 (not stirred) - Figure/Table B.1
- F_G=0,48 - Figure/Table B.2
- F_G=0,56 (MG) - Figure/Table B.3
- F_G=0,60 - Figure/Table B.4
- F_G=0,62 (Ba) - Figure/Table B.5
- F_G=0,68 - Figure/Table B.6
- F_G=0,85 - Figure/Table B.7

The chromatograms and data tables obtained by the HPAEC-PAD analyses of epimerized alginates degraded with G-lyase are given in the following figures:

- F_G=0,48 (not stirred) - Figure/Table B.8
- F_G=0,48 - Figure/Table B.9
- F_G=0,56 (MG) - Figure/Table B.10
- F_G=0,60 - Figure/Table B.11
- F_G=0,62 (Ba) - Figure/Table B.12
- F_G=0,68 - Figure/Table B.13
- F_G=0,85 - Figure/Table B.14

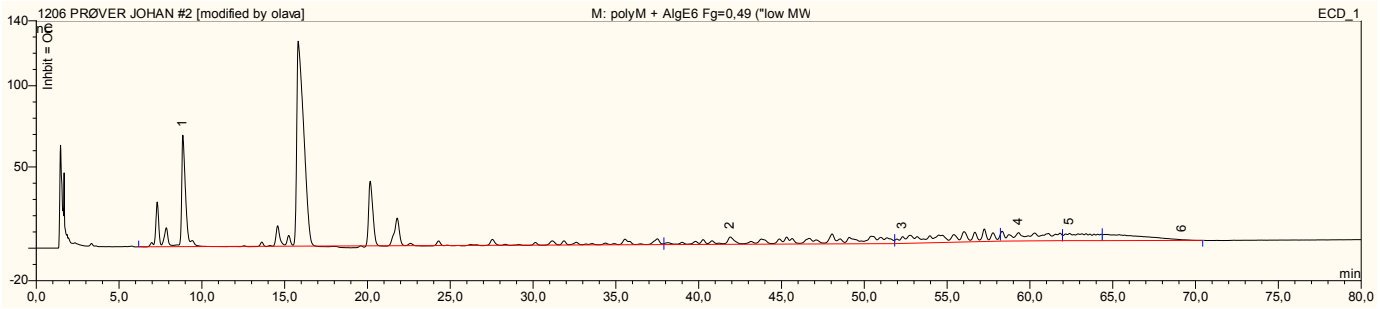

Figure B.1: HPAEC-PAD chromatogram of F_G=0,48 (not stirred) degraded with M-lyase.

Table B.1: HPAEC-PAD data of F_G=0,48 (not stirred) degraded with M-lyase.

F_G=0,48 (not stirred) DP	No.	Peakname	Ret.Time min	Area nC*min	Amount	Type	Height nC	Rel.Area %	Resolution
1-10	1	n.a.	8,85	118,7794	n.a.	BM *	68,587	59,8	17,76
11-20	2	n.a.	41,9	25,331	n.a.	M *	4,48	12,75	2,41
21-30	3	n.a.	52,317	20,5637	n.a.	M *	4,136	10,35	n.a.
31-40	4	n.a.	59,317	13,4372	n.a.	M *	5,122	6,76	n.a.
41-50	5	n.a.	62,4	9,091	n.a.	M *	4,361	4,58	n.a.
>50	6	n.a.	69,2	11,4274	n.a.	MB*	0,405	5,75	n.a.
	Total:			198,6298	0		87,092	100	

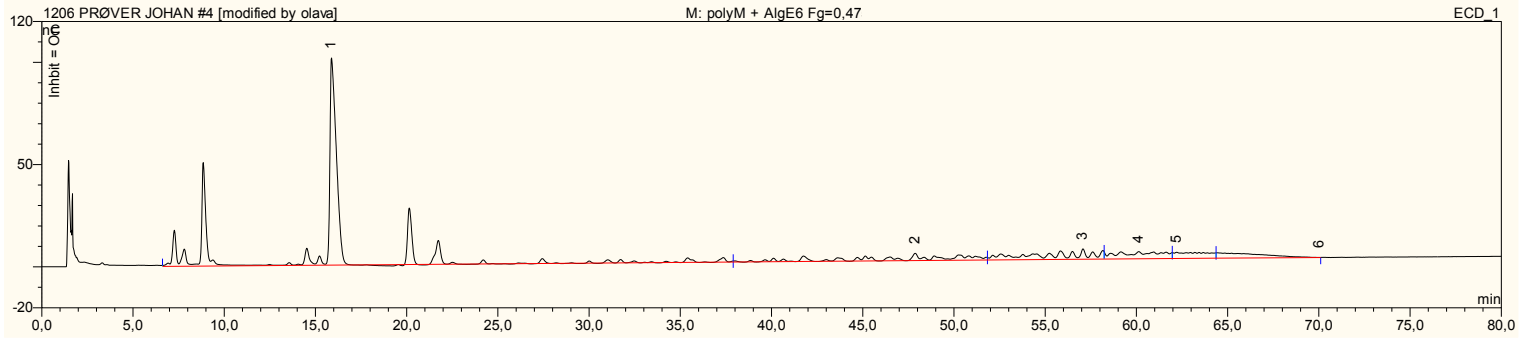

Figure B.2: HPAEC-PAD chromatogram of F_G=0,48 degraded with M-lyase.

Table B.2: HPAEC-PAD data of F_G=0,48 degraded with M-lyase.

F_G=0,48									
DP	**No.**	**Peakname**	**Ret.Time min**	**Area nC*min**	**Amount**	**Type**	**Height nC**	**Rel.Area %**	**Resolution**
1-10	1	n.a.	15,883	80,8138	n.a.	M *	101,3	62,25	5,58
11-20	2	n.a.	47,883	12,4272	n.a.	M *	3,556	9,57	0,98
21-30	3	n.a.	57,067	13,2293	n.a.	M *	5,056	10,19	n.a.
31-40	4	n.a.	60,133	9,4807	n.a.	M *	3,513	7,3	n.a.
41-50	5	n.a.	62,217	6,366	n.a.	M *	3,024	4,9	n.a.
>50	6	n.a.	70,033	7,5014	n.a.	M *	0,063	5,78	n.a.
	Total:			129,8185	0		116,51	100	

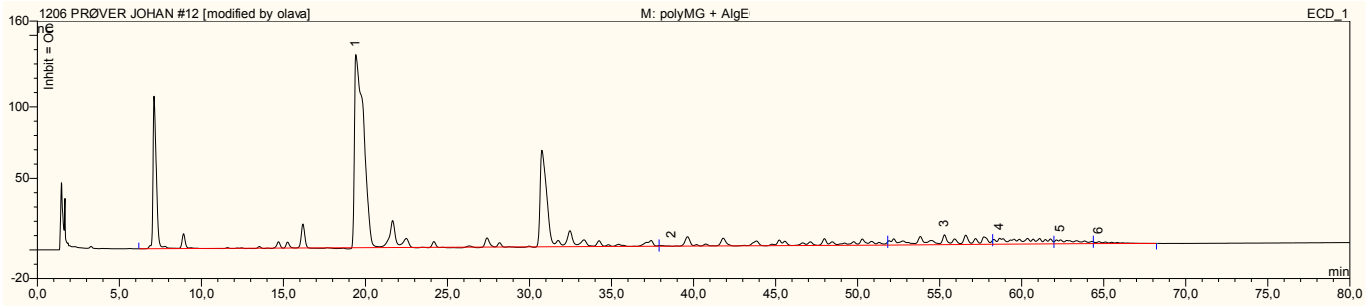

Figure B.3: HPAEC-PAD chromatogram of F_G=0,56 (MG) degraded with M-lyase.

Table B.3: HPAEC-PAD data of F_G=0,56 (MG) degraded with M-lyase.

F_G=0,56 (MG) DP	No.	Peakname	Ret.Time min	Area nC*min	Amount	Type	Height nC	Rel.Area %	Resolution
1-10	1	n.a.	19,417	175,5757	n.a.	BM *	135,04	78,01	n.a.
11-20	2	n.a.	38,683	17,6152	n.a.	M *	0,072	7,83	n.a.
21-30	3	n.a.	55,3	16,2156	n.a.	M *	6,874	7,2	n.a.
31-40	4	n.a.	58,65	10,035	n.a.	M *	4,152	4,46	n.a.
41-50	5	n.a.	62,367	4,0898	n.a.	M *	2,721	1,82	n.a.
>50	6	n.a.	64,7	1,5385	n.a.	MB*	1,309	0,68	n.a.
	Total:			225,0698	0		150,17	100	

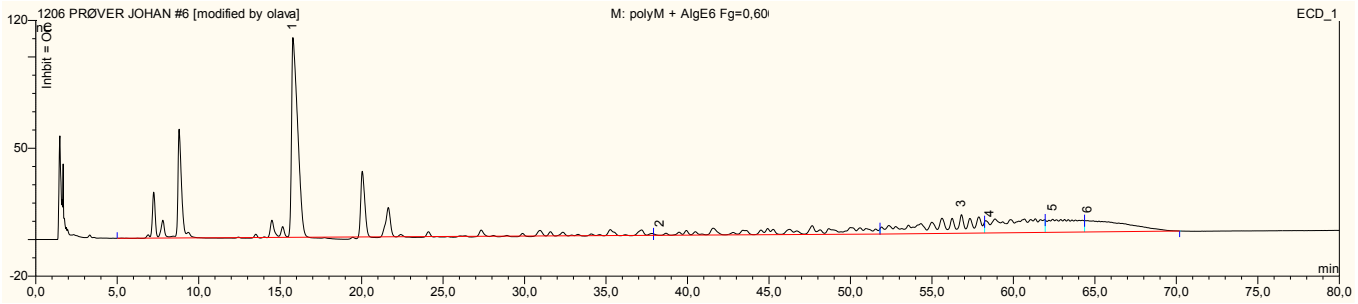

Figure B.4: HPAEC-PAD chromatogram of F_G=0,60 degraded with M-lyase.

Table B.4: HPAEC-PAD data of F_G=0,60 degraded with M-lyase.

F_G=0,60 DP	No.	Peakname	Ret.Time min	Area nC*min	Amount	Type	Height nC	Rel.Area %	Resolution
1-10	1	n.a.	15,783	93,9036	n.a.	BM *	109,35	46,75	n.a.
11-20	2	n.a.	38,317	20,9054	n.a.	M *	0,018	10,41	n.a.
21-30	3	n.a.	56,817	28,1912	n.a.	M *	10,195	14,04	n.a.
31-40	4	n.a.	58,567	23,2801	n.a.	M *	4,493	11,59	n.a.
41-50	5	n.a.	62,417	15,5292	n.a.	M *	7,14	7,73	n.a.
>50	6	n.a.	64,567	19,054	n.a.	MB*	6,192	9,49	n.a.
	Total:			200,8635	0		137,38	100	

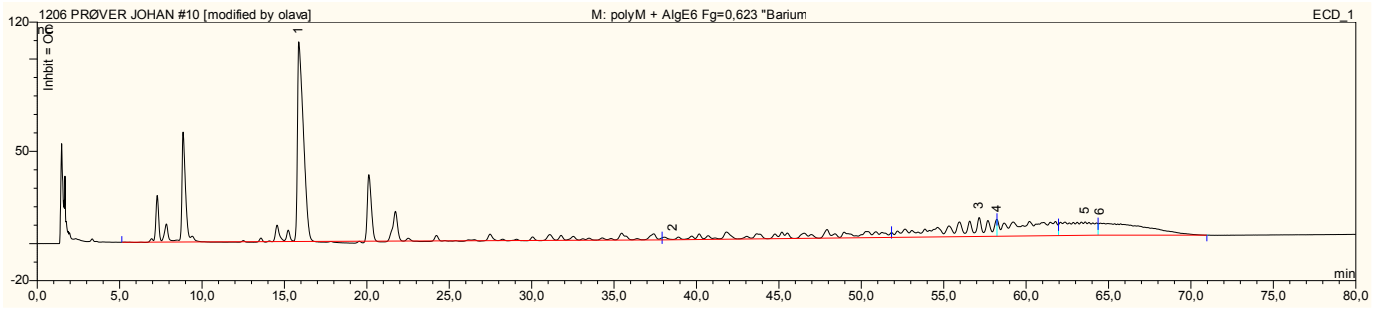

Figure B.5: HPAEC-PAD chromatogram of F_G=0,62 (Ba) degraded with M-lyase.

Table B.5: HPAEC-PAD data of F_G=0,62 (Ba) degraded with M-lyase.

F_G=0,62 (Ba) DP	No.	Peakname	Ret.Time min	Area nC*min	Amount	Type	Height nC	Rel.Area %	Resolution
1-10	1	n.a.	15,867	95,0962	n.a.	BM *	108,13	46,95	n.a.
11-20	2	n.a.	38,583	20,164	n.a.	M *	0,193	9,96	n.a.
21-30	3	n.a.	57,15	25,5099	n.a.	M *	10,271	12,59	n.a.
31-40	4	n.a.	58,25	23,2134	n.a.	M *	8,988	11,46	n.a.
41-50	5	n.a.	63,583	15,9317	n.a.	M *	7,254	7,87	n.a.
>50	6	n.a.	64,5	22,6279	n.a.	MB*	6,504	11,17	n.a.
	Total:			202,543	0		141,34	100	

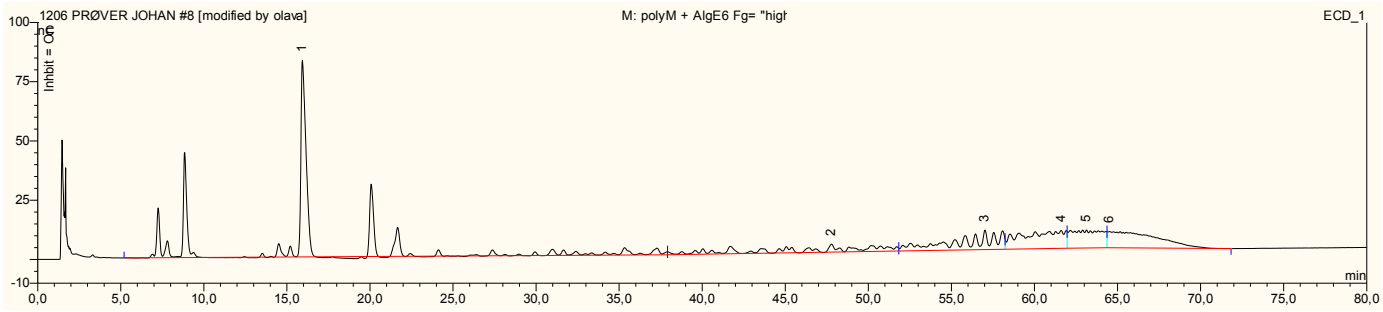

Figure B.6: HPAEC-PAD chromatogram of F_G=0,68 degraded with M-lyase.

Table B.6: HPAEC-PAD data of F_G=0,68 degraded with M-lyase.

F_G=0,68 DP	No.	Peakname	Ret.Time min	Area nC*min	Amount	Type	Height nC	Rel.Area %	Resolution
1-10	1	n.a.	15,933	67,8822	n.a.	BM *	82,888	41,37	2,45
11-20	2	n.a.	47,783	14,5272	n.a.	M *	3,353	8,85	1,09
21-30	3	n.a.	57,017	19,4708	n.a.	M *	8,219	11,87	n.a.
31-40	4	n.a.	61,617	21,9292	n.a.	M *	7,475	13,36	n.a.
41-50	5	n.a.	63,133	16,5466	n.a.	M *	7,556	10,08	n.a.
>50	6	n.a.	64,517	23,7405	n.a.	MB*	6,816	14,47	n.a.
	Total:			164,0965	0		116,31	100	

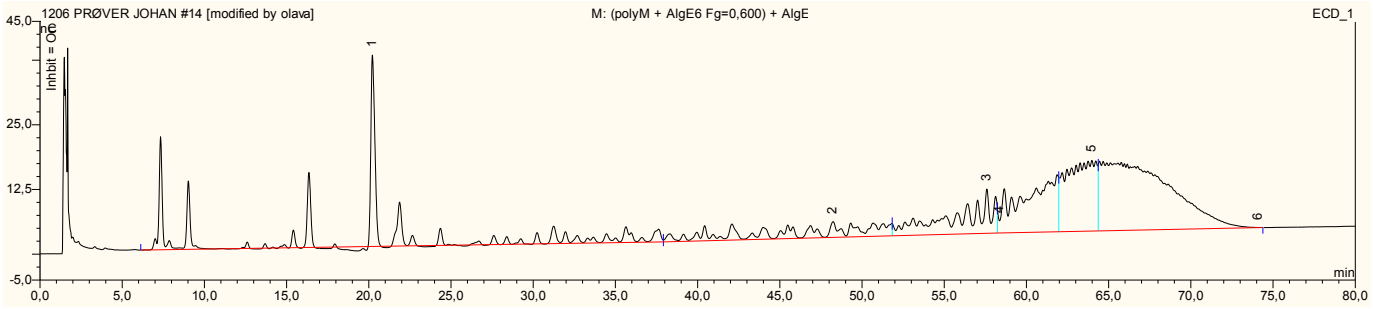

Figure B.7: HPAEC-PAD chromatogram of F_G=0,85 degraded with M-lyase.

Table B.7: HPAEC-PAD data of F_G=0,85 degraded with M-lyase.

F_G=0,85 DP	No.	Peakname	Ret.Time min	Area nC*min	Amount	Type	Height nC	Rel.Area %	Resolution
1-10	1	n.a.	20,217	35,1123	n.a.	BM *	37,009	18,4	1,42
11-20	2	n.a.	48,233	16,3436	n.a.	M *	3,044	8,56	0,96
21-30	3	n.a.	57,6	18,7626	n.a.	M *	8,551	9,83	n.a.
31-40	4	n.a.	58,367	26,0026	n.a.	M *	2,343	13,62	n.a.
41-50	5	n.a.	63,983	28,9186	n.a.	M *	13,657	15,15	n.a.
>50	6	n.a.	74,1	65,7304	n.a.	MB*	0,004	34,44	n.a.
	Total:			190,8699	0		64,609	100	

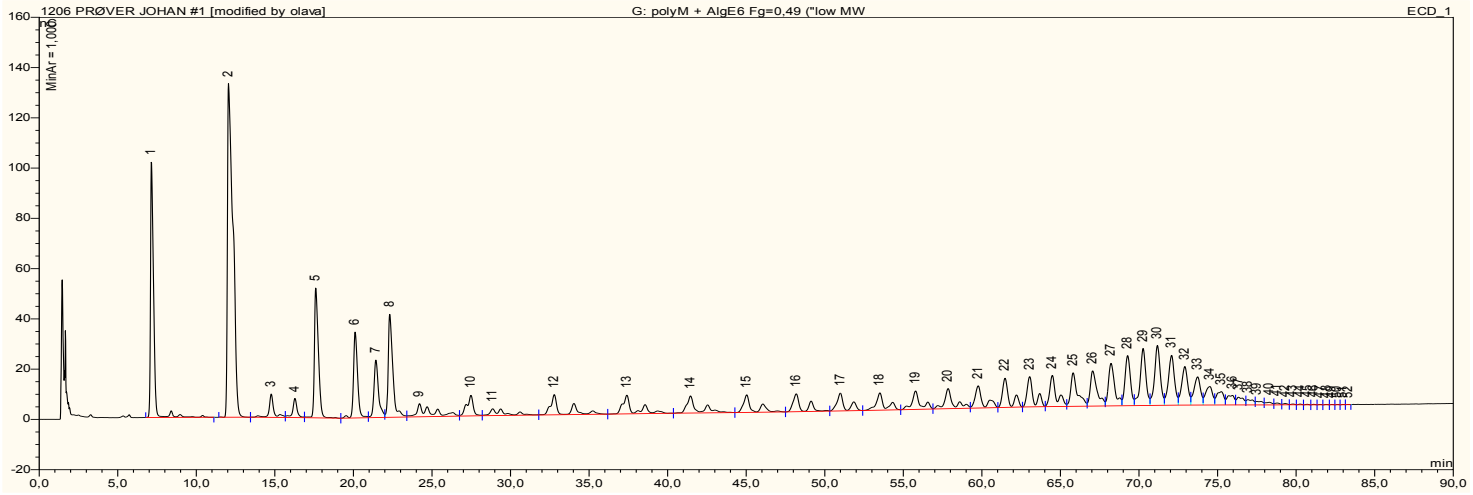

Figure B.8: HPAEC-PAD chromatogram of F_G=0,48 (not stirred) degraded with G-lyase.

Table B.8: HPAEC-PAD chromatogram of F_G=0,48 (not stirred) degraded with G-lyase.

F_G=0,48 (not stirred)	DP	No.	Peakname	Ret.Time min	Area nC*min	Amount	Type	Height nC	Rel.Area %	Resolution
ΔG2	2	1	n.a.	7,133	23,5532	n.a.	BMB*	101,56	8,08	9,01
ΔG3	3	2	n.a.	12,05	53,3677	n.a.	BMb*	132,724	18,32	4,8
ΔGM	3	3	n.a.	14,767	3,1135	n.a.	bM *	9,283	1,07	3,81
ΔMM	3	4	n.a.	16,283	2,4029	n.a.	M *	7,623	0,82	3,06
ΔG4	4	5	n.a.	17,6	15,1711	n.a.	Mb*	51,621	5,21	5,58
ΔGMG	4	6	n.a.	20,1	10,2708	n.a.	bM *	34,128	3,53	2,91
ΔMMG	4	7	n.a.	21,433	7,6266	n.a.	M *	22,856	2,62	1,85
ΔG5	5	8	n.a.	22,317	13,7486	n.a.	M *	40,973	4,72	4
	5	9	n.a.	24,2	5,0119	n.a.	M *	5,21	1,72	4,95
	5	10	n.a.	27,483	3,885	n.a.	M *	8,202	1,33	1,96
	5	11	n.a.	28,867	2,7449	n.a.	M *	2,709	0,94	7,27
	6	12	n.a.	32,783	5,8734	n.a.	Mb*	8,048	2,02	6,73
	7	13	n.a.	37,4	5,5869	n.a.	bMb*	7,411	1,92	5,35
	8	14	n.a.	41,467	5,0501	n.a.	bMb*	6,796	1,73	5,48
	9	15	n.a.	45,033	4,5676	n.a.	bMb*	7,009	1,57	4,92
	10	16	n.a.	48,183	4,4923	n.a.	bM *	7,105	1,54	4,38
	11	17	n.a.	51	4,3078	n.a.	Mb*	7,091	1,48	4,06
	12	18	n.a.	53,5	4,3208	n.a.	bMb*	6,862	1,48	3,78
	13	19	n.a.	55,783	4,3918	n.a.	bM *	7,331	1,51	3,42
	14	20	n.a.	57,85	5,0324	n.a.	M *	7,996	1,73	3,08
	15	21	n.a.	59,767	5,0574	n.a.	M *	8,812	1,74	2,78
	16	22	n.a.	61,467	5,8139	n.a.	Mb*	11,62	2	2,72
	17	23	n.a.	63,05	5,8826	n.a.	bM *	12,031	2,02	2,51
	18	24	n.a.	64,483	6,1328	n.a.	M *	12,418	2,11	2,31
	19	25	n.a.	65,817	6,6703	n.a.	M *	13,338	2,29	1,92
	20	26	n.a.	67,05	7,0548	n.a.	M *	14,026	2,42	1,69
	21	27	n.a.	68,217	7,872	n.a.	M *	16,94	2,7	1,61
	22	28	n.a.	69,267	7,9141	n.a.	M *	19,922	2,72	1,61
	23	29	n.a.	70,267	9,627	n.a.	M *	22,716	3,3	1,43
	24	30	n.a.	71,167	10,1969	n.a.	M *	23,826	3,5	1,36
	25	31	n.a.	72,067	8,8874	n.a.	M *	19,843	3,05	1,22
	26	32	n.a.	72,917	6,9265	n.a.	M *	15,373	2,38	1,09
	27	33	n.a.	73,733	5,4024	n.a.	M *	11,216	1,85	0,92
	28	34	n.a.	74,517	3,8423	n.a.	M *	7,352	1,32	0,74
	29	35	n.a.	75,233	2,828	n.a.	M *	5,276	0,97	n.a.
	30	36	n.a.	75,95	2,0545	n.a.	M *	3,772	0,71	n.a.
	31	37	n.a.	76,333	1,5913	n.a.	M *	3,041	0,55	n.a.
	32	38	n.a.	76,933	1,0801	n.a.	M *	2,067	0,37	n.a.
	33	39	n.a.	77,5	0,6956	n.a.	M *	1,351	0,24	n.a.
	34	40	n.a.	78,3	0,5062	n.a.	M *	1,039	0,17	n.a.
	35	41	n.a.	78,783	0,2702	n.a.	M *	0,716	0,09	n.a.
	36	42	n.a.	79,3	0,165	n.a.	M *	0,525	0,06	0,88
	37	43	n.a.	79,767	0,083	n.a.	Mb*	0,292	0,03	1,19
	38	44	n.a.	80,267	0,0618	n.a.	bMb*	0,287	0,02	1,29
	39	45	n.a.	80,733	0,045	n.a.	bMb*	0,212	0,02	1,11
	40	46	n.a.	81,117	0,0432	n.a.	bMb*	0,226	0,01	1,26
	41	47	n.a.	81,533	0,0318	n.a.	bMb*	0,164	0,01	1,25
	42	48	n.a.	81,933	0,0264	n.a.	bMb*	0,145	0,01	1
	43	49	n.a.	82,267	0,0191	n.a.	bMb*	0,1	0,01	1,04
	44	50	n.a.	82,617	0,0181	n.a.	bMb*	0,108	0,01	1,32
	45	51	n.a.	82,967	0,0133	n.a.	bMb*	0,098	0	1,48
	46	52	n.a.	83,317	0,0123	n.a.	bMB*	0,07	0	n.a.
Total		1378	0			0	0	711,46		

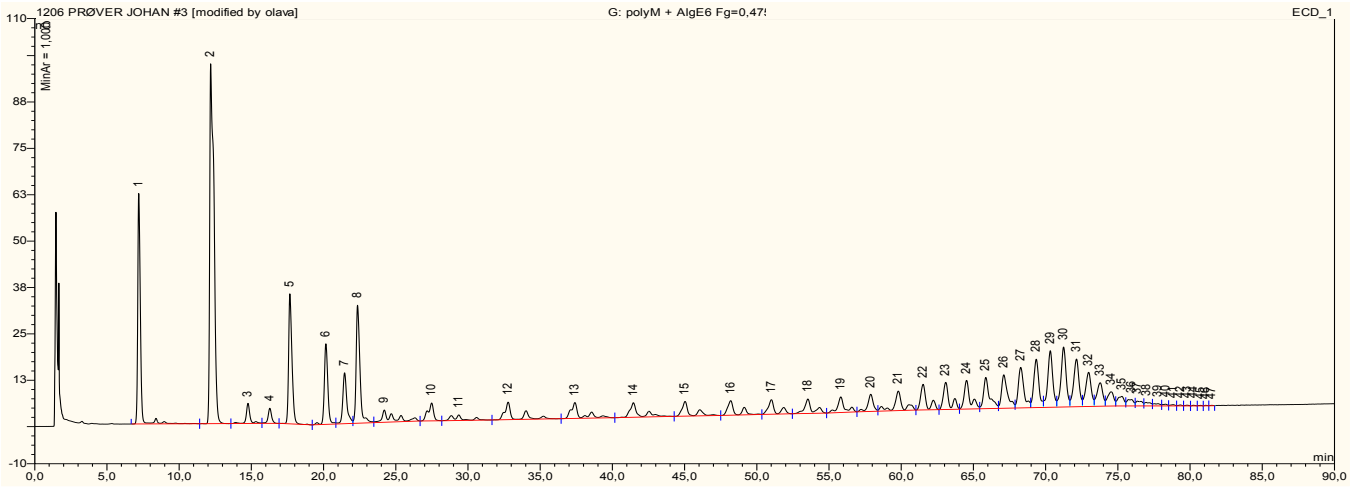

Figure B.9: HPAEC-PAD chromatogram of F_G=0,48 degraded with G-lyase.

Table B.9: HPAEC-PAD chromatogram of F_G=0,48 degraded with G-lyase.

	F_G=0,48 DP	No.	Peakname	Ret.Time min	Area nC*min	Amount	Type	Height nC	Rel.Area %	Resolution
ΔG2	2	1	n.a.	7,2	13,4048	n.a.	BMb*	62,096	7,8	11,12
ΔG3	3	2	n.a.	12,183	32,5654	n.a.	bMb*	97,004	18,94	5,36
ΔGM	3	3	n.a.	14,767	1,6498	n.a.	bM *	5,438	0,96	3,86
ΔMM	3	4	n.a.	16,283	1,1488	n.a.	Mb*	4,089	0,67	3,4
ΔG4	4	5	n.a.	17,667	9,4512	n.a.	bMb*	35,057	5,5	6
ΔGMG	4	6	n.a.	20,167	6,1705	n.a.	bM *	21,724	3,59	2,93
ΔMMG	4	7	n.a.	21,45	4,4678	n.a.	M *	13,718	2,6	2,01
ΔG5	5	8	n.a.	22,35	9,6608	n.a.	M *	31,821	5,62	4,16
	5	9	n.a.	24,2	2,7218	n.a.	Mb*	3,295	1,58	5,02
	5	10	n.a.	27,483	2,1492	n.a.	bMb*	4,821	1,25	1,71
	5	11	n.a.	29,367	1,2439	n.a.	bMb*	1,499	0,72	3,66
	6	12	n.a.	32,783	3,1861	n.a.	bMb*	4,725	1,85	6,67
	7	13	n.a.	37,4	3,0375	n.a.	bMb*	4,277	1,77	5,25
	8	14	n.a.	41,467	2,7369	n.a.	bMb*	3,93	1,59	5,44
	9	15	n.a.	45,033	2,4604	n.a.	bMb*	3,959	1,43	4,92
	10	16	n.a.	48,2	2,4053	n.a.	bMb*	3,93	1,4	4,39
	11	17	n.a.	51,017	2,2952	n.a.	bMb*	3,924	1,33	4,16
	12	18	n.a.	53,533	2,346	n.a.	bMb*	3,891	1,36	3,86
	13	19	n.a.	55,817	2,3458	n.a.	bMb*	4,193	1,36	3,52
	14	20	n.a.	57,9	2,0139	n.a.	bM *	4,61	1,17	3,15
	15	21	n.a.	59,8	3,3371	n.a.	Mb*	5,245	1,94	2,87
	16	22	n.a.	61,517	3,3268	n.a.	bMb*	6,909	1,93	2,7
	17	23	n.a.	63,083	3,5156	n.a.	bM *	7,331	2,04	2,53
	18	24	n.a.	64,517	3,7013	n.a.	M *	7,73	2,15	2,34
	19	25	n.a.	65,85	4,0843	n.a.	M *	8,416	2,38	1,99
	20	26	n.a.	67,1	4,3608	n.a.	M *	9,025	2,54	1,77
	21	27	n.a.	68,283	4,9796	n.a.	M *	10,926	2,9	1,66
	22	28	n.a.	69,35	5,3227	n.a.	M *	13,058	3,1	1,6
	23	29	n.a.	70,333	6,2065	n.a.	M *	15,242	3,61	1,49
	24	30	n.a.	71,25	6,7371	n.a.	M *	16,162	3,92	1,38
	25	31	n.a.	72,133	5,5814	n.a.	M *	12,853	3,25	1,25
	26	32	n.a.	72,983	4,1466	n.a.	M *	9,227	2,41	1,1
	27	33	n.a.	73,783	2,9598	n.a.	M *	6,33	1,72	0,91
	28	34	n.a.	74,533	1,9306	n.a.	M *	3,828	1,12	0,8
	29	35	n.a.	75,283	1,3636	n.a.	M *	2,586	0,79	n.a.
	30	36	n.a.	75,95	0,9211	n.a.	M *	1,717	0,54	n.a.
	31	37	n.a.	76,333	0,6605	n.a.	M *	1,299	0,38	n.a.
	32	38	n.a.	76,983	0,4702	n.a.	M *	0,932	0,27	n.a.
	33	39	n.a.	77,783	0,3199	n.a.	M *	0,605	0,19	n.a.
	34	40	n.a.	78,333	0,1714	n.a.	M *	0,463	0,1	n.a.
	35	41	n.a.	78,833	0,1226	n.a.	M *	0,334	0,07	0,93
	36	42	n.a.	79,333	0,0685	n.a.	M *	0,268	0,04	1,07
	37	43	n.a.	79,8	0,0576	n.a.	Mb*	0,213	0,03	1,05
	38	44	n.a.	80,233	0,0415	n.a.	bM *	0,191	0,02	1,19
	39	45	n.a.	80,733	0,0379	n.a.	Mb*	0,163	0,02	0,84
	40	46	n.a.	81,083	0,0335	n.a.	bM *	0,15	0,02	1,03
	41	47	n.a.	81,5	0,0287	n.a.	MB*	0,116	0,02	n.a.
		Total:			171,9483	0		459,319	100	

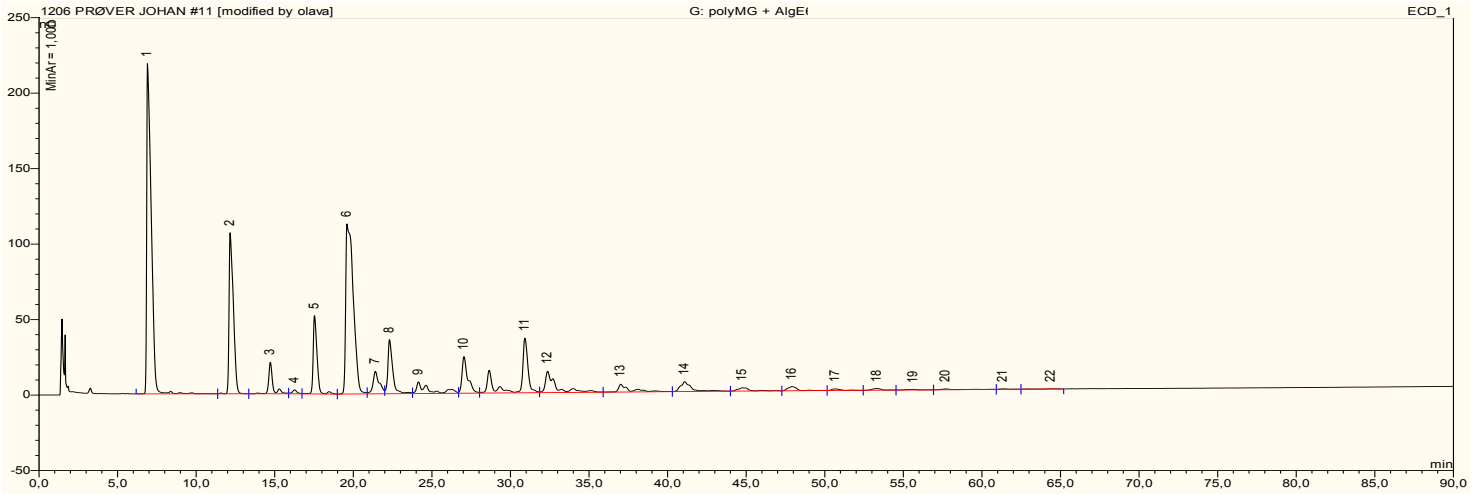

Figure B.10: HPAEC-PAD chromatogram of F_G=0,56 (MG) degraded with G-lyase.

Table B.10: HPAEC-PAD chromatogram of F_G=0,56 (MG) degraded with G-lyase.

F_G=0,56 (MG)	DP	No.	Peakname	Ret.Time min	Area nC*min	Amount	Type	Height nC	Rel.Area %	Resolution
ΔG2	2	1	n.a.	6,9	72,381	n.a.	BMb*	218,704	26,45	10,11
ΔG3	3	2	n.a.	12,167	33,6135	n.a.	bMb*	106,655	12,28	5,75
ΔGM	3	3	n.a.	14,717	6,2503	n.a.	bM *	20,849	2,28	3,7
ΔMM	3	4	n.a.	16,267	0,934	n.a.	M *	2,677	0,34	2,84
ΔG4	4	5	n.a.	17,533	14,8216	n.a.	Mb*	51,831	5,42	3,11
ΔGMG	4	6	n.a.	19,6	63,2209	n.a.	bM *	112,715	23,1	2,39
ΔMMG	4	7	n.a.	21,4	6,8557	n.a.	M *	14,904	2,5	1,64
ΔG5	5	8	n.a.	22,3	12,6431	n.a.	M *	35,832	4,62	3,9
	5	9	n.a.	24,15	6,4541	n.a.	M *	7,726	2,36	5,98
	5	10	n.a.	27,033	10,1786	n.a.	M *	24,25	3,72	7,39
	5	11	n.a.	30,917	20,4744	n.a.	M *	36,209	7,48	1,9
	6	12	n.a.	32,367	10,3901	n.a.	M *	14,155	3,8	4,85
	7	13	n.a.	37,017	4,2329	n.a.	M *	5,177	1,55	3,8
	8	14	n.a.	41,083	5,1114	n.a.	Mb*	6,52	1,87	3
	9	15	n.a.	44,75	1,831	n.a.	bMb*	2,179	0,67	2,71
	10	16	n.a.	47,917	1,8714	n.a.	bMb*	2,763	0,68	2,59
	11	17	n.a.	50,667	0,6736	n.a.	bMb*	1,014	0,25	2,53
	12	18	n.a.	53,317	0,758	n.a.	bMb*	1,131	0,28	1,94
	13	19	n.a.	55,633	0,2817	n.a.	bMb*	0,343	0,1	1,85
	14	20	n.a.	57,683	0,4241	n.a.	bMb*	0,543	0,15	4,29
	15	21	n.a.	61,333	0,1501	n.a.	bMb*	0,287	0,05	1,56
	16	22	n.a.	64,383	0,1469	n.a.	bMB*	0,162	0,05	n.a.
		Total:			273,6984	0		666,624	100	

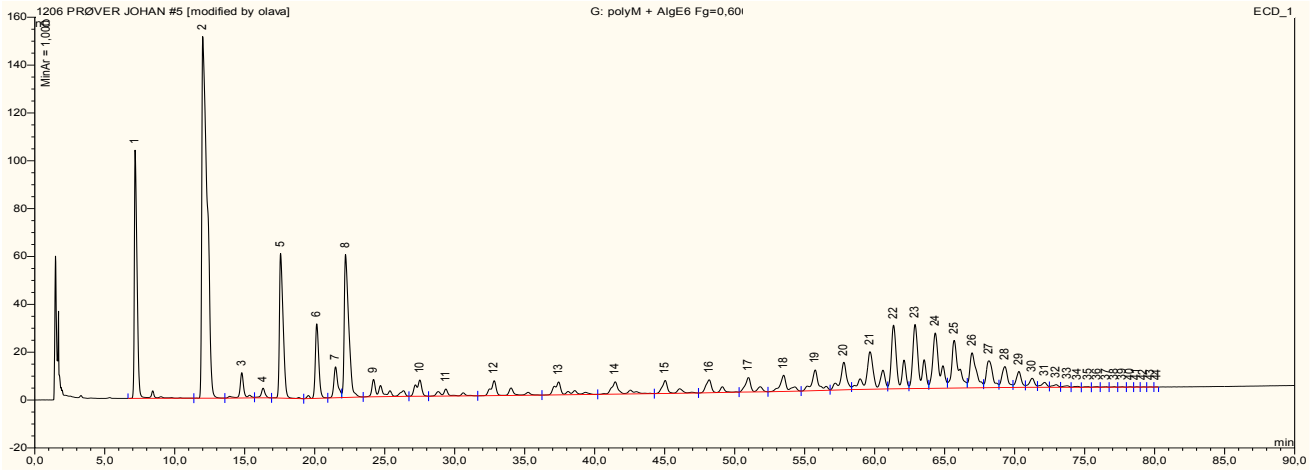

Figure B.11: HPAEC-PAD chromatogram of F_G=0,60 degraded with G-lyase.

Table B.11: HPAEC-PAD chromatogram of F_G=0,60 with G-lyase.

	F_G=0,60 DP	No.	Peakname	Ret.Time min	Area nC*min	Amount	Type	Height nC	Rel.Area %	Resolution
ΔG2	2	1	n.a.	7,167	23,9966	n.a.	BMb*	103,725	8,37	8,46
ΔG3	3	2	n.a.	12	66,1582	n.a.	bM *	151,127	23,07	4,72
ΔGM	3	3	n.a.	14,8	3,4146	n.a.	M *	10,588	1,19	3,68
ΔMM	3	4	n.a.	16,317	1,2859	n.a.	Mb*	4,043	0,45	2,74
ΔG4	4	5	n.a.	17,567	18,4238	n.a.	bMb*	60,397	6,42	5,62
ΔGMG	4	6	n.a.	20,15	9,1587	n.a.	bM *	31,139	3,19	2,94
ΔMMG	4	7	n.a.	21,483	4,3049	n.a.	M *	12,92	1,5	1,4
ΔG5	5	8	n.a.	22,2	21,8966	n.a.	Mb*	59,781	7,64	4,06
	5	9	n.a.	24,2	5,1931	n.a.	bMb*	7,262	1,81	4,84
	5	10	n.a.	27,517	3,3013	n.a.	bMb*	6,778	1,15	1,64
	5	11	n.a.	29,367	2,1508	n.a.	bMb*	2,951	0,75	3,72
	6	12	n.a.	32,817	4,4234	n.a.	bMb*	6,243	1,54	6,21
	7	13	n.a.	37,417	4,188	n.a.	bMb*	5,396	1,46	4,67
	8	14	n.a.	41,467	3,7426	n.a.	bMb*	5,143	1,31	4,96
	9	15	n.a.	45,033	3,3217	n.a.	bMb*	5,437	1,16	4,55
	10	16	n.a.	48,183	3,2876	n.a.	bMb*	5,424	1,15	4,05
	11	17	n.a.	50,983	3,5228	n.a.	bMb*	6,092	1,23	3,94
	12	18	n.a.	53,5	4,0119	n.a.	bMb*	6,784	1,4	3,61
	13	19	n.a.	55,75	4,9708	n.a.	bM *	8,638	1,73	3,27
	14	20	n.a.	57,8	6,0868	n.a.	M *	11,529	2,12	2,77
	15	21	n.a.	59,667	12,3077	n.a.	M *	15,7	4,29	2,53
	16	22	n.a.	61,35	14,3128	n.a.	M *	26,607	4,99	2,42
	17	23	n.a.	62,883	14,6279	n.a.	M *	26,777	5,1	2,21
	18	24	n.a.	64,333	12,8735	n.a.	M *	23,1	4,49	2,05
	19	25	n.a.	65,683	11,1228	n.a.	M *	19,912	3,88	1,76
	20	26	n.a.	66,967	7,7674	n.a.	M *	14,636	2,71	1,49
	21	27	n.a.	68,167	5,9139	n.a.	M *	11,206	2,06	1,5
	22	28	n.a.	69,3	4,0968	n.a.	M *	8,746	1,43	1,51
	23	29	n.a.	70,317	2,784	n.a.	M *	6,643	0,97	1,46
	24	30	n.a.	71,25	1,6625	n.a.	M *	3,785	0,58	1,36
	25	31	n.a.	72,133	0,9384	n.a.	M *	2,055	0,33	1,1
	26	32	n.a.	72,967	0,5234	n.a.	M *	1,104	0,18	0,93
	27	33	n.a.	73,767	0,3034	n.a.	M *	0,638	0,11	0,87
	28	34	n.a.	74,483	0,1697	n.a.	Mb*	0,384	0,06	1
	29	35	n.a.	75,25	0,1014	n.a.	bMb*	0,253	0,04	0,89
	30	36	n.a.	75,883	0,09	n.a.	bM *	0,242	0,03	0,93
	31	37	n.a.	76,517	0,0758	n.a.	M *	0,202	0,03	1
	32	38	n.a.	77,133	0,067	n.a.	M *	0,195	0,02	0,98
	33	39	n.a.	77,683	0,0573	n.a.	M *	0,169	0,02	1,06
	34	40	n.a.	78,233	0,0462	n.a.	M *	0,161	0,02	1,01
	35	41	n.a.	78,7	0,0404	n.a.	M *	0,147	0,01	1,19
	36	42	n.a.	79,2	0,0307	n.a.	Mb*	0,125	0,01	1,32
	37	43	n.a.	79,7	0,019	n.a.	bMb*	0,078	0,01	1,37
	38	44	n.a.	80,167	0,0132	n.a.	bMB*	0,075	0	n.a.
		Total:			286,7853	0		674,334	100	

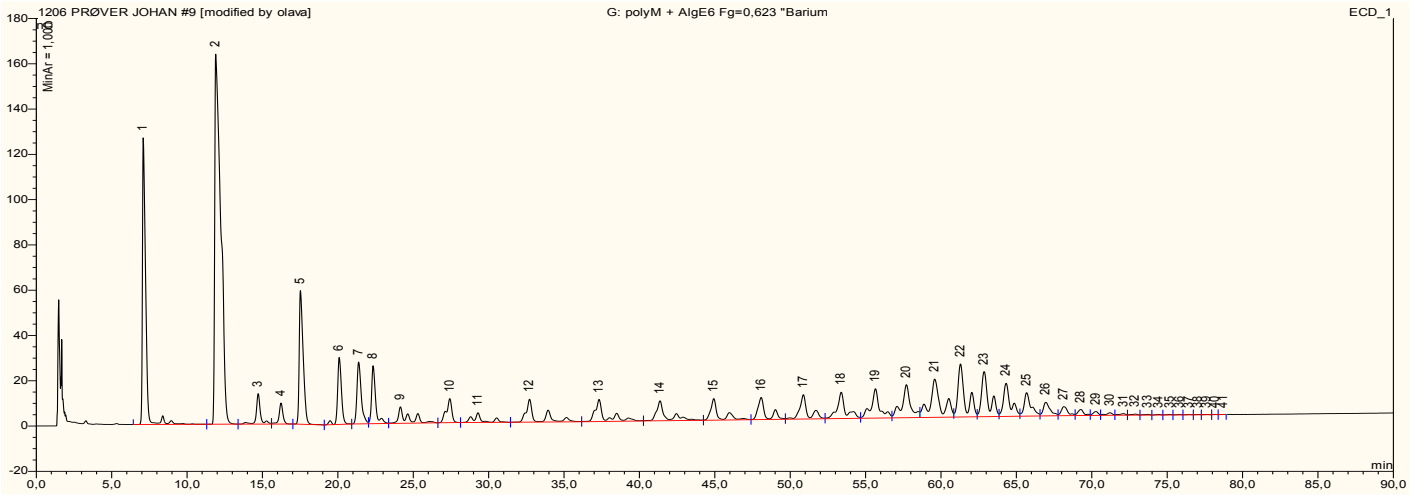

Figure B.12: HPAEC-PAD chromatogram of F_G=0,62 (Ba) degraded with G-lyase.

Table B.12: HPAEC-PAD chromatogram of F_G=0,62 (Ba) degraded with G-lyase.

F_G=0,62 (Ba)	DP	No.	Peakname	Ret.Time min	Area nC*min	Amount	Type	Height nC	Rel.Area %	Resolution
ΔG2	2	1	n.a.	7,083	31,7128	n.a.	BMb*	126,576	10,78	8,5
ΔG3	3	2	n.a.	11,9	75,3027	n.a.	bMb*	163,42	25,6	4,9
ΔGM	3	3	n.a.	14,717	4,2341	n.a.	bM *	13,457	1,44	3,81
ΔMM	3	4	n.a.	16,233	2,6959	n.a.	Mb*	9,295	0,92	2,93
ΔG4	4	5	n.a.	17,517	17,8746	n.a.	bMb*	58,952	6,08	5,63
ΔGMG	4	6	n.a.	20,083	8,8717	n.a.	bMb*	29,549	3,02	2,8
ΔMMG	4	7	n.a.	21,383	9,028	n.a.	bM *	27,315	3,07	2,08
ΔG5	5	8	n.a.	22,333	7,8202	n.a.	M *	25,565	2,66	4,24
	5	9	n.a.	24,15	4,9435	n.a.	Mb*	7,264	1,68	6,95
	5	10	n.a.	27,433	4,4677	n.a.	bMb*	10,611	1,52	2,22
	5	11	n.a.	29,3	2,8701	n.a.	bMb*	4,255	0,98	4,03
	6	12	n.a.	32,717	7,2503	n.a.	bM *	10,117	2,46	6,93
	7	13	n.a.	37,333	7,0959	n.a.	M *	9,751	2,41	5,55
	8	14	n.a.	41,367	6,2365	n.a.	M *	8,814	2,12	5,68
	9	15	n.a.	44,933	5,7294	n.a.	M *	9,522	1,95	4,92
	10	16	n.a.	48,083	5,7734	n.a.	M *	9,741	1,96	4,24
	11	17	n.a.	50,867	6,5889	n.a.	M *	10,753	2,24	3,95
	12	18	n.a.	53,383	7,448	n.a.	M *	11,624	2,53	3,58
	13	19	n.a.	55,65	8,47	n.a.	M *	12,975	2,88	3,13
	14	20	n.a.	57,7	9,6307	n.a.	M *	14,582	3,27	2,6
	15	21	n.a.	59,583	13,815	n.a.	M *	16,905	4,7	2,43
	16	22	n.a.	61,3	13,2204	n.a.	M *	23,426	4,49	2,44
	17	23	n.a.	62,867	11,0302	n.a.	M *	19,922	3,75	2,29
	18	24	n.a.	64,317	7,9324	n.a.	M *	14,602	2,7	2,18
	19	25	n.a.	65,683	5,4516	n.a.	M *	10,369	1,85	1,81
	20	26	n.a.	66,95	3,1757	n.a.	M *	5,989	1,08	1,59
	21	27	n.a.	68,15	2,0208	n.a.	M *	3,99	0,69	1,61
	22	28	n.a.	69,267	1,2031	n.a.	M *	2,663	0,41	1,59
	23	29	n.a.	70,283	0,6718	n.a.	M *	1,722	0,23	1,52
	24	30	n.a.	71,217	0,5347	n.a.	M *	1,13	0,18	1,17
	25	31	n.a.	72,117	0,3341	n.a.	M *	0,684	0,11	0,83
	26	32	n.a.	72,883	0,2202	n.a.	M *	0,454	0,07	0,96
	27	33	n.a.	73,717	0,1278	n.a.	M *	0,302	0,04	1,03
	28	34	n.a.	74,45	0,0897	n.a.	M *	0,249	0,03	1,11
	29	35	n.a.	75,183	0,0799	n.a.	M *	0,209	0,03	0,92
	30	36	n.a.	75,833	0,0599	n.a.	M *	0,158	0,02	0,99
	31	37	n.a.	76,45	0,0545	n.a.	M *	0,163	0,02	0,94
	32	38	n.a.	77,05	0,0453	n.a.	M *	0,127	0,02	0,87
	33	39	n.a.	77,633	0,0409	n.a.	M *	0,111	0,01	0,99
	34	40	n.a.	78,183	0,0201	n.a.	Mb*	0,077	0,01	1,24
	35	41	n.a.	78,733	0,016	n.a.	bMB*	0,073	0,01	n.a.
		Total:			294,1883	0		677,462	100	

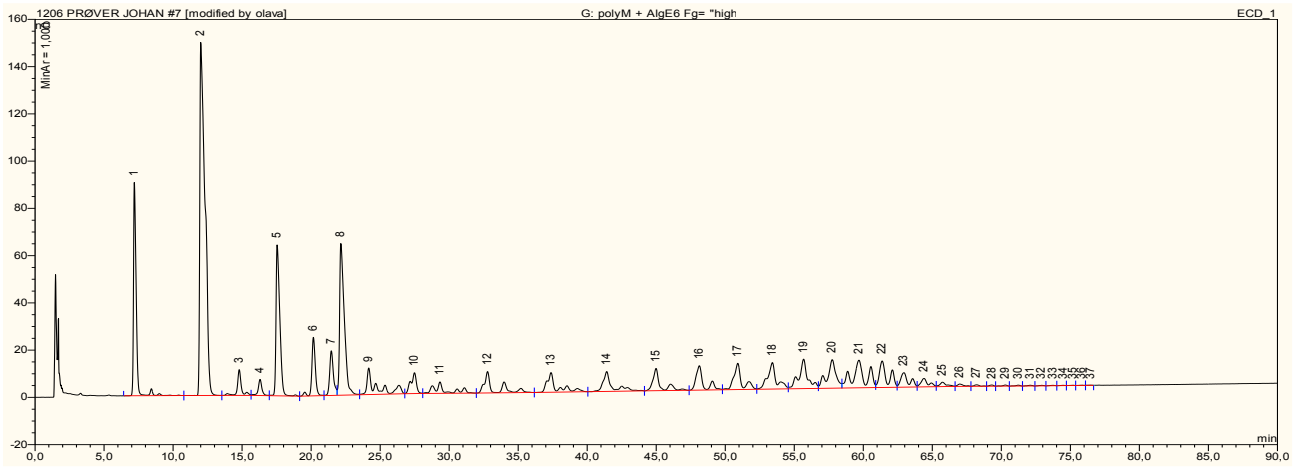

Figure B.13: HPAEC-PAD chromatogram of F_G=0,68 degraded with G-lyase.

Table B.13: HPAEC-PAD chromatogram of F_G=0,68 degraded with G-lyase.

	F_G=0,68 DP	No.	Peakname	Ret.Time min	Area nC*min	Amount	Type	Height nC	Rel.Area %	Resolution
ΔG2	2	1	n.a.	7,183	20,3668	n.a.	BMb*	90,244	7,9	8,57
ΔG3	3	2	n.a.	12	64,6516	n.a.	bMb*	149,445	25,08	4,76
ΔGM	3	3	n.a.	14,8	3,5595	n.a.	bM *	10,892	1,38	3,72
ΔMM	3	4	n.a.	16,3	2,1321	n.a.	M *	6,852	0,83	2,72
ΔG4	4	5	n.a.	17,533	20,3027	n.a.	Mb*	63,892	7,88	5,71
ΔGMG	4	6	n.a.	20,167	7,3853	n.a.	bM *	24,802	2,87	2,93
ΔMMG	4	7	n.a.	21,467	5,9714	n.a.	M *	18,888	2,32	1,3
ΔG5	5	8	n.a.	22,15	25,0317	n.a.	M *	64,204	9,71	3,91
	5	9	n.a.	24,167	7,7466	n.a.	M *	11,228	3,01	4,96
	5	10	n.a.	27,483	4,0865	n.a.	M *	8,817	1,59	1,65
	5	11	n.a.	29,333	4,1769	n.a.	Mb*	4,839	1,62	3,69
	6	12	n.a.	32,783	6,4111	n.a.	bMb*	9,053	2,49	6,48
	7	13	n.a.	37,383	6,2774	n.a.	bMb*	8,312	2,44	4,89
	8	14	n.a.	41,417	6,0853	n.a.	bMb*	8,411	2,36	5,07
	9	15	n.a.	44,983	5,7058	n.a.	bMb*	9,428	2,21	4,46
	10	16	n.a.	48,117	6,2406	n.a.	bM *	10,319	2,42	3,69
	11	17	n.a.	50,917	7,1906	n.a.	M *	11,123	2,79	3,27
	12	18	n.a.	53,417	8,0699	n.a.	M *	11,199	3,13	3,12
	13	19	n.a.	55,683	9,035	n.a.	M *	12,474	3,51	2,69
	14	20	n.a.	57,75	8,8095	n.a.	M *	12,077	3,42	1,4
	15	21	n.a.	59,683	12,0893	n.a.	M *	11,685	4,69	1,28
	16	22	n.a.	61,367	7,456	n.a.	M *	11,209	2,89	2,11
	17	23	n.a.	62,933	4,0752	n.a.	M *	6,087	1,58	1,98
	18	24	n.a.	64,4	2,1642	n.a.	M *	3,551	0,84	1,96
	19	25	n.a.	65,733	1,0237	n.a.	M *	1,841	0,4	1,85
	20	26	n.a.	66,983	0,4879	n.a.	M *	0,973	0,19	1,77
	21	27	n.a.	68,2	0,2759	n.a.	M *	0,611	0,11	1,82
	22	28	n.a.	69,317	0,1719	n.a.	M *	0,499	0,07	1,82
	23	29	n.a.	70,3	0,1812	n.a.	Mb*	0,474	0,07	1,77
	24	30	n.a.	71,233	0,1435	n.a.	bMb*	0,387	0,06	1,52
	25	31	n.a.	72,1	0,1211	n.a.	bMb*	0,31	0,05	1,3
	26	32	n.a.	72,9	0,0902	n.a.	bMb*	0,239	0,04	1,37
	27	33	n.a.	73,733	0,0695	n.a.	bMb*	0,194	0,03	1,34
	28	34	n.a.	74,5	0,046	n.a.	bMb*	0,133	0,02	1,25
	29	35	n.a.	75,2	0,0389	n.a.	bMb*	0,116	0,02	1,19
	30	36	n.a.	75,833	0,0341	n.a.	bM *	0,098	0,01	1,18
	31	37	n.a.	76,467	0,0318	n.a.	MB*	0,102	0,01	n.a.
		Total:			257,7367	0		585,005	100	

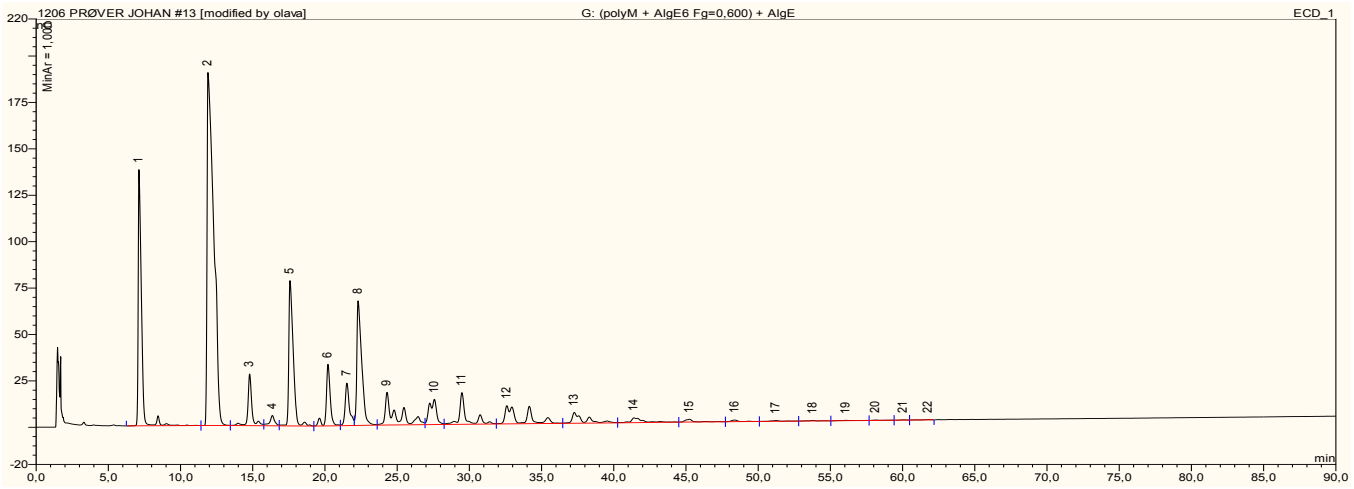

Figure B.14: HPAEC-PAD chromatogram of F_G=0,85 degraded with G-lyase.

Table B.14: HPAEC-PAD chromatogram of F_G=0,85 degraded with G-lyase.

	F_G=0,85 DP	No.	Peakname	Ret.Time min	Area nC*min	Amount	Type	Height nC	Rel.Area %	Resolution
ΔG2	2	1	n.a.	7,117	35,7633	n.a.	BMb*	137,949	13,22	7,71
ΔG3	3	2	n.a.	11,9	100,6394	n.a.	bM *	190,144	37,2	4,64
ΔGM	3	3	n.a.	14,783	8,6868	n.a.	M *	27,885	3,21	3,6
ΔMM	3	4	n.a.	16,367	2,1718	n.a.	M *	5,54	0,8	2,37
ΔG4	4	5	n.a.	17,583	27,5336	n.a.	Mb*	78,25	10,18	5,36
ΔGMG	4	6	n.a.	20,217	10,8388	n.a.	bM *	33,14	4,01	2,87
ΔMMG	4	7	n.a.	21,517	7,8517	n.a.	M *	22,881	2,9	1,48
ΔG5	5	8	n.a.	22,3	26,3163	n.a.	M *	67,15	9,73	3,83
	5	9	n.a.	24,3	13,2556	n.a.	M *	17,615	4,9	4,51
	5	10	n.a.	27,583	7,7424	n.a.	M *	13,624	2,86	2,56
	5	11	n.a.	29,483	8,7285	n.a.	M *	17,068	3,23	3,92
	6	12	n.a.	32,6	11,0759	n.a.	M *	9,808	4,09	4,52
	7	13	n.a.	37,267	5,1518	n.a.	M *	5,81	1,9	4,25
	8	14	n.a.	41,4	2,4858	n.a.	Mb*	2,592	0,92	4,14
	9	15	n.a.	45,25	0,9705	n.a.	bMb*	1,486	0,36	3,82
	10	16	n.a.	48,383	0,4779	n.a.	bMb*	0,837	0,18	3,32
	11	17	n.a.	51,233	0,2728	n.a.	bMb*	0,398	0,1	3,39
	12	18	n.a.	53,783	0,1965	n.a.	bMb*	0,312	0,07	4,16
	13	19	n.a.	56,067	0,1336	n.a.	bMb*	0,211	0,05	3,73
	14	20	n.a.	58,133	0,1057	n.a.	bMb*	0,19	0,04	3,23
	15	21	n.a.	60,05	0,058	n.a.	bMb*	0,149	0,02	2,88
	16	22	n.a.	61,767	0,0776	n.a.	bMB*	0,144	0,03	n.a.
		Total:			270,5344	0		633,183	100	

Appendix B – Block structure analysis

9 Appendix C – Molecular weight

The molecular weights of the epimerized alginates were measured by SEC-MALLS. A mannuronan sample with a molecular weight of 242 kDa was used as a start material. The results for each AlgE6 epimerized sample are given in the following figures:

- F_G=0,48 – Figure C.1
- F_G=0,56 (MG) - Figure C.2
- F_G=0,60 - Figure C.3
- F_G=0,62 (Ba) - Figure C.4
- F_G=0,68 - Figure C.5
- F_G=0,85 - Figure C.6

Figure C.1: Molecular weight determined by SEC-MALLS of F_G=0,48

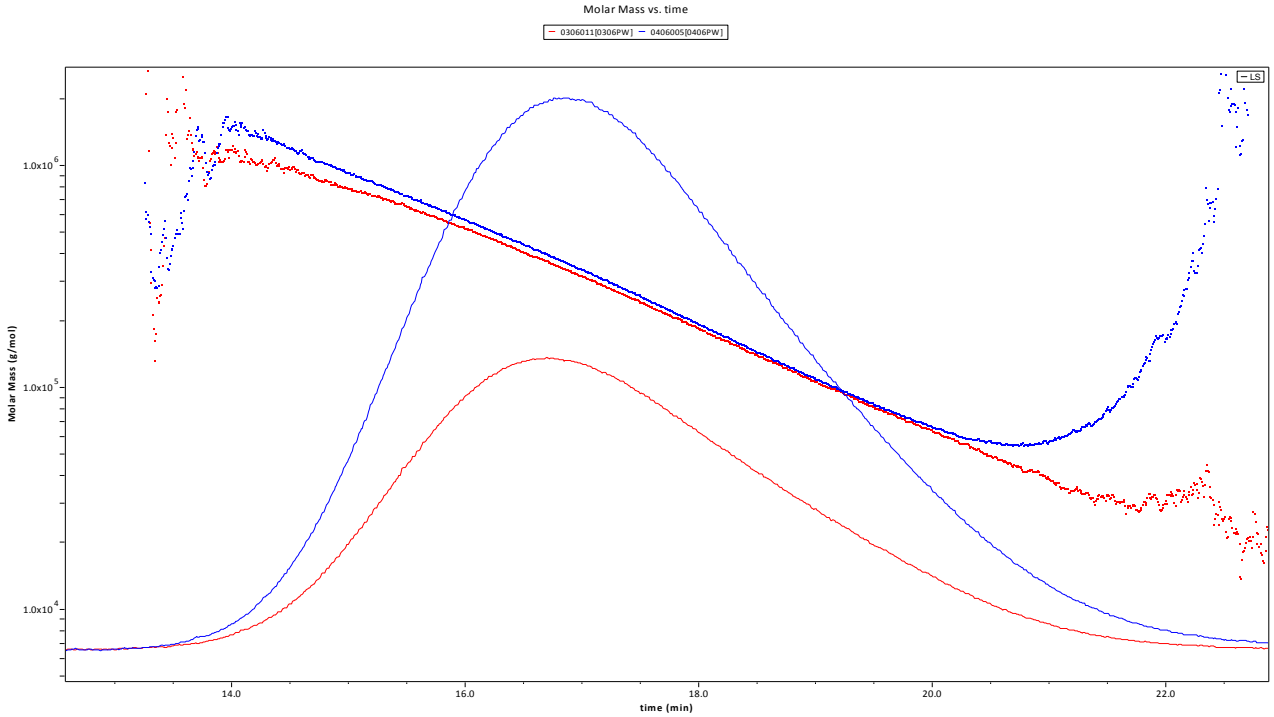

	Sample description	Mn (kDa)	Uncertainty	**Mw (kDa)**	Uncertainty	Polydispersity (Mw/Mn)	Uncertainty	Rw (nm)	Uncertainty	Injected mass (µg)	Mass recovery (%)
0406005[0406PW]	1) F_G=0.48	125,6	9,20%	**244,3**	4,50%	1,945	10,20%	80,4	6,20%	100	40
0306011[0306PW]	1) F_G=0.48	106,2	6,30%	**240**	2,10%	2,261	6,60%	73,5	2,50%	50	39,3
Average		115,9		**242,2**		2,103		77		75	39,6
Standard deviation		13,8		**3**		0,224		4,9		35,36	0,5
% Standard deviation		11,9		**1,3**		10,629		6,3		47,14	1,2

Figure C.2: Molecular weight determined by SEC-MALLS of F_G=0,56 (MG)

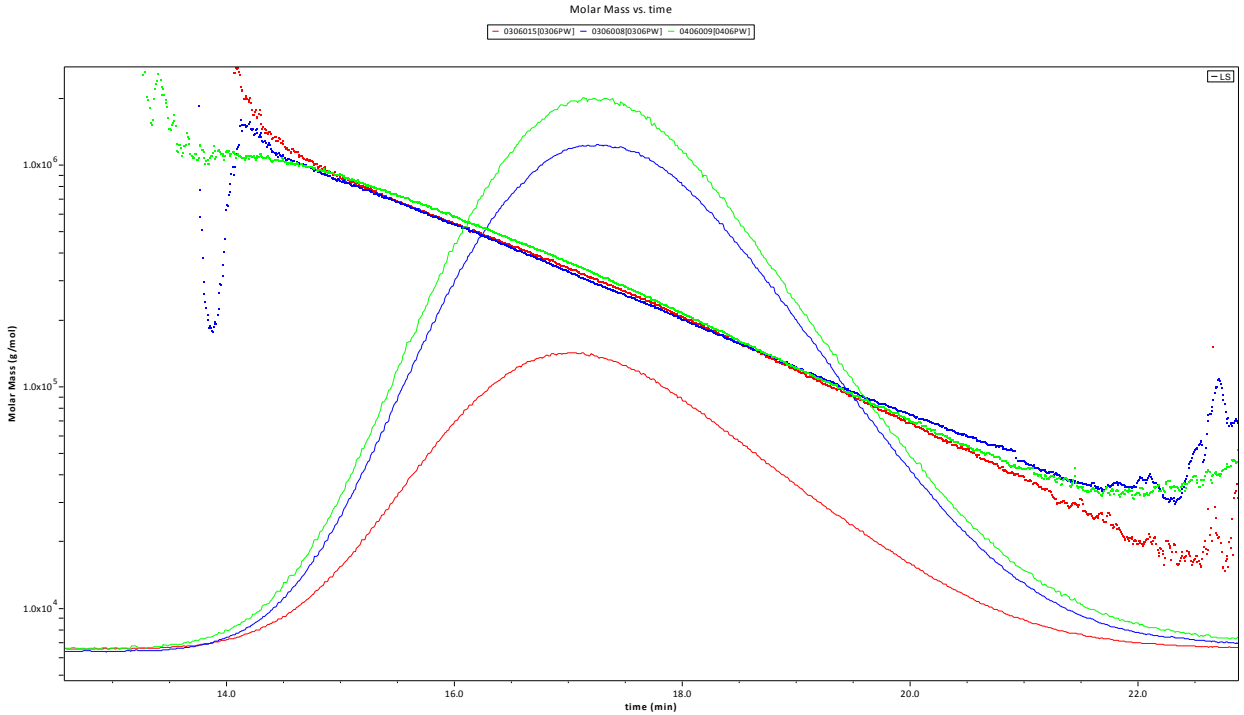

	Sample description	Mn (kDa)	Uncertainty	**Mw (kDa)**	Uncertainty	Polydispersity (Mw/Mn)	Uncertainty	Rw (nm)	Uncertainty	Injected mass (µg)	Mass recovery (%)
0306015[0306PW]	5) F_G=0,56 (MG)	106,3	3,80%	**237,6**	3,20%	2,234	5,00%	64,7	3,60%	50	59,7
0306008[0306PW]	5) F_G=0,56 (MG)	114,9	5,70%	**220,7**	4,10%	1,921	7,00%	70	3,80%	100	60,1
0406009[0406PW]	5) F_G=0,56 (MG)	100,4	4,60%	**218,6**	2,70%	2,177	5,30%	61,7	3,60%	100	65,6
Average		107,2		**225,6**		2,111		65,5		83,33	61,8
Standard deviation		9,1		**11**		0,234		5,1		40,82	3,4
% Standard deviation		8,4		**4,9**		11,074		7,8		48,99	5,4

Figure C.3: Molecular weight determined by SEC-MALLS of F_G=0,60

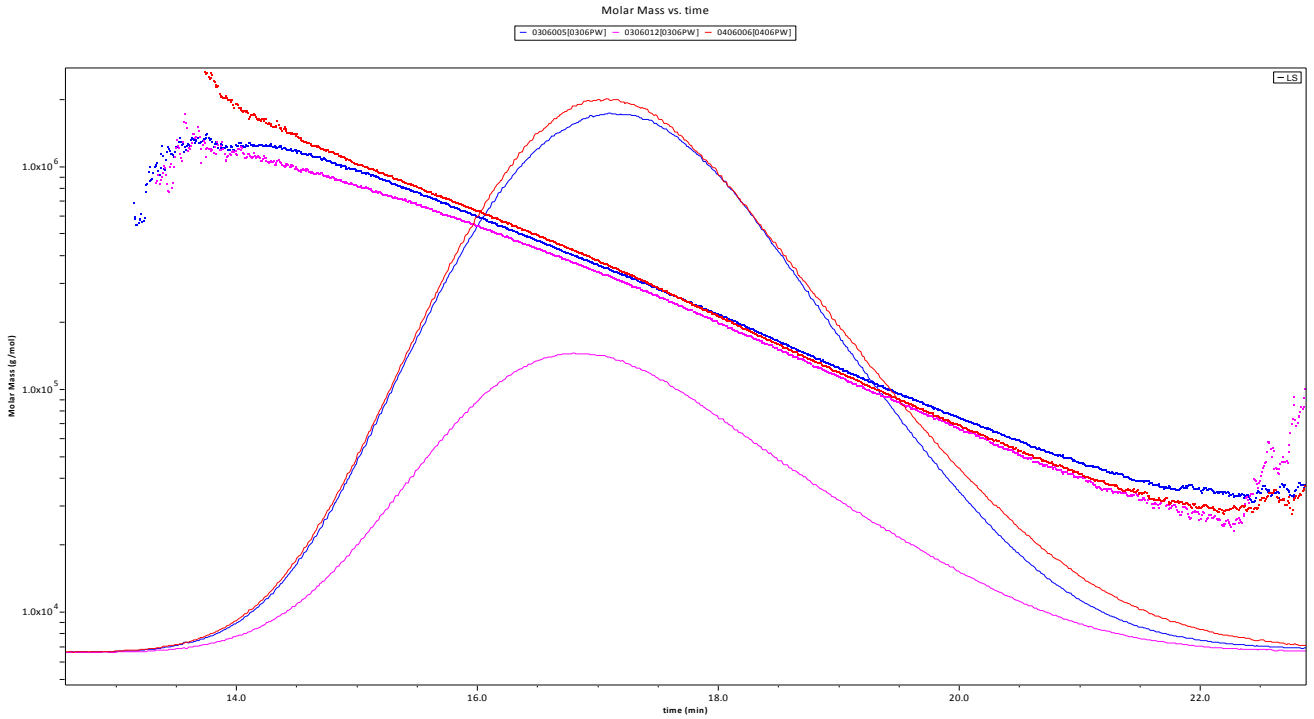

	Sample description	Mn (kDa)	Uncertainty	**Mw (kDa)**	Uncertainty	Polydispersity (Mw/Mn)	Uncertainty	Rw (nm)	Uncertainty	Injected mass (㎍)	Mass recovery (%)
0306005[0306PW]	2) F_G=0,60	130,3	1,50%	**270,5**	1,10%	2,075	1,80%	75,3	0,90%	100	57,8
0306012[0306PW]	2) F_G=0,60	111,9	4,30%	**251,3**	2,40%	2,246	4,90%	74,9	2,30%	50	64,6
0406006[0406PW]	2) F_G=0,60	99,1	3,20%	**248,9**	2,10%	2,511	3,90%	74,5	1,90%	100	67,2
Average		113,8		**256,9**		2,278		74,9		83,33	63,2
Standard deviation		19,5		**12,6**		0,27		0,5		40,82	6,7
% Standard deviation		17,1		**4,9**		11,871		0,7		48,99	10,6

Figure C.4: Molecular weight determined by SEC-MALLS of F_G=0,62 (Ba)

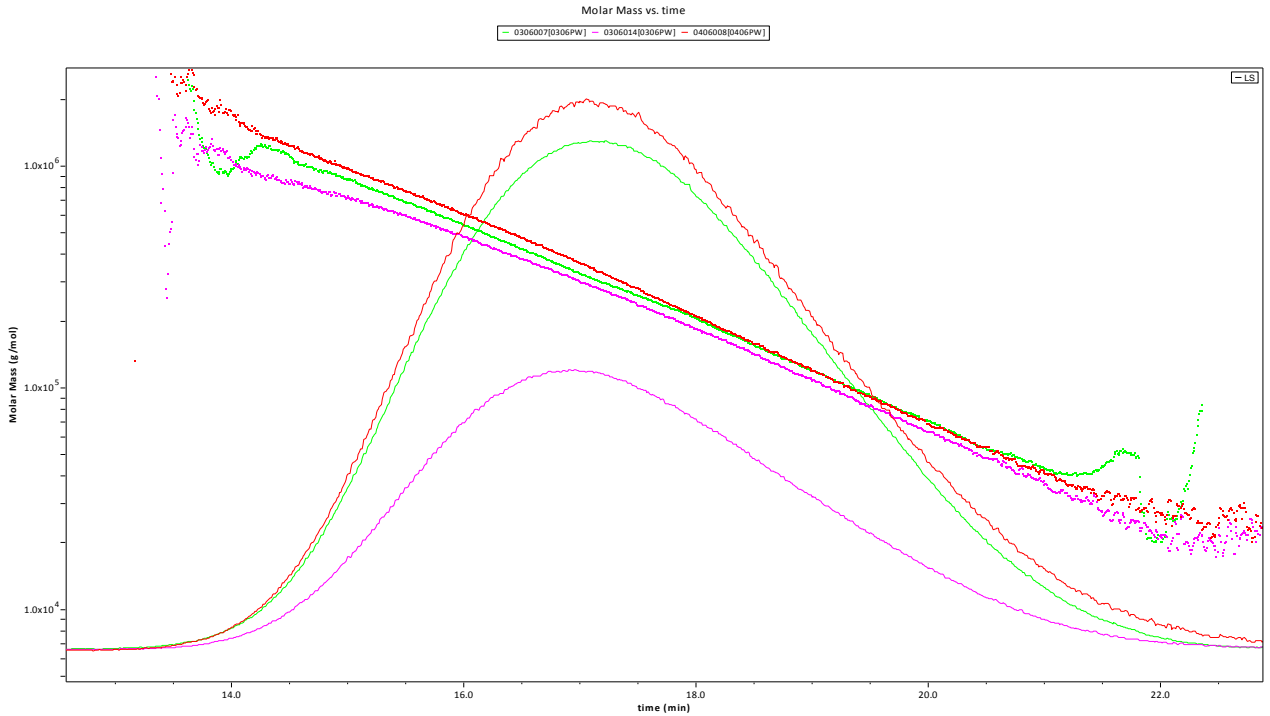

	Sample description	Mn (kDa)	Uncertainty	**Mw (kDa)**	Uncertainty	Polydispersity (Mw/Mn)	Uncertainty	Rw (nm)	Uncertainty	Injected mass (µg)	Mass recovery (%)
0306007[0306PW]	4) F_G=0.62 (Ba)	116,5	5,10%	**234,6**	2,80%	2,013	5,80%	69,1	2,80%	100	57,4
0306014[0306PW]	4) F_G=0.62 (Ba)	91,4	5,10%	**213**	1,50%	2,33	5,30%	68,1	2,00%	50	65,4
0406008[0406PW]	4) F_G=0.62 (Ba)	92	4,10%	**228,2**	2,00%	2,481	4,50%	66,4	2,40%	100	64,7
Average		100		**225,3**		2,275		67,9		83,33	62,5
Standard deviation		14,5		**15,3**		0,326		1,9		40,82	6,2
% Standard deviation		14,5		**6,8**		14,348		2,8		48,99	10

Figure C.5: Molecular weight determined by SEC-MALLS of F_G=0,68

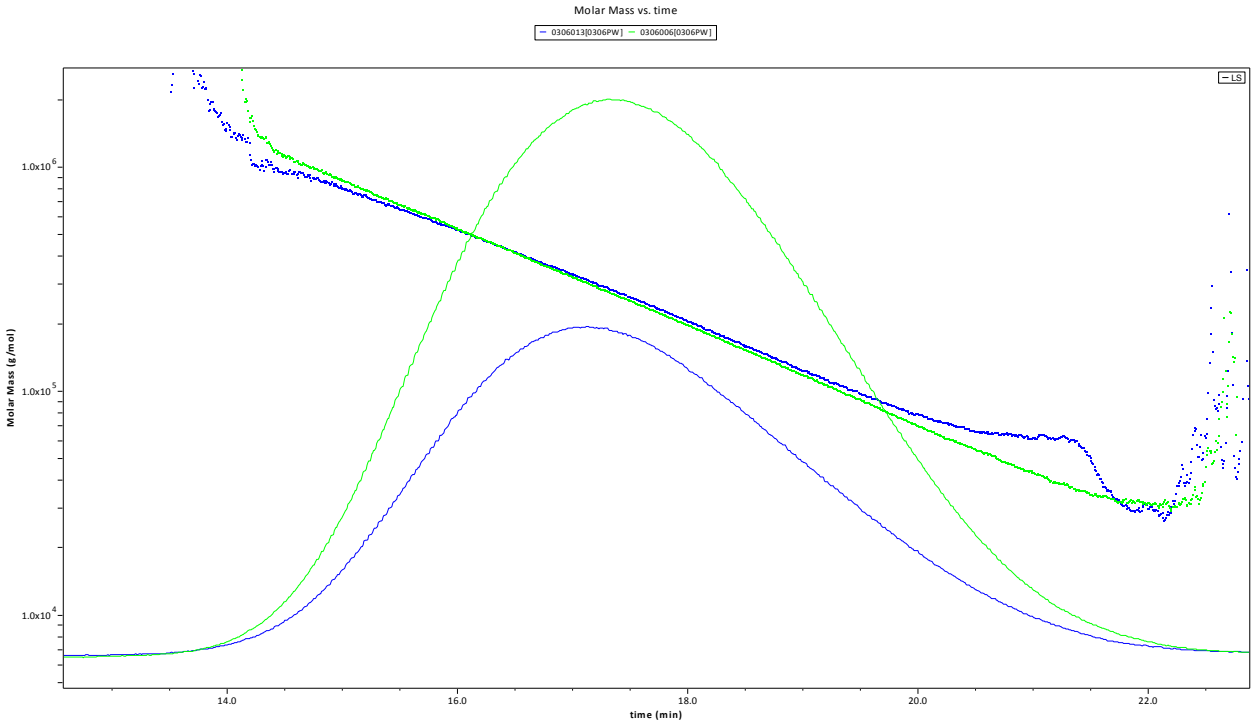

	Sample description	Mn (kDa)	Uncertainty	**Mw (kDa)**	Uncertainty	Polydispersity (Mw/Mn)	Uncertainty	Rw (nm)	Uncertainty	Injected mass (µg)	Mass recovery (%)
0306013[0306PW]	3) F_G= 0,68	127,5	7,20%	**233,4**	3,50%	1,83	8,00%	71,8	3,80%	50	64,2
0306006[0306PW]	3) F_G= 0,68	112,5	2,30%	**219,5**	1,90%	1,951	3,00%	69,7	1,40%	100	58,7
Average		120		**226,5**		1,891		70,8		75	61,5
Standard deviation		10,6		**9,8**		0,086		1,5		35,36	3,9
% Standard deviation		8,9		**4,3**		4,528		2,1		47,14	6,3

Figure C.6: Molecular weight determined by SEC-MALLS of F_G=0,85

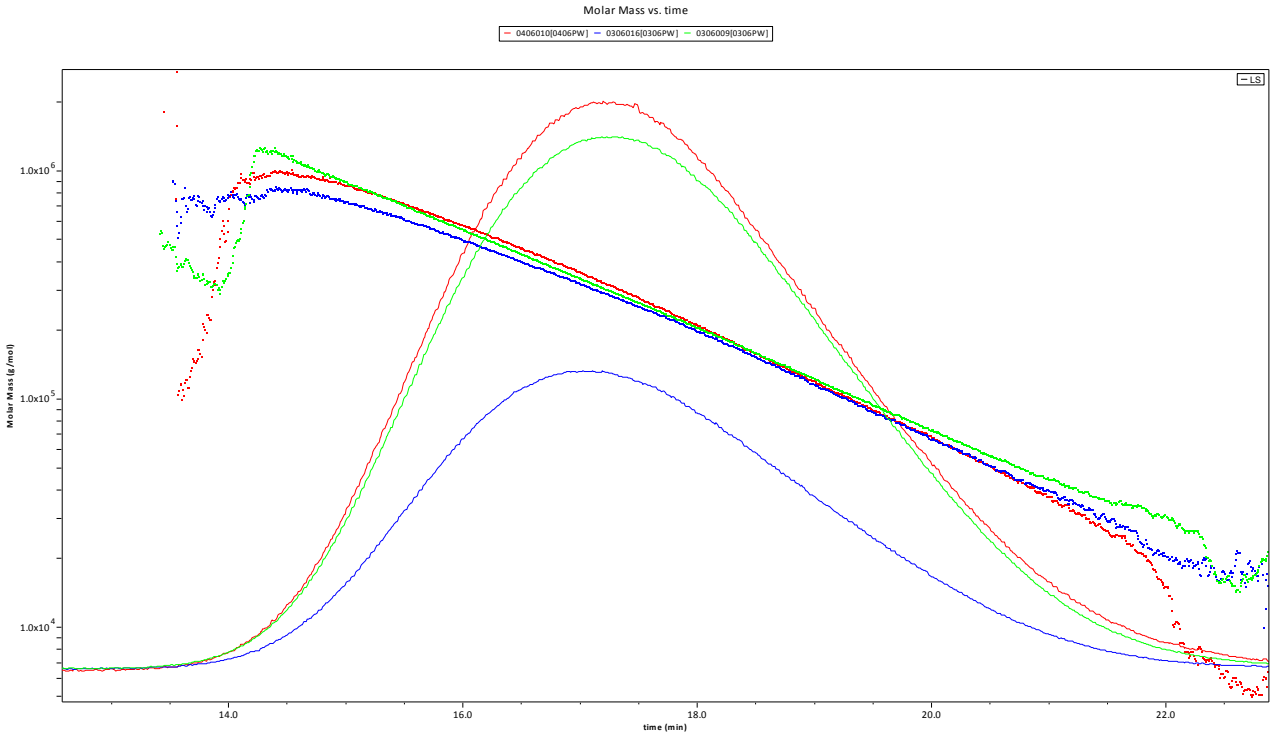

	Sample description	Mn (kDa)	Uncertainty	**Mw (kDa)**	Uncertainty	Polydispersity (Mw/Mn)	Uncertainty	Rw (nm)	Uncertainty	Injected mass (µg)	Mass recovery (%)
0406010[0406PW]	6) F_G=0,85	61,6	11,10%	**207,9**	1,40%	3,374	11,20%	60,3	3,40%	100	67,4
0306016[0306PW]	6) F_G=0,85	88,6	7,00%	**212,6**	1,10%	2,399	7,10%	65,4	2,30%	50	66,1
0306009[0306PW]	6) F_G=0,85	103	5,10%	**220,4**	2,20%	2,14	5,60%	68,4	2,50%	100	61,9
Average		84,4		**213,7**		2,638		64,7		83,33	65,2
Standard deviation		28,5		**7,7**		0,728		5,5		40,82	4
% Standard deviation		33,8		**3,6**		27,616		8,5		48,99	6,1

10 Appendix D – Data from rheology study

The data, given in the Tables D.1-D.9, were determined by deformation compression measurements performed on saturated alginate gel cylinders after 0-4 saline treatments (0.15 M NaCl). The experimental setup for the measurements is given in (section 2.7.2).

Gradient, rupture strength and deformation at rupture were measured with a texture analyzer (Stable Micro Systems). Young's modulus was calculated from the linear are between 0.1-0.3 mm, and is given as

$$\frac{F}{A} = E * \left(\frac{\Delta L}{L}\right) \Longrightarrow E = (L\left(\frac{L}{\Delta L}\right) * \frac{F}{A} \quad \text{(D.1)}$$

Example of calculation:

Cylinder no. 1 of SF60 (not stirred) is used in the following calculations (divergence from these values compared to the values in Table D.1 are caused by different number of digits used here).

Measured height: 15.62, measured diameter: 13.85. The force is applied to the area (A):

$$A = \pi(\frac{D}{2})^2 = 150{,}58\ mm^2 = 1{,}5058 * 10^{-4} m^2 \quad \text{(D.2)}$$

The gradient were determined from the graph obtained by the computer program Texture Exponent 32 (Stable Micro Systems), hence Young's modulus was calculated from the following equation:

$$E = \left(\frac{F}{\Delta L}\right) * \left(\frac{L}{A}\right) = \left(511\frac{N}{m}\right) * \frac{0{,}01562\ m}{1{,}5058 * 10^{-4} m^2} = 53007{,}17\ N/m^2 \quad \text{(D.3)}$$

The polymer concentration increases due to syneresis; hence Young's modulus was corrected based on the gel cylinders change in volume:
Initial volume of the cylinder was calculated from the measures of the well plate (Height: 18mm, diameter: 16mm).

$$V = \pi(\frac{D}{2})^2 * h = \pi\left(\frac{16mm}{2}\right)^2 * 18mm = 3617\ mm^3 \quad \text{(D.4)}$$

Actual volume of the cylinder:

$$V = \pi(\frac{D}{2})^2 * h = \pi\left(\frac{13{,}85mm}{2}\right)^2 * 15{,}62mm = 2260\, mm^3 \quad \text{(D.5)}$$

Correction factor: $\frac{V_{initial}}{V_{actual}} = \frac{3617mm^3}{2260mm^3} = 1{,}6004$ (D.6)

When the polymer concentration is much higher than the critical polymer concentration Young's modulus is corrected by:

$$E_{corr} = \frac{E}{c^2} \quad \text{(D.7)}$$

Young's modulus is given as: $E \propto C^2$
Hence Young's modulus is corrected to be:

$$E_{corr} = \frac{53007{,}17\,\frac{N}{m^2}}{1{,}6004} = 33121{,}2\,\frac{N}{m^2}$$

The degree of syneresis is calculated based on change in weight:

$$1 - \frac{2{,}41g}{3{,}62\,g} * 100\% = 33{,}4\% \quad \text{(D.8)}$$

Elasticity is calculated as percentage deformation at gel rupture from the measured height:

$$\frac{10{,}96mm}{15{,}62mm} * 100\% = 70{,}17\% \quad \text{(D.9)}$$

Table D.1: Data of SF60 (not stirred). The gel cylinders were prepared from *L.hyp.,* stipe and during the saline treatments the saline was not stirred.

Alginate	n	Diameter [mm]	Height [mm]	Weight before compression [g]	Weight after compression [g]	Gradient [N/m]	Youngs´s modulus [kPa]	Syneresis [%]	Rupture Strength [g]	Deform. at rupture [mm]	Elasticity [%]
	1	13,85	15,62	2,41	2,04	511,00	22,41	33,43	6002,62	10,96	70,17
SF60	2	13,78	15,65	2,45	1,90	616,00	26,90	32,32	6130,96	11,08	70,78
(not stirred)	3	13,61	15,82	2,44	2,00	566,00	24,90	32,60	5787,23	10,89	68,82
Intial	4	13,72	15,57	2,41	1,93	558,00	23,79	33,43	5766,16	10,70	68,71
	5	13,71	15,50	2,43	1,90	561,00	23,56	32,87	5290,59	10,41	67,14
Average		**13,73**	**15,63**	**2,43**	**1,95**	**562,40**	**24,31**	**32,93**	**5795,51**	**10,81**	**69,12**
St. deviation		**0,09**	**0,12**	**0,02**	**0,06**	**37,25**	**1,70**	**0,49**	**320,66**	**0,26**	**1,42**
	1	13,70	15,34	2,30	1,89	498,00	20,23	36,42	2808,47	9,09	59,28
SF60	2	13,77	15,39	2,35	1,90	433,00	17,97	35,03	3128,24	9,51	61,76
(not stirred)	3	13,77	15,42	2,37	1,72	527,00	21,98	34,48	4291,13	10,13	65,68
1 shift in NaCl	4	13,44	15,37	2,36	1,84	453,00	17,82	34,76	5558,96	10,64	69,21
	5	13,71	15,36	2,35	1,88	457,00	18,67	35,03	3633,99	9,58	62,37
Average		**13,68**	**15,38**	**2,35**	**1,85**	**473,60**	**19,33**	**35,14**	**3884,16**	**9,79**	**63,66**
St. deviation		**0,14**	**0,03**	**0,03**	**0,07**	**38,06**	**1,76**	**0,75**	**1091,07**	**0,60**	**3,85**
	1	13,74	15,40	2,45	2,11	274,00	11,33	32,27	3063,04	9,75	63,33
SF60	2	13,70	15,30	2,42	2,28	251,00	10,12	33,10	2941,68	9,70	63,39
(not stirred)	3	13,60	15,33	2,34	2,15	221,00	8,84	35,31	3293,16	10,14	66,12
2 shifs in NaCl	4	13,48	15,44	2,43	2,23	217,00	8,70	32,82	2405,50	9,60	62,17
	5	13,61	15,52	2,48	2,34	203,00	8,43	31,44	2629,84	9,99	64,38
Average		**13,63**	**15,40**	**2,42**	**2,22**	**233,20**	**9,48**	**32,99**	**2866,64**	**9,84**	**63,88**
St. deviation		**0,10**	**0,09**	**0,05**	**0,09**	**28,74**	**1,22**	**1,44**	**351,73**	**0,22**	**1,48**
	1	14,25	15,56	2,51	2,43	94,00	4,31	30,61	1999,79	10,31	66,24
SF60	2	14,28	15,58	2,60	2,33	80,00	3,70	28,12	2067,50	10,40	66,75
(not stirred)	3	14,20	15,66	2,54	2,39	99,00	4,59	29,78	1969,20	10,12	64,63
3 shifts in NaCl	4	14,19	15,71	2,57	2,43	104,00	4,87	28,95	2354,94	10,60	67,43
	5	14,07	15,62	2,59	2,49	113,00	5,11	28,40	1741,67	9,75	62,44
Average		**14,20**	**15,63**	**2,56**	**2,41**	**98,00**	**4,52**	**29,17**	**2026,62**	**10,23**	**65,50**
St. deviation		**0,08**	**0,06**	**0,04**	**0,06**	**12,27**	**0,55**	**1,02**	**220,61**	**0,32**	**2,00**
	1	14,90	15,51	2,65	2,59	67,00	3,33	26,80	1390,43	10,01	64,53
SF60	2	14,36	15,27	2,70	2,58	57,00	2,51	25,41	694,68	8,47	55,43
(not stirred)	3	14,35	15,58	2,74	2,63	53,00	2,47	24,31	1286,20	9,68	62,13
4 shifts in NaCl	4	14,91	15,64	2,78	2,58	49,00	2,50	23,20	726,95	9,03	57,74
	5	14,24	15,51	2,79	2,62	57,00	2,58	22,93	601,83	8,49	54,72
Average		**14,55**	**15,50**	**2,73**	**2,60**	**56,60**	**2,68**	**24,53**	**940,02**	**9,13**	**58,91**
St. deviation		**0,33**	**0,14**	**0,06**	**0,02**	**6,69**	**0,37**	**1,60**	**368,33**	**0,70**	**4,27**

Table D.2: Data of SF60. The gel cylinders were prepared from *L.hyp.,* stipe. During the saline treatments the saline was stirred.

Alginate	n	Diameter [mm]	Height [mm]	Weight before compression [g]	Weight after compression [g]	Gradient [N/m]	Youngs´s modulus [kPa]	Syneresis [%]	Rupture Strength [g]	Deform. at rupture [mm]	Elasticity [%]
	1	13,830	15,516	2,280	1,110	511,000	21,903	37,017	4501,913	10,017	64,559
SF60	2	14,090	15,609	2,300	1,510	645,000	29,215	36,464	5368,604	10,047	64,367
Initial	3	13,940	15,705	2,320	0,910	689,000	31,114	35,912	5663,660	10,590	67,431
	4	13,840	15,579	2,310	1,470	634,000	27,547	36,188	5788,958	10,319	66,237
	5	14,080	15,617	2,310	1,740	649,000	29,400	36,188	5738,290	10,517	67,343
	6	14,010	15,645	2,390	1,600	664,000	29,941	33,978	4854,493	9,967	63,707
	7	14,170	15,592	2,300	1,760	659,000	30,091	36,464	6204,548	10,651	68,311
Average		**13,994**	**15,609**	**2,316**	**1,443**	**635,857**	**28,459**	**36,030**	**5445,781**	**10,301**	**65,993**
St. deviation		**0,130**	**0,058**	**0,035**	**0,320**	**57,736**	**3,087**	**0,968**	**587,792**	**0,291**	**1,791**
	1	14,3	15,182	2,320	2,020	227,000	9,745	35,912	3680,000	8,988	59,202
SF60	2	14,18	15,501	2,450	2,100	213,000	9,570	32,320	3861,400	9,963	64,273
1 shift in NaCl	3	13,9	15,669	2,490	2,060	217,000	9,676	31,215	3480,219	8,917	56,909
	4	14,2	15,538	2,430	2,290	199,000	9,031	32,873	4171,500	10,972	70,614
	5	14,44	14,601	2,210	1,960	169,000	6,581	38,950	2500,000	9,714	66,53
Average		**14,204**	**15,298**	**2,380**	**2,086**	**205,000**	**8,921**	**34,254**	**3538,624**	**9,711**	**63,505**
St. deviation		**0,199**	**0,429**	**0,114**	**0,125**	**22,494**	**1,338**	**3,150**	**633,809**	**0,838**	**5,530**
	1	14,89	15,433	2,76	2,500	36	1,760	23,757	401,960	9,658	62,58
SF60	2	15,43	15,435	2,69	2,190	32	1,681	25,691	284,300	8,965	58,082
2 shifts in NaCl	3	15,62	15,649	2,82	2,400	31	1,739	22,099	529,000	9,873	63,09
	4	15,71	15,903	2,75	2,680	38	2,263	24,033	334,344	8,730	54,895
	5	15,91	15,929	2,91	2,740	40	2,455	19,613	294,572	8,453	53,067
	6	15,62	15,569	2,82	2,560	33	1,823	22,099	421,700	9,398	60,364
	7	15,46	15,494	2,73	2,280	30	1,600	24,586	354,194	9,310	60,088
	8	15,82	15,691	2,90	2,720	35	2,030	19,890	339,000	9,202	58,645
Average		**15,558**	**15,638**	**2,798**	**2,509**	**34,375**	**1,919**	**22,721**	**369,884**	**9,199**	**58,851**
St. deviation		**0,315**	**0,195**	**0,079**	**0,206**	**3,503**	**0,303**	**2,189**	**79,724**	**0,470**	**3,494**
	1	16,8	17,48	3,05	2,8	30	2,713	15,746	262,9	8,889	50,852
SF60	2	16,3	17,58	3,01	2,3	28	2,425	16,851	324,215	8,420	47,895
3 shifts in NaCl	3	15,64	18,10	2,74	2,2	20	1,740	24,309	138,145	7,255	40,083
	4	15,58	18,25	2,91	1,85	22	1,947	19,613	283,1	8,323	45,605
	5	16,18	17,79	3,09	2,32	29	2,564	14,641	292,53	8,129	45,694
	6	15,95	17,83	3,13	2,62	18	1,557	13,536	175,893	7,003	39,277
Average		**16,075**	**17,838**	**2,988**	**2,348**	**24,500**	**2,158**	**17,449**	**246,131**	**8,003**	**44,901**
St. deviation		**0,455**	**0,295**	**0,143**	**0,332**	**5,128**	**0,474**	**3,955**	**72,790**	**0,726**	**4,480**
	1	13,06	17,50	1,76	1,1	23	1,261	51,381	Dissolved	Dissolved	Dissolved
SF60	2	14,41	18,64	2,07	1,32	20	1,614	42,818	Dissolved	Dissolved	Dissolved
4 shifts in NaCl	3	14,49	18,73	1,75	1,01	21	1,738	51,657	Dissolved	Dissolved	Dissolved
	4	13,90	18,24	1,86	1,06	18	1,266	48,619	Dissolved	Dissolved	Dissolved
	5	14,3	18,29	1,88	1,13	19	1,426	48,066	Dissolved	Dissolved	Dissolved
	6	14,01	18,03	2,02	1,37	18	1,242	44,199	Dissolved	Dissolved	Dissolved
Average		**14,028**	**18,238**	**1,890**	**1,165**	**19,833**	**1,425**	**47,790**	**Dissolved**	**Dissolved**	**Dissolved**
St. deviation		**0,527**	**0,446**	**0,132**	**0,146**	**1,941**	**0,209**	**3,640**	-	-	-

D.3: Data of F_G=0,48 (not stirred). The gel cylinders were prepared from AlgE6 + mannuronan, F_G=0,48. During the saline treatments the saline was not stirred.

Alginate	n	Diameter [mm]	Height [mm]	Weight before compression [g]	Weight after compression [g]	Gradient [N/m]	Youngs´s modulus [kPa]	Syneresis [%]	Rupture Strength [g]	Deform. at rupture [mm]	Elasticity [%]
F_G=0,48	1	11,51	12,74	1,28	0,81	201,00	3,31	64,61	6265,70	10,52	82,53
(not stirred)	2	11,20	12,28	1,28	0,99	208,00	2,90	68,48	6083,30	10,06	81,92
Initial	3	11,32	12,46	1,28	0,88	213,00	3,16	66,55	3913,54	9,62	77,23
	4	11,51	11,84	1,28	0,96	299,00	3,94	69,04	4128,61	9,34	78,92
Average		**11,39**	**12,33**	**1,28**	**0,91**	**230,25**	**3,33**	**67,17**	**5097,79**	**9,88**	**80,15**
St. deviation		**0,15**	**0,38**	**0,00**	**0,08**	**46,10**	**0,44**	**2,01**	**1248,60**	**0,52**	**2,50**
	1	11,11	12,45	1,20	1,16	98,00	1,40	66,83	4982,93	10,24	82,31
F_G=0,48	2	11,40	12,37	1,27	1,22	110,00	1,62	64,89	4786,10	10,43	84,36
(not stirred)	3	11,17	12,47	1,25	1,07	105,00	1,52	65,44	2083,50	9,82	78,76
1 shifts in saline	4	11,34	12,22	1,24	1,01	120,00	1,69	65,72	2367,82	9,61	78,70
	5	10,54	12,45	1,24	1,17	89,00	1,15	65,72	3782,53	10,18	81,75
	6	11,19	12,60	1,29	1,12	79,00	1,19	64,34	2006,79	10,34	82,08
	7	11,20	12,28	1,15	1,11	124,00	1,73	68,21	4001,44	10,30	83,90
	8	11,02	12,50	1,21	1,14	119,00	1,69	66,55	2173,10	9,65	77,26
Average		**11,12**	**12,42**	**1,23**	**1,13**	**105,50**	**1,50**	**65,96**	**3273,03**	**10,07**	**81,14**
St. deviation		**0,26**	**0,12**	**0,04**	**0,06**	**15,97**	**0,23**	**1,21**	**1256,46**	**0,33**	**2,60**
	1	13,41	12,11	1,60	1,47	29,00	0,56	55,77	750,59	9,61	79,32
F_G=0,48	2	12,45	11,84	1,41	1,26	45,00	0,69	61,02	1412,03	9,89	83,51
(not stirred)	3	13,56	12,08	1,56	1,34	34,00	0,66	56,87	1024,65	9,69	80,20
2 shifts in saline	4	13,30	12,70	1,73	1,55	29,00	0,63	52,17	791,73	10,34	81,42
	5	13,16	11,94	1,55	1,32	43,00	0,76	57,15	1401,35	9,87	82,68
	6	13,23	12,76	1,64	1,51	36,00	0,79	54,66	888,00	11,09	86,87
Average		**13,19**	**12,24**	**1,58**	**1,41**	**36,00**	**0,68**	**56,27**	**1044,72**	**10,08**	**82,33**
St. deviation		**0,39**	**0,40**	**0,11**	**0,12**	**6,81**	**0,08**	**2,94**	**295,83**	**0,55**	**2,70**
	1	13,86	14,54	1,80	1,63	14,00	0,50	50,28	322,64	8,92	61,33
F_G=0,48	2	14,80	14,91	1,89	1,73	18,00	0,78	47,79	358,87	9,44	63,29
(not stirred)	3	14,47	15,04	1,95	1,61	14,00	0,60	46,13	460,00	7,50	49,83
3 shifts in saline	4	14,02	15,24	1,91	1,69	13,00	0,54	47,24	209,17	7,64	50,14
	5	14,10	15,17	1,92	1,58	6,00	0,25	46,96	277,31	8,04	52,97
	6	13,87	15,60	1,99	1,71	15,00	0,66	45,03	370,22	7,33	46,97
	7	14,30	14,41	1,78	1,52	18,00	0,66	50,83	316,10	7,51	52,12
Average		**14,20**	**14,99**	**1,89**	**1,64**	**14,00**	**0,57**	**47,75**	**330,62**	**8,05**	**53,81**
St. deviation		**0,34**	**0,41**	**0,08**	**0,08**	**4,04**	**0,17**	**2,11**	**78,50**	**0,81**	**6,14**
	1	14,68	16,38	1,53	1,38	12,00	0,68	57,73	Dissolved	Dissolved	Dissolved
F_G=0,48	2	15,61	16,91	2,21	1,85	13,00	0,92	38,95	Dissolved	Dissolved	Dissolved
(not stirred)	3	16,47	18,08	2,29	1,78	14,00	1,35	36,74	Dissolved	Dissolved	Dissolved
4 shifts in saline	4	14,81	17,10	1,81	1,46	11,00	0,72	50,00	Dissolved	Dissolved	Dissolved
	5	15,20	17,15	2,30	1,95	14,00	0,98	36,46	Dissolved	Dissolved	Dissolved
	6	16,70	17,30	2,35	1,87	18,00	1,56	35,08	Dissolved	Dissolved	Dissolved
Average		**15,58**	**17,15**	**2,08**	**1,72**	**13,67**	**1,03**	**42,50**	**Dissolved**	**Dissolved**	**Dissolved**
St. deviation		**0,85**	**0,56**	**0,33**	**0,24**	**2,42**	**0,35**	**9,23**	-	-	-

D.4: Data of F_G=0,48. The gel cylinders were prepared from AlgE6 + mannuronan, F_G=0,48. During the saline treatments the saline was stirred. This alginate (242 kDa) had a considerably higher molecular weight than F_G=0,48 (not stirred) (155 kDa).

Alginate	n	Diameter [mm]	Height [mm]	Weight before compression [g]	Weight after compression [g]	Gradient [N/m]	Youngs´s modulus [kPa]	Syneresis [%]	Rupture Strength [g]	Deform. at rupture [mm]	Elasticity [%]
	1	10,90	12,71	1,13	0,95	343,00	5,02	68,78	5009,50	9,95	78,32
F_G=0,48	2	10,93	12,55	1,12	0,64	561,00	7,95	69,06	3265,10	8,63	68,79
Initial	3	11,000	12,300	1,030	0,530	570,000	7,700	71,547	6001,000	9,845	80,041
	4	11,130	12,061	1,150	0,670	775,000	10,105	68,232	6517,632	9,001	74,629
Average		**10,990**	**12,405**	**1,108**	**0,698**	**562,250**	**7,693**	**69,406**	**5198,308**	**9,358**	**75,445**
St. deviation		**0,102**	**0,284**	**0,053**	**0,179**	**176,441**	**2,085**	**1,468**	**1432,698**	**0,644**	**4,978**
	1	11,41	12,240	1,160	1,030	186,000	2,664	67,956	14308,083	10,855	88,685
F_G=0,48	2	11,58	12,744	1,200	1,110	291,000	4,845	66,851	11785,600	11,738	92,106
1 shift in NaCl	3	10,95	12,341	1,170	1,030	222,000	3,001	67,680	17297,364	11,334	91,84
	4	11,02	12,340	1,170	0,940	366,000	5,011	67,680	14800,300	11,074	89,741
	5	11,15	12,280	1,170	1,010	245,000	3,384	67,680	11377,100	11,078	90,212
Average		**11,222**	**12,389**	**1,174**	**1,024**	**262,000**	**3,781**	**67,569**	**13913,689**	**11,216**	**90,517**
St. deviation		**0,266**	**0,203**	**0,015**	**0,061**	**69,502**	**1,079**	**0,419**	**2416,295**	**0,338**	**1,443**
	1	13,37	12,564	1,79	1,490	37	0,787	50,552	6322,500	11,800	93,919
F_G=0,48	2	13,01	12,958	1,75	1,410	28	0,619	51,657	4925,000	12,044	92,946
2 shifts in NaCl	3	12,82	12,920	1,82	1,410	35	0,744	49,724	4631,300	11,974	92,678
	4	13,43	13,250	1,88	1,470	20	0,503	48,066	6232,500	12,672	95,638
	5	13,1	13,385	1,85	1,320	38	0,938	48,895	5843,800	12,589	94,053
	6	13,28	13,139	1,99	1,410	12	0,288	45,028	4405,200	12,261	93,318
Average		**13,168**	**13,036**	**1,847**	**1,418**	**28,333**	**0,647**	**48,987**	**5393,383**	**12,223**	**93,759**
St. deviation		**0,234**	**0,290**	**0,084**	**0,059**	**10,482**	**0,230**	**2,309**	**842,248**	**0,349**	**1,064**
	1	14,43	17,92	2,16	1,53	10	0,719	40,331	Dissolved	Dissolved	Dissolved
F_G=0,48	2	14,71	18,54	2,33	2,18	16	1,324	35,635	Dissolved	Dissolved	Dissolved
3 shifts in NaCl	3	15,25	18,6	2,59	2,06	18	1,616	28,453	Dissolved	Dissolved	Dissolved
	4	14,84	17,47	2,10	1,71	16	1,127	41,989	Dissolved	Dissolved	Dissolved
	5	14,42	17,1	2,06	1,74	15	0,936	43,094	Dissolved	Dissolved	Dissolved
	6	15,35	17,01	2,39	2,04	16	1,113	33,978	Dissolved	Dissolved	Dissolved
	7	14,54	17,04	2,33	2,11	10	0,628	35,635	Dissolved	Dissolved	Dissolved
	8	14,77	17,28	2,35	2,09	17	1,148	35,083	Dissolved	Dissolved	Dissolved
	9	14,82	17,77	2,40	1,97	16	1,183	33,702	Dissolved	Dissolved	Dissolved
Average		**14,792**	**17,637**	**2,301**	**1,937**	**14,889**	**1,088**	**36,433**	**Dissolved**	**Dissolved**	**Dissolved**
St. deviation		**0,329**	**0,616**	**0,167**	**0,222**	**2,892**	**0,300**	**4,619**	**-**	**-**	**-**
	1	16,89	20,43	2,48	-	8	1,167	31,492	Dissolved	Dissolved	Dissolved
F_G=0,48	2	16,31	18,92	2,71	-	13	1,405	25,138	Dissolved	Dissolved	Dissolved
4 shifts in NaCl	3	18,03	20,55	2,63	-	12	2,031	27,348	Dissolved	Dissolved	Dissolved
	4	17,89	20,49	2,86	-	13	2,147	20,994	Dissolved	Dissolved	Dissolved
	5	17,81	19,62	2,51	-	12	1,725	30,663	Dissolved	Dissolved	Dissolved
	6	17,05	19,57	2,91	-	10	1,307	19,613	Dissolved	Dissolved	Dissolved
	7	16,75	19,3	2,64	-	5	0,605	27,072	Dissolved	Dissolved	Dissolved
	8	16,83	19,04	2,73	-	11	1,290	24,586	Dissolved	Dissolved	Dissolved
Average		**17,195**	**19,740**	**2,684**	**-**	**10,500**	**1,460**	**25,863**	**Dissolved**	**Dissolved**	**Dissolved**
St. deviation		**0,631**	**0,665**	**0,152**	**-**	**2,777**	**0,499**	**4,197**	-	-	-

D.5: Data of F_G=0,56 (MG). The gel cylinders were prepared from polyMG (F_G= 0,45) + AlgE6 = F_G=0,56.

Alginate	n	Diameter [mm]	Height [mm]	Weight before compression [g]	Weight after compression [g]	Gradient [N/m]	Youngs´s modulus [kPa]	Syneresis [%]	Rupture Strength [g]	Deform. at rupture [mm]	Elasticity [%]
	1	9,510	10,785	0,740	0,510	839,000	5,711	79,558	16413,223	9,289	86,129
F_G=0,56 (MG)	2	9,840	11,259	0,770	0,540	613,000	5,082	78,729	13868,876	9,179	81,526
Initial	3	9,710	10,874	0,790	0,550	497,000	3,615	78,177	15859,206	9,066	83,373
	4	9,880	11,114	0,750	0,490	869,000	6,986	79,282	10036,373	8,852	79,647
Average		**9,735**	**11,008**	**0,763**	**0,523**	**704,500**	**5,348**	**78,936**	**14044,420**	**9,097**	**82,669**
St. deviation		**0,167**	**0,218**	**0,022**	**0,028**	**179,424**	**1,401**	**0,613**	**2886,747**	**0,187**	**2,763**
	1	9,98	10,840	0,840	0,710	361,000	2,748	76,796	11227,600	9,481	87,463
F_G=0,56 (MG)	2	10,37	10,801	0,870	0,720	372,000	3,024	75,967	6240,000	8,940	82,77
1 shift in NaCl	3	10,41	10,719	0,840	0,710	385,000	3,083	76,796	10501,319	9,295	86,715
	4	10,01	10,763	0,870	0,700	327,000	2,451	75,967	6091,504	9,101	84,558
	5	9,93	10,880	0,890	0,700	325,000	2,476	75,414	4420,700	8,594	78,989
	6	10,04	10,613	0,840	0,660	320,000	2,313	76,796	6803,249	8,793	82,851
	7	10,01	10,837	0,840	0,700	372,000	2,846	76,796	10536,607	9,394	86,685
	8	10,03	10,879	0,860	0,690	372,000	2,891	76,243	10043,733	9,441	86,782
	9	9,99	10,978	0,800	0,750	372,000	2,947	77,901	5636,949	9,387	85,507
Average		**10,086**	**10,812**	**0,850**	**0,704**	**356,222**	**2,753**	**76,519**	**7944,629**	**9,158**	**84,702**
St. deviation		**0,176**	**0,105**	**0,026**	**0,024**	**24,969**	**0,276**	**0,718**	**2593,868**	**0,319**	**2,748**
	1	10,71	11,992	1,15	0,980	149	1,768	68,232	627,932	7,816	65,177
F_G=0,56 (MG)	2	11,2	11,971	1,14	0,850	131	1,691	68,508	1297,582	8,655	72,3
2 shifts in NaCl	3	10,74	12,013	1,08	0,990	136	1,632	70,166	726,453	7,777	64,738
	4	10,69	12,000	1,12	1,000	147	1,741	69,061	862,072	8,321	69,342
	5	10,92	12,029	1,09	0,810	129	1,606	69,890	532,876	7,471	62,108
Average		**10,852**	**12,001**	**1,116**	**0,926**	**138,400**	**1,688**	**69,171**	**809,383**	**8,008**	**66,733**
St. deviation		**0,215**	**0,022**	**0,030**	**0,089**	**9,154**	**0,069**	**0,842**	**298,903**	**0,473**	**4,049**
	1	11,14	12,18	1,24	0,91	85	1,144	65,746	159,864	5,614	46,081
F_G=0,56 (MG)	2	11,64	12,28	1,26	1,07	96	1,446	65,193	273,61	6,907	56,232
3 shifts in NaCl	3	11,68	12,28	1,27	0,99	91	1,378	64,917	287,9	6,729	54,819
	4	11,42	12,36	1,28	1,01	90	1,330	64,641	296,705	7,001	56,642
	5	11,57	12,20	1,26	0,95	93	1,357	65,193	225,687	6,068	49,725
Average		**11,490**	**12,261**	**1,262**	**0,986**	**91,000**	**1,331**	**65,138**	**248,753**	**6,464**	**52,700**
St. deviation		**0,219**	**0,071**	**0,015**	**0,061**	**4,062**	**0,113**	**0,410**	**56,752**	**0,599**	**4,614**
	1	11,82	12,75	1,39	0,97	69	1,198	61,602	263,26	7,506	58,875
F_G=0,56 (MG)	2	11,67	12,34	1,34	0,95	67	1,028	62,983	262,3	8,853	71,748
4 shifts in NaCl	3	11,53	12,71	1,39	1,01	74	1,213	61,602	232,3	7,387	58,106
	4	11,41	12,61	1,35	1	66	1,033	62,707	287,075	7,500	59,486
	5	11,75	12,82	1,34	0,95	64	1,117	62,983	169,301	6,175	48,163
Average		**11,636**	**12,646**	**1,362**	**0,976**	**68,000**	**1,118**	**62,376**	**242,847**	**7,484**	**59,276**
St. deviation		**0,166**	**0,188**	**0,026**	**0,028**	**3,808**	**0,088**	**0,715**	**45,474**	**0,948**	**8,376**

D.6: Data of F_G=0,60. The gel cylinders were prepared from AlgE6 + mannuronan, F_G=0,60.

Alginate	n	Diameter [mm]	Height [mm]	Weight before compression [g]	Weight after compression [g]	Gradient [N/m]	Youngs´s modulus [kPa]	Syneresis [%]	Rupture Strength [g]	Deform. at rupture [mm]	Elasticity [%]
	1	11,530	13,670	1,180	0,580	1153,000	23,491	67,403	9611,777	9,730	71,178
	2	11,220	13,490	1,270	0,760	604,000	11,198	64,917	7676,505	9,252	68,584
Initial	3	11,110	13,210	1,180	0,840	568,000	9,696	67,403	7679,319	9,615	72,786
Average		**11,287**	**13,457**	**1,210**	**0,727**	**775,000**	**14,795**	**66,575**	**8322,534**	**9,532**	**70,849**
St. deviation		**0,218**	**0,232**	**0,052**	**0,133**	**327,852**	**7,568**	**1,435**	**1116,518**	**0,249**	**2,120**
	1	11,01	12,253	1,120	0,990	505,000	6,756	69,061	12615,885	10,792	88,076
F_G=0,60	2	11,29	12,321	1,180	1,010	561,000	8,024	67,403	10106,593	10,774	87,444
1 shift in NaCL	3	11,28	12,388	1,150	0,930	401,000	5,819	68,232	14544,078	10,767	86,915
	4	11,19	12,330	1,120	1,040	539,000	7,590	69,061	15640,026	11,081	89,87
	5	11,75	12,196	1,150	1,050	273,000	4,102	68,232	22836,360	11,193	91,776
	6	11,2	12,177	1,120	0,920	336,000	4,566	69,061	14162,813	10,643	87,402
Average		**11,287**	**12,278**	**1,140**	**0,990**	**435,833**	**6,143**	**68,508**	**14984,293**	**10,875**	**88,581**
St. deviation		**0,248**	**0,083**	**0,024**	**0,055**	**117,294**	**1,598**	**0,677**	**4297,787**	**0,213**	**1,875**
	1	13,44	13,781	1,73	1,470	45	1,276	52,210	7524,291	12,575	91,249
F_G=0,60	2	13,32	13,639	1,75	1,610	65	1,755	51,657	4589,115	11,353	83,239
2 shifts in NaCL	3	13,81	13,856	1,79	1,600	46	1,400	50,552	3673,700	10,449	75,411
	4	13,22	13,515	1,77	1,530	69	1,786	51,105	7028,514	11,125	82,316
	5	13,08	12,554	1,71	1,410	61	1,239	52,762	8985,000	10,711	85,319
	6	13,37	13,715	1,79	1,380	63	1,743	50,552	8082,100	12,545	91,469
Average		**13,373**	**13,510**	**1,757**	**1,500**	**58,167**	**1,533**	**51,473**	**6647,120**	**11,460**	**84,834**
St. deviation		**0,248**	**0,483**	**0,033**	**0,096**	**10,167**	**0,256**	**0,902**	**2074,433**	**0,909**	**6,051**
	1	14,9	12,90	2,21	1,32	22	0,629	38,950	3656,7	11,690	90,62
F_G=0,60	2	15,61	12,83	2,23	1,22	16	0,494	38,398	3859,4	12,493	97,404
3 shifts in NaCL	3	15,1	13,35	2,14	1,52	18	0,586	40,884	3403,8	12,822	96,052
	4	15,18	12,74	2,35	1,42	16	0,457	35,083	4304,3	12,578	98,736
	5	15,81	12,84	2,10	1,12	18	0,571	41,989	3467,9	12,447	96,954
	6	15,92	12,87	2,29	1,61	22	0,713	36,740	6125,6	12,475	96,946
	7	15,3	12,91	2,12	1,5	19	0,575	41,436	8972,4	12,742	98,668
Average		**15,403**	**12,919**	**2,206**	**1,387**	**18,714**	**0,575**	**39,069**	**4827,157**	**12,464**	**96,483**
St. deviation		**0,383**	**0,198**	**0,093**	**0,176**	**2,498**	**0,084**	**2,556**	**2054,362**	**0,369**	**2,760**
	1	17,09	18,55	2,25	1,21	11	1,230	37,845	Dissolved	Dissolved	Dissolved
F_G=0,60	2	14,96	18,39	2,51	1,13	12	1,002	30,663	Dissolved	Dissolved	Dissolved
4 shifts inNaCL	3	15,34	19,20	2,58	1,51	16	1,599	28,729	Dissolved	Dissolved	Dissolved
	4	15,2	18,86	2,27	1,22	15	1,395	37,293	Dissolved	Dissolved	Dissolved
	5	14,8	19,62	2,49	1,63	16	1,588	31,215	Dissolved	Dissolved	Dissolved
	6	16,2	19,01	2,42	1,71	15	1,622	33,149	Dissolved	Dissolved	Dissolved
	7	15,01	19,09	2,44	1,45	8	0,752	32,597	Dissolved	Dissolved	Dissolved
Average		**15,514**	**18,960**	**2,423**	**1,409**	**13,286**	**1,313**	**33,070**	**Dissolved**	**Dissolved**	**Dissolved**
St. deviation		**0,832**	**0,411**	**0,123**	**0,225**	**3,039**	**0,336**	**3,390**	-	-	-

D.7: Data of F_G=0,62 (Ba). The gel cylinders were prepared from AlgE6 + mannuronan, F_G=0,62. The cylinders were saturated in 20 mM $BaCl_2$ and 30 mM $CaCl_2$.

Alginate	n	Diameter [mm]	Height [mm]	Weight before compression [g]	Weight after compression [g]	Gradient [N/m]	Youngs´s modulus [kPa]	Syneresis [%]	Rupture Strength [g]	Deform. at rupture [mm]	Elasticity [%]
	1	13,260	14,457	1,490	0,710	156,000	4,972	58,840	5321,957	10,206	70,596
F_G=0,62 (Ba)	2	13,400	13,562	1,370	0,550	185,000	4,971	62,155	4655,747	9,272	68,367
Initial	3	13,190	14,555	1,460	0,930	158,000	5,085	59,669	3734,513	9,928	68,210
	4	13,230	14,204	1,480	0,690	160,000	4,815	59,116	2776,620	10,154	71,487
	5	13,040	12,012	1,130	0,370	176,000	3,112	68,785	4774,600	8,513	70,871
	6	13,270	14,284	1,470	1,110	171,000	5,265	59,392	6138,338	10,722	75,063
Average		**13,232**	**13,846**	**1,400**	**0,727**	**167,667**	**4,703**	**61,326**	**4566,963**	**9,799**	**70,766**
St. deviation		**0,118**	**0,963**	**0,139**	**0,264**	**11,570**	**0,794**	**3,844**	**1182,246**	**0,786**	**2,502**
	1	13,2	13,279	1,280	0,740	159,000	3,892	64,641	5067,918	9,805	73,838
F_G=0,62 (Ba)	2	12,68	13,657	1,240	1,100	124,000	3,047	65,746	4435,800	10,588	77,528
1 shift in NaCl	3	12,61	13,443	1,240	0,950	121,000	2,804	65,746	5750,127	10,184	75,757
	4	12,53	13,808	1,300	1,180	120,000	2,976	64,088	3363,912	10,237	74,138
	5	12,72	13,621	1,290	1,150	127,000	3,115	64,365	5653,050	10,276	75,442
	6	12,69	13,978	1,360	1,190	139,000	3,668	62,431	4895,056	10,549	75,469
	7	13,02	13,856	1,310	1,210	148,000	4,004	63,812	4538,579	10,257	74,026
	8	12,80	13,149	1,180	0,870	133,000	2,972	67,403	4942,200	10,087	76,713
Average		**12,781**	**13,599**	**1,275**	**1,049**	**133,875**	**3,310**	**64,779**	**4830,830**	**10,248**	**75,364**
St. deviation		**0,223**	**0,289**	**0,055**	**0,174**	**13,943**	**0,469**	**1,506**	**754,718**	**0,249**	**1,325**
	1	11,9	12,849	1,20	1,060	82	1,478	66,851	7971,200	10,823	84,232
F_G=0,62 (Ba)	2	12,07	13,349	1,26	1,100	78	1,622	65,193	8241,240	10,860	81,354
2 shifts in NaCl	3	12,3	13,082	1,21	1,070	78	1,585	66,575	4955,210	10,418	79,636
	4	12,08	13,402	1,21	1,150	78	1,644	66,575	7039,400	11,483	85,681
	5	12,38	12,017	1,07	0,820	79	1,261	70,442	8807,739	10,062	83,731
Average		**12,146**	**12,940**	**1,190**	**1,040**	**79,000**	**1,518**	**67,127**	**7402,958**	**10,729**	**82,927**
St. deviation		**0,193**	**0,561**	**0,071**	**0,128**	**1,732**	**0,157**	**1,963**	**1510,188**	**0,533**	**2,410**
	1	11,58	12,04	1,08	0,85	77	1,081	70,166	5845,599	9,878	82,036
F_G=0,62 (Ba)	2	12,01	13,09	1,14	1	75	1,455	68,508	6454,759	10,551	80,61
3 shifts in NaCl	3	12,03	12,80	1,07	0,95	68	1,237	70,442	7401,74	9,702	75,815
	4	12,42	12,94	1,06	0,89	70	1,405	70,718	6057,16	10,892	84,154
	5	11,92	12,72	1,18	0,76	72	1,262	67,403	8658,174	9,984	78,515
	6	12,41	13,11	1,11	0,98	72	1,498	69,337	8586	10,841	82,712
Average		**12,062**	**12,782**	**1,107**	**0,905**	**72,333**	**1,323**	**69,429**	**7167,239**	**10,308**	**80,640**
St. deviation		**0,318**	**0,395**	**0,046**	**0,090**	**3,266**	**0,158**	**1,280**	**1247,189**	**0,518**	**3,046**
	1	11,92	12,96	1,11	0,87	66	1,226	69,337	10397,188	10,948	84,449
F_G=0,62 (Ba)	2	11,8	12,93	1,12	1,06	63	1,138	69,061	8166,5	11,429	88,371
4 shifts in NaCl	3	11,58	12,60	1,08	0,98	64	1,031	70,166	6981,925	10,450	82,917
	4	12,15	12,97	1,14	0,89	62	1,199	68,508	4606,027	10,088	77,756
	5	11,82	12,59	1,06	0,89	64	1,071	70,718	10748,117	10,694	84,927
	6	11,88	12,95	1,12	0,87	67	1,232	69,061	9716,257	11,417	88,169
	7	12,05	12,52	1,07	0,94	64	1,095	70,442	11421,182	10,673	85,22
Average		**11,886**	**12,791**	**1,100**	**0,929**	**64,286**	**1,142**	**69,613**	**8862,457**	**10,814**	**84,544**
St. deviation		**0,184**	**0,206**	**0,030**	**0,071**	**1,704**	**0,080**	**0,829**	**2426,421**	**0,492**	**3,585**

D.8: Data of F_G=0,68. The gel cylinders were prepared from AlgE6 + mannuronan, F_G=0,68.

Alginate	n	Diameter [mm]	Height [mm]	Weight before compression [g]	Weight after compression [g]	Gradient [N/m]	Youngs´s modulus [kPa]	Syneresis [%]	Rupture Strength [g]	Deform. at rupture [mm]	Elasticity [%]
	1	12,020	13,175	1,360	0,780	1049,000	20,794	62,431	8276,000	10,191	77,351
F_G=0,68	2	11,440	12,931	1,250	0,800	812,000	13,785	65,470	6536,400	9,762	75,493
Initial	3	11,780	13,330	1,380	0,880	663,000	13,074	61,878	4850,327	9,967	74,771
	4	11,650	12,840	1,280	0,960	1074,000	18,512	64,641	7246,401	9,552	74,393
Average		**11,723**	**13,069**	**1,318**	**0,855**	**899,500**	**16,541**	**63,605**	**6727,282**	**9,868**	**75,502**
St. deviation		**0,243**	**0,224**	**0,062**	**0,082**	**196,968**	**3,723**	**1,723**	**1440,765**	**0,274**	**1,315**
	1	11,84	12,966	1,350	1,180	507,000	9,295	62,707	13867,409	11,132	85,855
F_G=0,68	2	11,67	12,678	1,240	1,060	554,000	9,224	65,746	13143,400	11,384	89,793
1 shift in NaCl	3	11,24	12,694	1,200	1,060	555,000	8,604	66,851	14728,573	11,167	87,971
	4	11,45	12,465	1,180	1,020	620,000	9,445	67,403	13809,594	11,022	88,424
	5	11,4	12,614	1,150	1,030	601,000	9,405	68,232	12795,771	10,970	86,967
	6	11,38	12,879	1,210	1,120	500,000	8,299	66,575	7704,500	10,728	83,298
Average		**11,497**	**12,716**	**1,222**	**1,078**	**556,167**	**9,045**	**66,252**	**12674,875**	**11,067**	**87,051**
St. deviation		**0,219**	**0,181**	**0,070**	**0,061**	**48,297**	**0,476**	**1,925**	**2524,526**	**0,220**	**2,270**
	1	12,56	13,082	1,61	1,460	36	0,763	55,525	3054,922	10,819	82,701
F_G=0,68	2	12,92	13,758	1,71	1,540	72	1,878	52,762	4348,008	11,478	83,428
2 shifts in NaCl	3	12,73	12,925	1,60	1,440	33	0,693	55,801	3193,057	10,667	82,53
	4	12,9	13,584	1,54	1,380	46	1,151	57,459	4504,200	11,851	87,242
	5	13,01	11,662	1,43	1,290	31	0,499	60,497	3614,608	9,646	82,713
	6	12,35	13,507	1,61	1,440	47	1,060	55,525	2529,951	11,068	81,943
Average		**12,745**	**13,086**	**1,583**	**1,425**	**44,167**	**1,007**	**56,262**	**3540,791**	**10,922**	**83,426**
St. deviation		**0,251**	**0,766**	**0,093**	**0,084**	**15,171**	**0,489**	**2,566**	**769,934**	**0,761**	**1,929**
	1	13,34	16,10	1,80	1,08	22	0,980	50,276	1748,863	10,121	62,863
F_G=0,68	2	13,81	16,13	1,61	1,1	20	0,960	55,525	2045,3	10,528	65,27
3 shifts in NaCl	3	13,69	16,05	1,72	1,16	19	0,883	52,486	1878,51	8,306	51,751
	4	13,72	16,26	1,79	1,21	19	0,922	50,552	2347,939	10,370	63,776
	5	13,68	16,09	1,70	1,16	20	0,935	53,039	2343,8	10,471	65,078
	6	13,31	16,67	1,56	0,97	18	0,886	56,906	2582,9	10,192	61,14
Average		**13,592**	**16,217**	**1,697**	**1,113**	**19,667**	**0,928**	**53,131**	**2157,885**	**9,998**	**61,646**
St. deviation		**0,212**	**0,233**	**0,096**	**0,084**	**1,366**	**0,039**	**2,653**	**319,170**	**0,844**	**5,081**
	1	14,02	18,73	1,34	-	14	1,085	62,983	Dissolved	Dissolved	Dissolved
F_G=0,68	2	13,86	17,45	1,35	1,23	19	1,164	62,707	Dissolved	Dissolved	Dissolved
4 shifts inNaCl	3	14,35	17,94	1,38	-	18	1,284	61,878	Dissolved	Dissolved	Dissolved
	4	14,71	17,61	1,33	-	17	1,205	63,260	Dissolved	Dissolved	Dissolved
	5	14,41	17,67	1,40	-	19	1,306	61,326	Dissolved	Dissolved	Dissolved
	6	14,36	17,49	1,25	-	16	1,059	65,470	Dissolved	Dissolved	Dissolved
Average		**14,285**	**17,815**	**1,342**	**-**	**17,167**	**1,184**	**62,937**	**Dissolved**	**Dissolved**	**Dissolved**
St. deviation		**0,302**	**0,481**	**0,052**	**-**	**1,941**	**0,101**	**1,435**	**-**	**-**	**-**

D.9: Data of F_G=0,85. The mannuronan first was epimerized with AlgE6 (F_G=0,60) and the resulting alginate was incubated with AlgE4. However, AlgE6 was re-activated and more G-blocks were introduced.

Alginate	n	Diameter [mm]	Height [mm]	Weight before compression [g]	Weight after compression [g]	Gradient [N/m]	Youngs´s modulus [kPa]	Syneresis [%]	Rupture Strength [g]	Deform. at rupture [mm]	Elasticity [%]
	1	12,540	13,788	1,630	0,750	654,000	16,173	54,972	5099,578	9,699	70,344
F_G=0,85	2	13,280	14,784	1,940	1,380	530,000	18,120	46,409	5391,274	10,179	68,851
Intial	3	12,860	13,970	1,650	1,090	631,000	17,069	54,420	5568,990	9,940	71,152
	4	12,930	14,838	1,960	1,330	643,000	21,069	45,856	3864,728	9,608	64,753
	5	12,470	13,877	1,640	0,950	614,000	15,307	54,696	6058,181	9,921	71,492
Average		**12,816**	**14,251**	**1,764**	**1,100**	**614,400**	**17,547**	**51,271**	**5196,550**	**9,869**	**69,319**
St. deviation		**0,326**	**0,515**	**0,170**	**0,263**	**49,460**	**2,229**	**4,699**	**821,917**	**0,224**	**2,748**
	1	12,57	14,492	1,800	0,910	550,000	15,868	50,276	6912,136	10,734	74,068
F_G=0,85	2	12,49	14,073	1,550	1,060	279,000	7,278	57,182	7002,707	10,906	77,496
1 shift in NaCl	3	12,74	12,410	1,790	1,240	666,000	12,395	50,552	5728,864	10,545	84,972
	4	11,97	14,112	1,500	0,970	545,000	13,166	58,564	6003,500	10,492	74,348
	5	12,63	14,079	1,560	0,930	519,000	13,861	56,906	6993,500	11,099	78,834
	6	11,84	13,865	1,600	1,080	671,000	15,041	55,801	7216,686	10,599	76,444
Average		**12,373**	**13,839**	**1,633**	**1,032**	**538,333**	**12,935**	**54,880**	**6642,899**	**10,729**	**77,694**
St. deviation		**0,374**	**0,729**	**0,129**	**0,123**	**142,624**	**3,041**	**3,571**	**616,181**	**0,235**	**4,005**
	1	12,59	13,576	1,64	1,330	193	4,592	54,696	7710,492	11,469	84,48
F_G=0,85	2	12,56	13,616	1,69	1,480	193	4,611	53,315	8364,792	11,661	85,642
2 shifts in NaCl	3	12,11	14,272	1,67	1,540	221	5,652	53,867	8001,372	11,956	83,772
	4	12,23	13,455	1,65	1,380	211	4,612	54,420	7574,074	11,402	84,742
	5	12,82	14,396	1,86	1,460	214	6,295	48,619	8607,100	12,051	83,711
	6	12,86	14,601	1,90	1,680	201	6,208	47,514	9146,400	12,330	84,446
Average		**12,528**	**13,986**	**1,735**	**1,478**	**205,500**	**5,328**	**52,072**	**8234,038**	**11,812**	**84,466**
St. deviation		**0,305**	**0,493**	**0,114**	**0,124**	**11,623**	**0,823**	**3,158**	**592,024**	**0,362**	**0,709**
	1	13,02	11,33	1,50	-	55	0,813	58,564	1173	8,258	72,899
F_G=0,85	2	12,41	12,45	1,51	-	35	0,625	58,287	817,6	9,043	72,617
3 shifts in NaCl	3	12,08	12,77	1,61	-	42	0,765	55,525	1040,3	9,151	71,688
	4	12,14	12,24	1,36	-	33	0,535	62,431	1269,6	9,592	78,379
Average		**12,503**	**12,182**	**1,540**	**-**	**44,000**	**0,734**	**57,459**	**1010,300**	**8,817**	**72,401**
St. deviation		**0,477**	**0,756**	**0,061**	**-**	**10,149**	**0,098**	**1,680**	**179,589**	**0,487**	**0,634**
	1	9,56	13,32	0,81	-	25	0,324	77,624	Dissolved	Dissolved	Dissolved
F_G=0,85	2	9,96	13,05	0,70	-	25	0,331	80,663	Dissolved	Dissolved	Dissolved
4 shifts in NaCl	3	13,16	14,06	0,89	-	27	0,780	75,414	Dissolved	Dissolved	Dissolved
	4	10,23	12,02	0,82	-	27	0,294	77,348	Dissolved	Dissolved	Dissolved
	5	11,81	12,95	0,92	-	9	0,164	74,586	Dissolved	Dissolved	Dissolved
Average		**10,944**	**13,080**	**0,828**	**-**	**22,600**	**0,378**	**77,127**	**Dissolved**	**Dissolved**	**Dissolved**
St. deviation		**1,505**	**0,735**	**0,085**	**-**	**7,668**	**0,234**	**2,355**	-	-	-